

Sedimentology, Behavior, and Hazards of Debris Flows at Mount Rainier, Washington



U.S. GEOLOGICAL SURVEY PROFESSIONAL PAPER 1547

AVAILABILITY OF BOOKS AND MAPS OF THE U.S. GEOLOGICAL SURVEY

Instructions on ordering publications of the U.S. Geological Survey, along with prices of the last offerings, are given in the current-year issues of the monthly catalog "New Publications of the U.S. Geological Survey." Prices of available U.S. Geological Survey publications released prior to the current year are listed in the most recent annual "Price and Availability List." Publications that may be listed in various U.S. Geological Survey catalogs (see back inside cover) but not listed in the most recent annual "Price and Availability List" may no longer be available.

Reports released through the NTIS may be obtained by writing to the National Technical Information Service, U.S. Department of Commerce, Springfield, VA 22161; please include NTIS report number with inquiry.

Order U.S. Geological Survey publications by mail or over the counter from the offices listed below.

BY MAIL

Books

Professional Papers, Bulletins, Water-Supply Papers, Techniques of Water-Resources Investigations, Circulars, publications of general interest (such as leaflets, pamphlets, booklets), single copies of Earthquakes & Volcanoes, Preliminary Determination of Epicenters, and some miscellaneous reports, including some of the foregoing series that have gone out of print at the Superintendent of Documents, are obtainable by mail from

U.S. Geological Survey, Information Services
Box 25286, Federal Center
Denver, CO 80225

Subscriptions to periodicals (Earthquakes & Volcanoes and Preliminary Determination of Epicenters) can be obtained ONLY from the

Superintendent of Documents
Government Printing Office
Washington, DC 20402

(Check or money order must be payable to Superintendent of Documents.)

Maps

For maps, address mail orders to

U.S. Geological Survey, Information Services
Box 25286, Federal Center
Denver, CO 80225

Residents of Alaska may order maps from

U.S. Geological Survey, Earth Science Information Center
101 Twelfth Ave., Box 12
Fairbanks, AK 99701

OVER THE COUNTER

Books and Maps

Books and maps of the U.S. Geological Survey are available over the counter at the following U.S. Geological Survey offices, all of which are authorized agents of the Superintendent of Documents.

- **ANCHORAGE, Alaska**—Rm. 101, 4230 University Dr.
- **LAKEWOOD, Colorado**—Federal Center, Bldg. 810
- **MENLO PARK, California**—Bldg. 3, Rm. 3128, 345 Middlefield Rd.
- **RESTON, Virginia**—USGS National Center, Rm. 1C402, 12201 Sunrise Valley Dr.
- **SALT LAKE CITY, Utah**—Federal Bldg., Rm. 8105, 125 South State St.
- **SPOKANE, Washington**—U.S. Post Office Bldg., Rm. 135, West 904 Riverside Ave.
- **WASHINGTON, D.C.**—Main Interior Bldg., Rm. 2650, 18th and C Sts., NW.

Maps Only

Maps may be purchased over the counter at the following U.S. Geological Survey offices:

- **FAIRBANKS, Alaska**—New Federal Bldg, 101 Twelfth Ave.
- **ROLLA, Missouri**—1400 Independence Rd.
- **STENNIS SPACE CENTER, Mississippi**—Bldg. 3101

**SEDIMENTOLOGY, BEHAVIOR, AND
HAZARDS OF DEBRIS FLOWS AT
MOUNT RAINIER, WASHINGTON**



Frontispiece. View of south side of Mount Rainier near the end of the 1987 drought; showing upper Kautz Glacier, right of center, and tributary Success Glacier, at lower left, separated by Kautz Cleaver. Sunset Amphitheater, far upper left, is above heads of Puyallup and Tahoma Glaciers. Note the volcanic edifice composed of steeply outward-dipping lava and pyroclastic flow units. Hydrothermal alteration has been intense along many of the stratigraphic contacts, converting them to potential planes of failure. Photograph by R. M. Krimmel, October 5, 1987.

SEDIMENTOLOGY, BEHAVIOR, AND HAZARDS OF DEBRIS FLOWS AT MOUNT RAINIER, WASHINGTON

By K.M. Scott, J.W. Vallance, *and* P.T. Pringle

U.S. GEOLOGICAL SURVEY PROFESSIONAL PAPER 1547



UNITED STATES GOVERNMENT PRINTING OFFICE, WASHINGTON : 1995

U.S. DEPARTMENT OF THE INTERIOR

BRUCE BABBITT, Secretary

U.S. GEOLOGICAL SURVEY

Gordon P. Eaton, Director

For sale by U.S. Geological Survey, Information Services
Box 25286, Federal Center
Denver, CO 80225

Any use of trade, product, or firm names in this publication is for descriptive purposes only and does not imply endorsement by the U.S. Government

Library of Congress Cataloging-in-Publication Data

Scott, Kevin M., 1935-

Sedimentology, behavior, and hazards of debris flows at Mount Rainier, Washington / by K. M. Scott, J. W. Vallance, and P. T. Pringle.

p. cm. — (U.S. Geological Survey professional paper ; 1547)

1. Lahars—Washington (State)—Rainier, Mount, Region.
2. Volcanic hazard analysis—Washington (State)—Rainier, Mount, Region. I. Vallance, J. W. II. Pringle, Patrick T. III. Title.
IV. Series.

QE599.U5S36 1995

363.3'495—dc20

94-43162
CIP

CONTENTS

Abstract.....	1
Introduction	1
Acknowledgments	4
Types of flows at Mount Rainier	4
General statement	4
Cohesive debris flows (more than 3 to 5 percent clay)	7
Noncohesive debris flows (less than 3 to 5 percent clay).....	8
Hyperconcentrated flows.....	9
Flow magnitude and frequency	9
Methods of study	9
Flows of high magnitude and low frequency (500 to 1,000 years)	10
Greenwater Lahar and Osceola Mudflow.....	12
Paradise Lahar	18
Round Pass Mudflow (branch on Tahoma Creek)	19
Round Pass Mudflow (branch on Puyallup River).....	20
Unnamed pre–Electron deposits, Puyallup River System	21
1,000–year–old lahar	22
Electron Mudflow	22
Other lahars and possible lahars	24
Synthesis of the record of large, low–frequency lahars.....	24
Flows of intermediate magnitude and frequency (100 to 500 years)	24
White River System.....	24
Cowlitz River System.....	26
Nisqually River System	26
Puyallup River System	30
Carbon River System.....	30
Flows of low magnitude and high frequency (less than 100 years)	31
Recurrence interval of small debris flows	31
Seasonal distribution.....	32
Flow texture and formative transformations	32
Flow dynamics and transformations.....	32
Debris avalanches and the Tahoma Lahar	38
Historical floods compared with debris flows	40
Summary of flow origins and transformations	41
Risk analysis	42
Flow frequency and risk at Mount Rainier	43
Debris flows and summit–cone volcanism	44
Design or planning cases and hazard zonation.....	44
Definition of cases	44
Measurements and estimates of flow dynamics	44
Maximum lahar.....	45
Design or planning case I	46
Design or planning case II	47
Design or planning case III.....	47
Hazard zonation.....	47
Zone I.....	48
Zone II	48
Zone III.....	48
Lateral erosion associated with hazard zone III	48

Probability of precursor volcanic activity.....	48
Travel times of lahars and potential reservoir effects.....	49
Travel times of lahars	49
Reservoir effects	51
White River	51
Cowlitz River.....	51
Nisqually River	52
Conclusions.....	52
References Cited.....	53

PLATE

[Plate is in pocket]

1. Cross sections of selected flows at Mount Rainier.

FIGURES

1. Maps showing location of Mount Rainier, localities of lahar cross sections, and other features of interest in southwestern Washington	2
2. Graph showing cumulative curves of particle sizes in a typical cohesive lahar (Electron Mudflow) and noncohesive lahar (National Lahar).....	6
3. Graph showing relation of sorting and mean grain size for selected cohesive and noncohesive debris flows.....	8
4. Photograph showing northeast side of Mount Rainier and Little Tahoma Peak	11
5. Graph showing relation of flow volume and clay content in several postglacial mudflows at Mount Rainier	13
6. Diagrammatic composite sequence of valley-fill deposits in the White River valley	14
7. Photographs showing mound-studded surface of the Osceola Mudflow.....	15
8. Graph showing lahar-bulking factors for four lahars at Mount Rainier, and composition changes in the Osceola Mudflow.....	17
9. Composite columnar sections of lahars and associated deposits in the upper Nisqually River drainage	19
10. Diagrammatic composite sequences of valley-fill deposits in the Puyallup River valley	21
11. Diagrammatic composite sequences of valley-fill deposits in the Nisqually River valley	27
12. Photograph showing dish structure in deposits of National Lahar at the type locality	28
13. Graph showing discharge versus distance for debris flows resulting from glacial outburst or collapse	30
14. Graph showing seasonal distribution of debris flows, hyperconcentrated flows, and floods in glacier-fed tributaries of the Nisqually River from 1925 to 1990.....	32
15-17. Photographs showing:	
15. Active front of the South Tahoma Glacier 5 days before and 1 day after the clear-weather glacial-outburst flood and debris flow of June 29, 1987	33
16. Area of stagnant, moraine-covered lower part of South Tahoma Glacier 5 days before and 1 day after the flow of June 29, 1987	34
17. Ice clast, more than 1 meter in maximum dimension, included with andesite clasts of similar size in lobate boulder front of flow of October 26, 1986	35
18. Graph showing cumulative curves of particle sizes within successive boulder fronts and hyperconcentrated-flow deposits formed during transformation of the Tahoma Creek debris flow of October 26, 1986.....	36
19. Photographs showing debris flow levees and underlying sole layers from flows of 1986 and 1987 along Tahoma Creek.....	37
20. Graph showing cumulative curves of particle sizes of debris flows derived by dewatering	38
21. Photograph showing debris avalanche on the surface of the Tahoma Glacier at the head of the South Puyallup River	39
22. Photograph showing megaclast at surface of the 1963 debris avalanche below the Emmons Glacier in the main fork of the White River.....	50

TABLES

1. Tephra units and other indications of volcanic activity 10

2. Mainly cohesive debris flows of sector-collapse or avalanche origin 12

3. Mainly noncohesive debris flows and their runout phases 23

4. Radiocarbon dates from hyperconcentrated-flow and normal streamflow deposits 25

5. Summary of origins and transformations of debris flows 41

6. Ranking of debris flows described in table 5 by magnitude, frequency, and risk 43

7. Characteristics of design- or planning-case lahars 45

8. Celerities and travel times of the maximum lahar, Case I lahar, and Case II lahar from Mount Rainier to the nearest downstream reservoir or the Puget Sound lowland 50

CONVERSION FACTORS

Multiply	By	To obtain
millimeters (mm)	0.03937	inches
centimeters (cm)	0.3937	inches
meters (m)	3.281	feet
kilometers (km)	0.6214	miles
square kilometers (km ²)	0.3861	square miles
meters per second (m/s)	3.281	feet per second
cubic meters per second (m ³ /s)	35.31	cubic feet per second

SEDIMENTOLOGY, BEHAVIOR, AND HAZARDS OF DEBRIS FLOWS AT MOUNT RAINIER, WASHINGTON

By K.M. Scott, J.W. Vallance, and P.T. Pringle

ABSTRACT

Mount Rainier is potentially the most dangerous volcano in the Cascade Range because of its great height, frequent earthquakes, active hydrothermal system, and extensive glacier mantle. Many debris flows and their distal phases have inundated areas far from the volcano during postglacial time. Two types of debris flows, cohesive and noncohesive, have radically different origins and behavior that relate empirically to clay content. The two types are the major subpopulations of debris flows at Mount Rainier. The behavior of cohesive flows is affected by the cohesion and adhesion of particles; noncohesive flows are dominated by particle collisions to the extent that particle cataclasis becomes common during near-boundary shear.

Cohesive debris flows contain more than 3 to 5 percent of clay-size sediment. The composition of these flows changed little as they traveled more than 100 kilometers from Mount Rainier to inundate parts of the now-populated Puget Sound lowland. They originate as deep-seated failures of sectors of the volcanic edifice, and such failures are sufficiently frequent that they are the major destructional process of Mount Rainier's morphologic evolution. In several deposits of large cohesive flows, a lateral, megaclast-bearing facies (with a mounded or hummocky surface) contrasts with a more clay-rich facies in the center of valleys and downstream. Cohesive flows at Mount Rainier do not correlate strongly with volcanic activity and thus can recur without warning, possibly triggered by non-magmatic earthquakes or by changes in the hydrothermal system.

Noncohesive debris flows contain less than 3 to 5 percent clay-size sediment. They form most commonly by bulking of sediment in water surges, but some originate directly or indirectly from shallow slope failures that do not penetrate the hydrothermally altered core of the volcano. In contrast with cohesive flows, most noncohesive flows transform both from and to other flow types and are, therefore, the middle segments of flow waves that begin and end as flood surges. Proximally, through the bulking of poorly sorted volcanoclastic debris on the flanks of the

volcano, flow waves expand rapidly in volume by transforming from water surges through hyperconcentrated streamflow (20 to 60 percent sediment by volume) to debris flow. Distally, the transformations occur more slowly in reverse order—from debris flow, to hyperconcentrated flow, and finally to normal streamflow with less than 20 percent sediment by volume. During runout of the largest noncohesive flows, hyperconcentrated flow has continued for as much as 40 to 70 kilometers.

Lahars (volcanic debris flows and their deposits) have occurred frequently at Mount Rainier over the past several thousand years, and generally they have not clustered within discrete eruptive periods as at Mount St. Helens. An exception is a period of large noncohesive flows during and after construction of the modern summit cone. Deposits from lahar-runout flows, the hyperconcentrated distal phases of lahars, document the frequency and extent of noncohesive lahars. These deposits also record the following transformations of debris flows: (1) the direct, progressive dilution of debris flow to hyperconcentrated flow, (2) deposition of successively finer grained lobes of debris until only the hyperconcentrated tail of the flow remains to continue downstream, and (3) dewatering of coarse debris flow deposits to yield fine-grained debris flow or hyperconcentrated flow.

Three planning or design case histories represent different lengths of postglacial time. Case I is representative of large, infrequent (500 to 1,000 years on average) cohesive debris flows. These flows need to be considered in long-term planning in valleys around the volcano. Case II generalizes the noncohesive debris flows of intermediate size and recurrence (100 to 500 years). This case is appropriate for consideration in some structural design. Case III flows are relatively small but more frequent (less than 100 years on average).

INTRODUCTION

Mount Rainier volcano is potentially the most dangerous of the periodically active volcanoes of the Cascade Range, which extends from northern California into

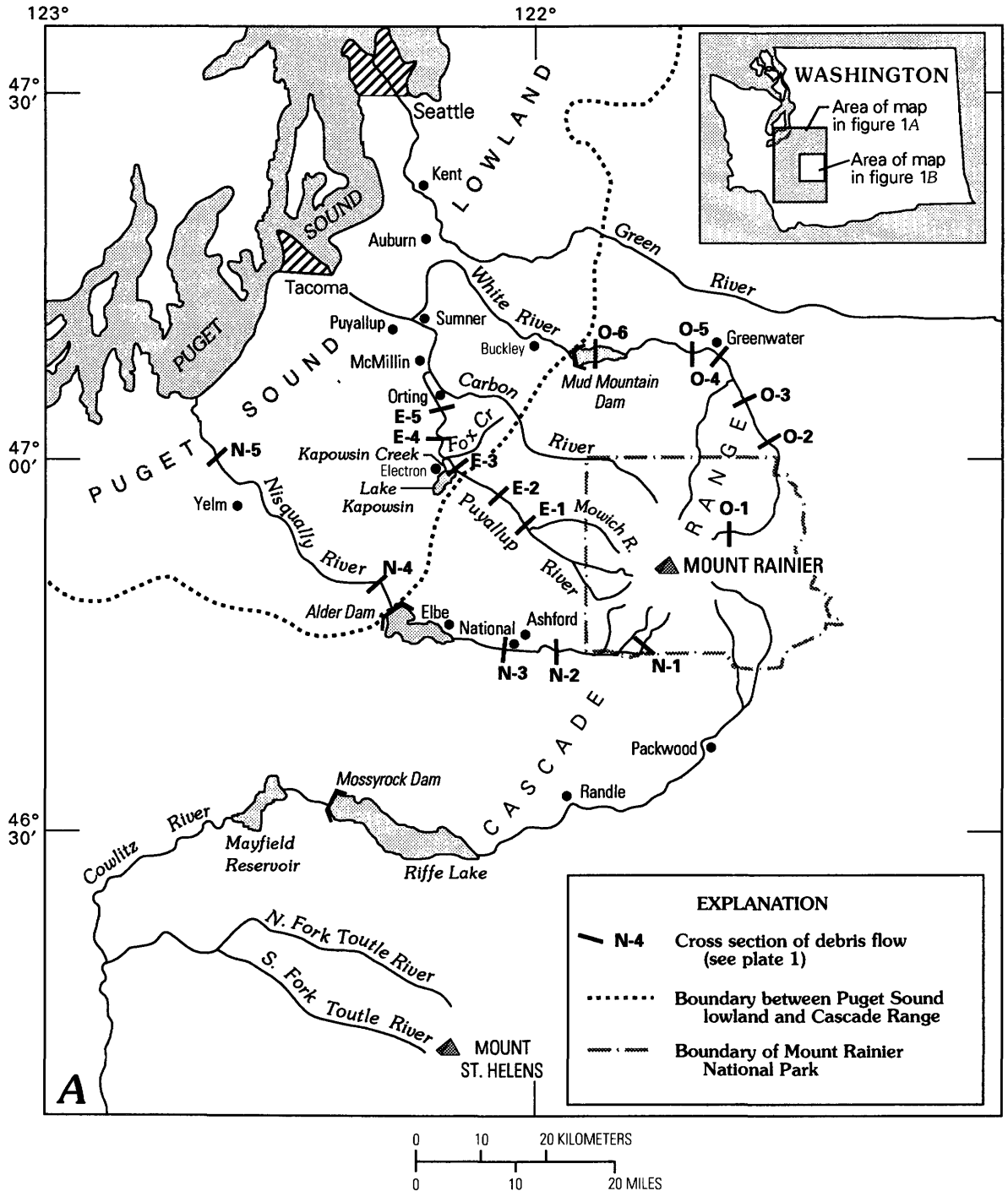


Figure 1 (above and facing page). Location of Mount Rainier, localities of lahar cross sections, and other features of interest in southwestern Washington. All cross sections are shown on plate 1. Cross-section localities for Tahoma Lahar (T) are shown on detailed map *B* (facing page); all other cross-section localities are shown above. *A*, Major streams, dams, reservoirs, and population centers in the region.

British Columbia. The mountain is second only to Mount St. Helens in seismic activity, and it is the highest volcano in the Cascade Range. It also has the largest mass at high altitude, above 3,000 m for example, and consequently has a perennial snow and glacier mantle that is approximately

equal in volume to that at all other Cascade Range volcanoes combined (Driedger and Kennard, 1986).

The volcano is the dominant feature of Mount Rainier National Park, located about 70 km southeast of Seattle, Wash. It is drained by five major river systems (fig. 1): the

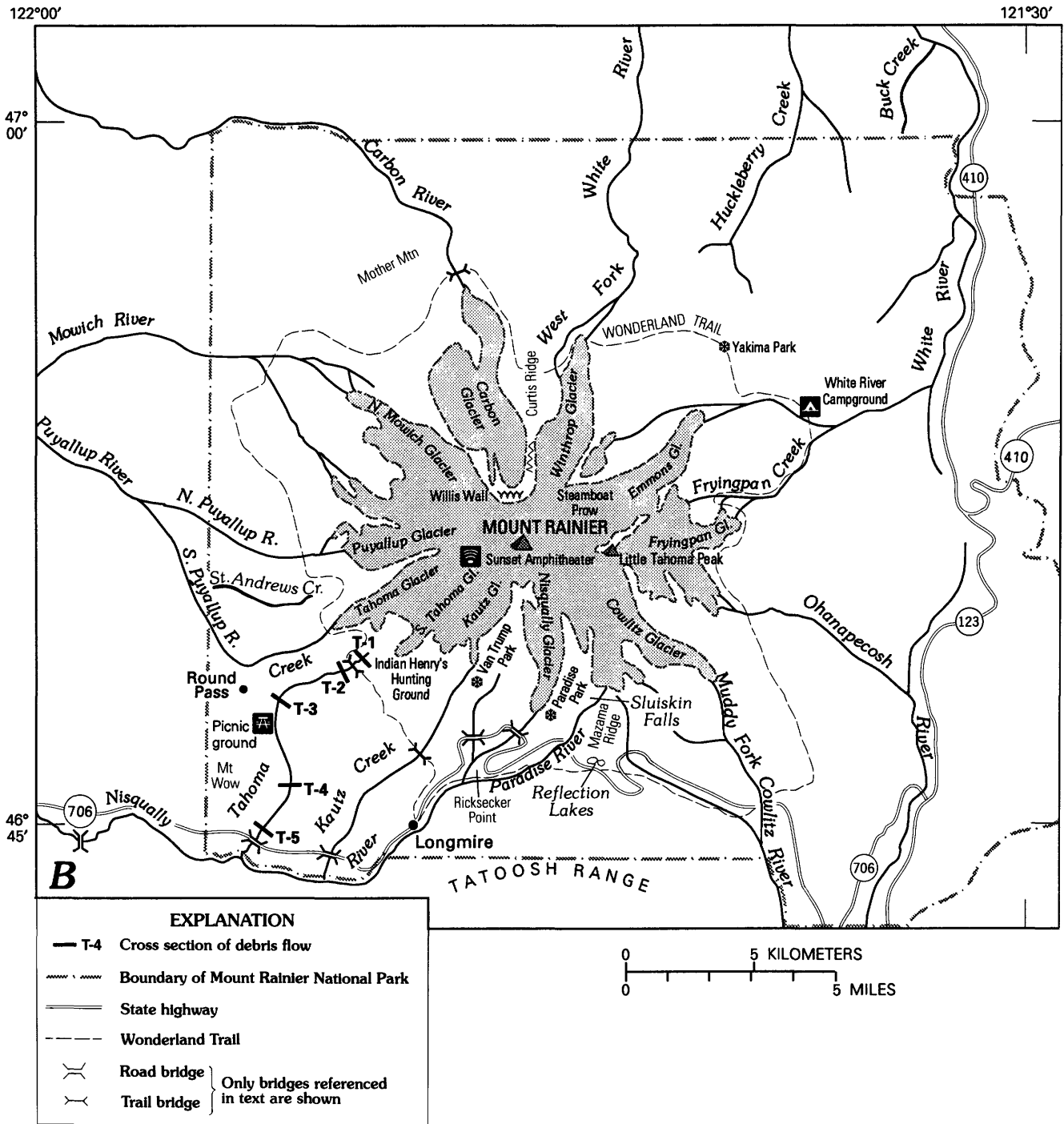


Figure 1, continued. B, Enlarged map of Mount Rainier National Park showing glaciers, streams, and major roads and trails.

White River on the northeast, the Cowlitz River on the southeast, the Nisqually River on the southwest, and the Puyallup and Carbon River systems on the northwest. All but the Cowlitz River traverse at least 100 km of both the Cascade Range and the Puget Sound lowland before emptying into Puget Sound. The Cowlitz flows more than 140 km southward and enters the Columbia River. For more than 45 km upstream of Riffe Lake, the Cowlitz's flood plain is unusually wide, averaging about 2 km in width.

Mount Rainier volcano has an extensive history of post-glacial debris flows that originated from collapse of major sectors of the mountain (Crandell, 1971). Many recent studies of similar composite volcanoes show that evolution by periodic sector collapses is a common morphologic progression. Risk analysis in this report shows that the debris flows of this origin pose the greatest hazard at Mount Rainier. These flows are distinguished here as cohesive debris flows to indicate the importance of their "sticky,"

relatively clay-rich matrix in determining flow behavior, and their defining characteristic is their ability to remain unchanged as debris flows to their distal ends. Evidence of the flows is traced downstream, and flow dynamics are defined where the flows left the canyons of the Cascade Range to inundate flood plains, now increasingly populated, on the Puget Sound lowland (fig. 1).

A second type of debris flow, which is common at Mount Rainier, is substantially different in origin and behavior and yields deposits distinctly more granular in texture. These relatively clay-poor flows, distinguished here as noncohesive to indicate the importance of grain-to-grain contact in determining behavior, readily transform both from and to other flow types. Noncohesive debris flows originate most commonly as water surges produced by melting of snow by volcanic heat. Although less of a general hazard than the debris flows that originate as large slope failures, noncohesive flows occur more often, and their runout phases could inundate parts of the Puget Sound lowland. Because of their shorter recurrence intervals, noncohesive flows pose a more likely threat to life and property locally on and near the base of the volcano. The recognition of the deposits of this flow type and its transformations has significant implications for the reconstruction of a volcano's history. As illustrated by the forecast of Crandell and Mullineaux (1978) at Mount St. Helens, 80 km south of Mount Rainier, a volcano's history is the best guide to its future behavior.

Some noncohesive debris flows reflect another factor contributing to the exceptional flow hazards at Mount Rainier: its mantle of ice and snow is subject to volcanically induced melting. A geothermally formed subglacial lake has existed in at least one of the two summit craters (Lokey and others, 1972; Kiver and Steele, 1972), and it may still exist but its presence hasn't been verified since 1978 (W. M. Lokey, Pierce County Dept. of Emergency Management; written commun., 1989). A subset of noncohesive flows consists of debris flows formed from glacial-outburst floods. Although these flows have been a hazard only locally, they provided important behavioral models of noncohesive flows from 1986 to 1992.

The purpose of this report is to define the origins, magnitude, and frequency of debris flows and other flow types associated with debris flows, with particular reference to volcanic hazards. The probability of such flows is similar in most of the drainage basins, as indicated by the present-day symmetry of hydrothermal activity, occasional small earthquake clusters centered beneath the summit, and our inability to forecast which sector of the volcano will be affected by renewed volcanic, seismic, or geothermal activity. However, several factors affect variations in probabilities between drainages. For example, sector collapses that produce huge, cohesive debris flows can occur on any flank of Mount Rainier, but northward- or northeastward-directed failure may be especially likely because the summit cone is formed in an amphitheater resembling a

"greased bowl" that is probably open to the north (Frank, 1985, p. 180).

In analyzing flows of sediment and water in populated valleys surrounding the volcano, this study complements ongoing studies by the U.S. Geological Survey of Mount Rainier's volcanic hazards and glacially related hydrologic hazards. There is necessarily some overlap in these investigations because many large debris flows were volcanically initiated, and many small debris flows originated as glacial-outburst floods. As at Mount St. Helens, however, there is a record of more large debris flows than the number of known volcanic events, and glaciers do not exert a primary influence in forming the larger flows. This report, therefore, concentrates on the actual downstream stratigraphic record of flows and their dynamics, as revealed by sedimentologic and paleohydrologic evidence, rather than evidence from volcanic or glacial activity.

ACKNOWLEDGMENTS

Although this study mainly focused on the flow record beyond the base of the volcano, some work within Mount Rainier National Park was necessary, and the writers are indebted to the personnel of the National Park Service cited herein for their observations of flow phenomena and for information on the 20th-century flow record. W.V. Steuben and D.J. Gooding, U.S. Geological Survey, overcame the extensive problems in laboratory analysis of the cohesive deposits. The manuscript benefited substantially from review by J.C. Brice, J.E. Costa, and C.L. Driedger, all of the U.S. Geological Survey, and K.S. Rodolfo, University of Illinois at Chicago; and from review of specific topics by D.R. Crandell, U.S. Geological Survey, R.R. Dibble, Victoria University of Wellington, and W.M. Lokey, Pierce County Department of Emergency Management.

TYPES OF FLOWS AT MOUNT RAINIER

GENERAL STATEMENT

Fundamental to the analysis of subaerial sediment-gravity flows at Mount Rainier is the recognition of two distinct types of debris flows that differ significantly in both texture and origin. Thus it is possible to deduce the origin of an ancient flow deposit, even one far from the volcano, from its texture, in particular the texture of the matrix phase of the characteristically bimodal flows. An earlier investigation at Mount St. Helens (Scott, 1988b) reported two distinctive types of debris flows: (1) relatively clay-rich flows that traveled long distances as debris flows and (2) more granular flows that began mainly as streamflow, then bulked (increased volume by incorporating sediment) to form

hyperconcentrated streamflow, and continued to incorporate eroded sediment until a debris flow was formed. Distally, the sequence of flow types was reversed. These two types of debris flows are the cohesive and noncohesive debris flows, respectively, of this report.

A subdivision of only mudflows (commonly defined as silt- and clay-rich debris flows) into cohesive and noncohesive types was made by Russian investigators (Kurdin, 1973, p. 311). However, noncohesive flow was defined as containing 80 percent sediment by weight (approximately 60 percent by volume), and the particles were described as being deposited and sorted as flow velocity slowed (Kurdin, 1973, p. 315). Although the sediment content was that of debris flow, the behavior described is mainly characteristic, not of debris flow, but of hyperconcentrated streamflow as noted by Costa (1984, p. 289). The subdivision of sediment-gravity flows and deposits into the cohesive and cohesionless classes of soil mechanics (for example, Postma, 1986) is probably only theoretically useful. Several workers have implicitly or explicitly questioned the reliability of clay or matrix content (for example, Lowe, 1979, 1982; Nemeč and Steel, 1984) as the main criterion for distinguishing between ancient deposits of cohesive and cohesionless debris flows. This criterion is probably not useful for deposits of subaqueous debris flows, for which only the texture may be known and nothing at all may be known about the involvement of processes such as fluidization, escaping pore fluids, and the modified grain flow of Lowe (1976).

Differences in behavior between flows having different matrix properties are more obvious where, as at a volcano, the deposit of a modern or postglacial flow can be seen from beginning to end, and each textural, stratigraphic, and morphologic nuance can be known. In some modern (1982) volcanic flows, even the postdepositional changes in matrix character can be defined (Scott, 1988b). Noncohesive debris flow, as defined here, is flow that retains sufficient strength (albeit with lower matrix cohesiveness than cohesive flow) to produce the diagnostic characteristics of debris flow deposits: transversely and longitudinally convex flow fronts, lateral levees, buoyed dense megaclasts, and a texture of commonly dispersed clasts, pebble size or coarser, in a finer grained granular matrix. Despite these similarities, however, the behavior of noncohesive debris flows differs radically from that of their cohesive counterparts.

Neither type of debris flow has truly irreversible sediment entrainment, one of Hooke's (1967) criteria for distinguishing a debris flow from a water flow; both cohesive and noncohesive types may leave coarse, clast-supported whaleback bars at sites of rapid energy loss (Scott, 1988b). Only noncohesive flows lose coarse sediment at a rate sufficient to cause transformation downstream to more dilute flow types, initially hyperconcentrated flow. Some cohesive flows show a slight textural change in the direction of that transformation, probably by particle

settling within the rigid central plug of the flow, and by periodic loss of coarse clasts at sites of energy loss where dispersive and other particle-impact stresses are minimal. However, cohesive flows at both Mount Rainier and Mount St. Helens traveled well over 100 km and did not transform. The net results of deposition of sediment, and its addition (bulking) in reaches of high shear stress at flow boundaries, are discussed in the subsequent section on the Osceola Mudflow.

Debris flow behavior correlates strongly with particle-size distribution (size classes shown in fig. 2), especially clay content (Hampton, 1975; Middleton and Hampton, 1976; Qian and others, 1980, fig. 3; Costa, 1984; Pierson and Costa, 1987). The description of debris flows as cohesive or noncohesive is intended to reflect an important empirical difference in behavior related to clay content, and thus to matrix cohesiveness. Silt content also contributes to the cohesiveness of a flow but is normally proportional to the clay content. Both cohesive and noncohesive debris flows have a matrix phase and a coarse-sediment phase (dispersed phase of Fisher and Schmincke, 1984). The coarse sediment is dispersed throughout the matrix phase in most cases, but not all. Figure 2 shows particle-size distributions for representative cohesive and noncohesive flow deposits and for the other flow types into which the noncohesive debris flows normally transform downstream.

The existence of a spectrum of debris flow behavior is implicit (see Lowe, 1979) in the original Coulomb viscoplastic model of a debris flow (Johnson, 1965; Yano and Daido, 1965) and, regardless of rheological model, a range of behavior in response to varying sediment properties and content has been observed as noted above. Some flows are clearly dominated by viscoplastic behavior resulting primarily from momentum exchange within a "sticky" fine-grained matrix (cohesive flows of this report); others are more granular flows dominated by momentum exchange between coarser particles (noncohesive flows of this report) that are, however, still part of the matrix. Sand-size sediment dominates the matrix of noncohesive flows at both Mount Rainier and Mount St. Helens.

Although the two flow behaviors are distinct, basic mechanisms of particle support likely overlap. A greater abundance of particle collisions probably explains the more pronounced shear-related boundary features and cataclasis in the noncohesive flows as well as the transformations of those flows to and from other flow types. It may also explain some previously divergent assumptions of debris flow rheology, and it clearly accounts for some of the difficulties in modeling their behavior. The fundamental distinction is pragmatic, however, and a view of debris flows as having only two distinct types of momentum exchange and particle support does not fully consider the evidence of other dynamic interactions between their solid and fluid constituents (Iverson and Denlinger, 1987). Nevertheless, the distinction based on clay content is highly useful and it

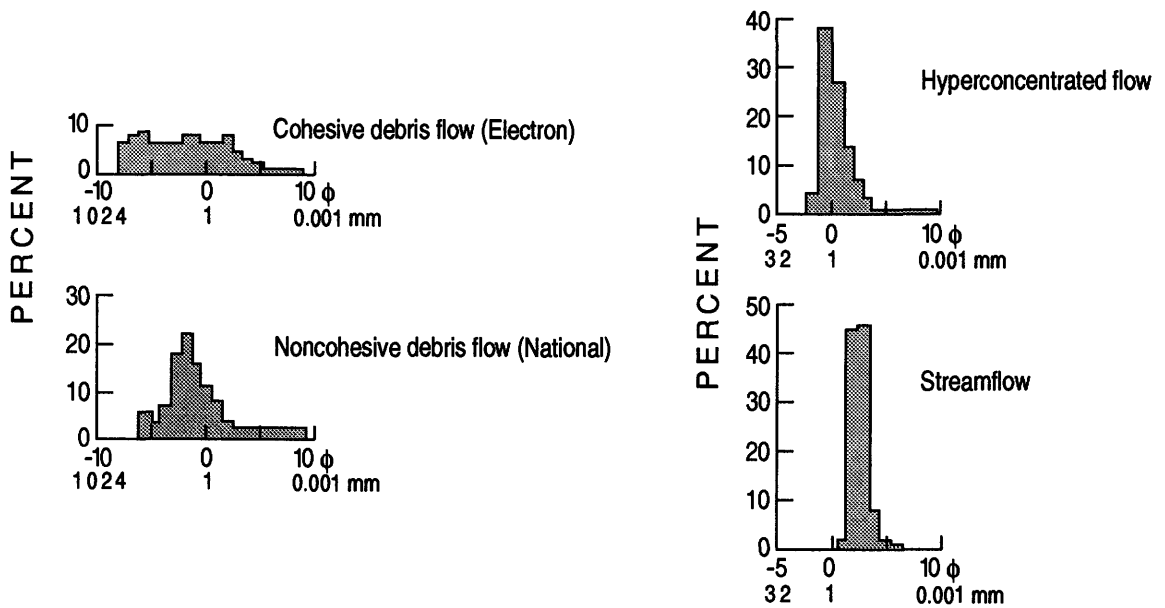
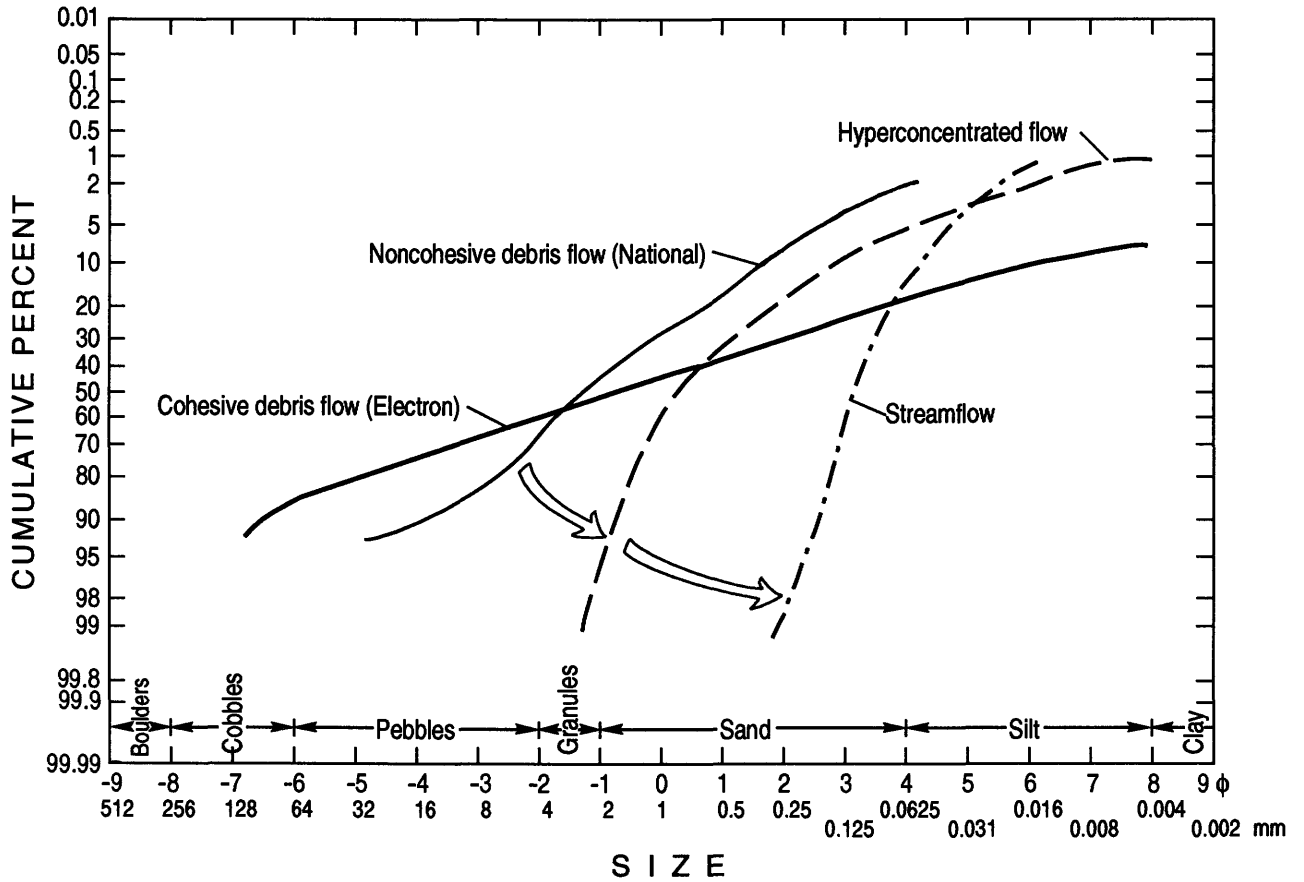


Figure 2. Cumulative curves of particle sizes in a typical cohesive lahar (Electron Mudflow) and noncohesive lahar (National Lahar). Other flow types into which the noncohesive debris flows normally transform downstream are also shown.

rationalizes many of the features and behavioral variations of lahars. Based on observations at volcanoes around the Pacific Rim by the senior writer, the distinction is generally applicable.

The observation that a species of debris flow transforms to and from other flow types also can add greatly to our knowledge of a volcano's past. For example, the presence of large noncohesive flows and their downstream

transformations, or of synchronous flows in more than one watershed, can indicate unrecognized eruptions (magmatic or phreatic) or shallow landslides mobilized to debris flow. Also, the identification of debris-flow-related deposits is aided by knowing that noncohesive flows attenuate more rapidly than cohesive flows and that a noncohesive debris flow upstream may be marked on flood plains downstream by deposits of hyperconcentrated or normal streamflow, which are less conspicuous than debris flow deposits (Scott, 1989).

The formation of debris flows from flood surges is the dominant formative process at some Cascade Range strato-volcanoes, such as Mount St. Helens (Scott, 1988b), but apparently is less common in other environments. The process probably does not involve pure autosuspension (Bagnold, 1962; Southard and Mackintosh, 1981) and is greatly facilitated by large sediment contributions from bed and bank mobilization. The efficacy of the process is dramatically illustrated at Mount St. Helens by the huge lahar (PC1) that consists almost entirely of stream-rounded alluvium (Scott, 1988a). In constructing a conceptual model of debris flow formation, Johnson (1984, p. 331) cited one example (Jahns, 1949) in which a debris flow resulted from the bulking of sediment from channel erosion by a clay-water mixture. Costa (1984) also cited several cases in which this mechanism probably occurred, and Rodolfo (1989) documented the process for rain-induced lahars. A surge from a moraine-dammed-lake breakout quickly bulked to debris flow in the Bol'shaya Almatinka River in Russia and continued to enlarge downstream (Yesenov and Degovets, 1979). The same mechanism formed debris flows from breakouts of moraine-dammed lakes at the Three Sisters volcanoes, Oregon (Laenen and others, 1987, 1992). The requisite factor both for bulking to debris flow and for continued enlargement is an abundance of loose, poorly sorted volcanoclastic and morainal sediment on steep slopes.

Usage here of the popular but variously defined term "lahar" for volcanic debris flows corresponds, with one exception, to its application by Crandell (for example, 1971) throughout the Cascade Range. Glacial-outburst floods that bulk to debris flows but lack evidence of triggering by volcanism are not here called lahars; the term is reserved for, and most usefully applied to, flows that are directly or indirectly related to volcanism rather than merely the alpine environment. Other characteristics, such as composition or angularity of debris, are not definitive. Even origin on a volcano is not a reliable criterion, for in some cases bulking may not produce a debris flow until the surge is beyond the volcanic edifice. Some details of terminology are discussed by Scott (1988b). To be consistent with most formal and informal usage in the Cascade Range, the term is applied here, as by Crandell (1971), to both the flow and the deposit. Future workers may wish to conform to the definition recommended by the 1988 Penrose Conference on Volcanic Influences on Terrestrial Sedimentation (Smith and Fritz,

1989), which is essentially the definition used here except that the flow deposit is excluded.

COHESIVE DEBRIS FLOWS (MORE THAN 3 TO 5 PERCENT CLAY)

The largest lahars at Mount Rainier were recognized as relatively clay-rich by Crandell (1971), who logically hypothesized that a clay content of about 5 percent or more reflected an origin directly from large landslides. The clay is an alteration product of the hydrothermal system of the volcano. These flows remained debris flows to their termini. At Mount St. Helens, the critical clay content that characterized the nontransforming cohesive flows was a minimum of 3 percent. The apparent difference in critical clay content between the two volcanoes, as it affects flow behavior, mainly reflects sampling procedure and is discussed below. Hydrothermal alteration is more intense at Mount Rainier, probably as a result of its greater age. This difference is the probable cause of the dominance of large cohesive flows at Mount Rainier, whereas large noncohesive flows dominate the record at Mount St. Helens (Scott, 1988a, 1989; Major and Scott, 1988). The original and type example of a cohesive flow is the 1980 North Fork Lahar at Mount St. Helens (Scott, 1988b).

The differences in behavior of cohesive and noncohesive debris flows correlate strongly with the texture of the matrix phase: the matrix of cohesive debris flows is a mix of sand, silt, and at least 3 percent clay; that of noncohesive debris flows is silty sand with commonly about 1 percent clay. In cohesive debris flows, (1) grain interaction is cushioned by the adhering clay aggregates, thereby reducing near-boundary shear and other particle interactions recorded by the boundary features characteristic of noncohesive debris flows; and (2) the clayey matrix retards each of the following: (a) the settling of coarse particles, (b) the differential movement of all coarse-phase particles (which produces the well-developed normal and inverse grading in noncohesive flows), and (c) the miscibility of the flow with associated streamflow. The latter effects prevent or greatly retard the transformation of a cohesive debris flow to hyperconcentrated streamflow. These conclusions are empirical; the actual physics and chemistry of clay in the matrix remain to be investigated. For example, clay content may affect the viscosity of the pore fluid and, therefore, the hydraulic diffusivity of that fluid through the granular phase (Iverson, 1989). Such movement may be slight in cohesive flows, where interparticle attractive forces can dominate, but in the noncohesive regime, the character of the medium around colliding and abrading particles of the matrix must be important.

Clay minerals compose most clay-size sediment, but their proportion is variable in lahars. They compose 75 percent of the clay-size sediment in the largest lahar from

Mount Rainier (Crandell, 1971). Clay minerals are layer-lattice silicates with powerful surface forces that can provide cohesion and strength to the entire flow. Clay aggregates in turn adhere to sand in the matrix as well as the coarse-phase clasts. Varieties of clay minerals reported from the edifice of Mount Rainier and the lahars derived from it include kaolinite, montmorillonite, smectite, halloysite, illite, and pyrophyllite (Crandell, 1971; Frank, 1985).

The failed sectors of the volcano contained enough water and clay to provide uninterrupted mobility as they rapidly disaggregated, first to a debris avalanche and then to a lahar. A debris avalanche is a rapid flow of rock debris (Varnes, 1978), wet or dry, commonly containing many large megaclasts. Studies of the May 18, 1980, eruption at Mount St. Helens suggest that some cohesive flows may have been derived from the surface of an immobilized debris avalanche. The surficial portion of the huge 1980 debris avalanche at Mount St. Helens was saturated by dewatering after emplacement, thereby forming a critical mass of ponded muddy debris which began flowing as a broadly peaked lahar wave several hours later. All large-scale debris avalanches recorded by known deposits at Mount Rainier mobilized directly to lahars. The only debris avalanches known to have yielded lahars secondarily were small examples of shallow origin.

NONCOHESIVE DEBRIS FLOWS (LESS THAN 3 TO 5 PERCENT CLAY)

These more granular debris flows commonly represent the middle segments of meltwater flood surges (either volcanically or climatically induced) that both begin and end as streamflow surges. They are generally better sorted and may be finer grained on average than the larger, boulder-rich cohesive debris flows (fig. 3). The initial water surges incorporate most sediment from stream-channel deposits that are partly depleted of fine sediment as a result of selective or hydraulic sorting by fluvial processes acting both subglacially and proglacially. Consequently, through bulking, the surges form debris flows that have an average clay content of only about 1 percent. The original and type example of a noncohesive flow is the lahar of March 19–20, 1982, at Mount St. Helens (Scott, 1988b).

On the volcano, glacial-outburst flows are characterized by a relatively high lahar-bulking factor (LBF; the percentage of sediment added to the flow beyond the point of origin as revealed from clast roundness or composition; Scott, 1988b). Noncohesive debris flows originating as slides of relatively unaltered volcanoclastic debris have a distinctively lower LBF. This origin resembles, at smaller scale, the process by which the large cohesive lahars are formed from deep-seated failures.

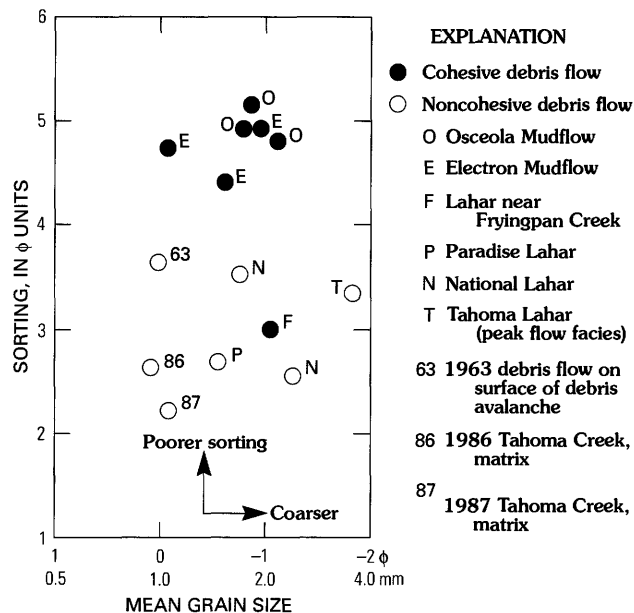


Figure 3. Sorting versus mean grain size for selected cohesive and noncohesive debris flows. Mean grain size and sorting values correspond to M_z and σ_G of Folk (1980).

In comparison with the deposits of cohesive lahars, those of noncohesive lahars document more intense particle interaction, especially near flow boundaries, where the group of boundary features described by Scott (1988b) records the effects of shearing on particles and their size distributions. These features include a distinctive sole layer, inverse graded bedding, a lahar-abraded pavement, truncated size distributions, and grain cataclasis. Such features are clearly best developed in the noncohesive flows, but are not exclusive to them.

A common but not consistent distinction between the debris flow types is a generally higher rate of attenuation of the noncohesive flows. The granularity of noncohesive flows increases their miscibility with overrun streamflow, a factor leading to their downstream transformations to hyperconcentrated flow. The effect is illustrated by the increase in transformation rate at sites of significant tributary inflow (Scott, 1988b, fig. 37). In effect, the flow becomes diluted and loses strength, and the fluid phase progressively outruns the sediment phase. The sediment component of the noncohesive debris flows is more readily deposited than that of the cohesive flows. Once transformation occurs, the peak sediment concentration characteristically lags behind peak discharge (Scott, 1988b), as in some storm-flood peaks (Guy, 1970). In cohesive debris flows, the entire mixture remains coherent and relatively constant in texture, although systematic downstream change can occur (Scott, 1988b).

HYPERCONCENTRATED FLOWS

Hyperconcentrated flow is an important flow type at most Cascade Range volcanoes. The history of its recognition and the criteria by which its deposits are recognized are described elsewhere (Scott, 1988b). The most obvious feature that differentiates these deposits from debris flow deposits is their undispersed, entirely clast-supported texture. They are distinguished from flood-surge and normal streamflow deposits by poor development of stratification, sorting in a range intermediate between those of debris-flow and flood-surge deposits, locally well-developed inverse or normal grading, and the local presence of dewatering structures such as the dish structure of Wentworth (1967) and Lowe and LoPiccolo (1974). Dish structure is previously reported only from deposits of sediment-gravity flows in the deep marine environment.

Bulking of a flood surge to a debris flow commonly occurs on the steep flanks of the volcano in confined channels. In this setting, the granular deposits of the hyperconcentrated flow interval are thin and rarely preserved. Channel steepness and an abundance of unstable detritus commonly result in rapid bulking in a short increment of channel. The debulking, in contrast, may occur over a long distance. In the streams draining Mount Rainier, the longest documented intervals of hyperconcentrated transport in single flows occurred in the Nisqually River from Longmire to below Alder Reservoir, more than 40 km, and in the White River from near the base of the volcano to beyond the boundary of the Puget Sound lowland, over 70 km.

A distinctive facies distinguishes the interval where debris flow transforms to hyperconcentrated flow (Scott, 1988b, fig. 10). This "transition facies" begins to form as the front of the flood wave transforms, continues as the change works its way progressively back through the debris flow, and ends at the point where the entire wave becomes hyperconcentrated flow. The preserved record of this transition interval, therefore, consists of downstream-thickening hyperconcentrated flow deposits overlain by downstream-thinning debris flow deposits. This transition facies thus documents the origin of hyperconcentrated flow from an upstream debris flow.

At Mount St. Helens, the hyperconcentrated flows were described as lahar-runout flows and interpreted as evidence of upstream lahars, based on the presence of the transition facies (Scott, 1988b). The record of ancient and modern flows at Mount Rainier confirms that most, if not all, of the significant hyperconcentrated flows there had such an origin. At most Cascade Range stratovolcanoes, the steep slopes and abundance of volcanoclastic sediment assure that any significant flood surge will bulk to debris flow.

FLOW MAGNITUDE AND FREQUENCY

METHODS OF STUDY

The distribution of past flows in time and space is an excellent guide to the probability and extent of future flows. This study amplifies the landmark work of Crandell (1971) by likewise focusing on lahars formed during postglacial time at Mount Rainier. Older lahars, however extensive (lahar deposit along lower Cowlitz River; Bethel, 1981), are not included because of their possible disturbance by, and potential confusion with, extensive glacial deposits. (See Dethier and Bethel, 1981.) Also, not only is the record of older lahars probably incomplete, but the conditions of their formation probably differed from present conditions.

Certain flow deposits that are distinctive and correlative over significant distances are named informally in accordance with the North American Stratigraphic Code for key or marker beds (North American Commission on Stratigraphic Nomenclature, 1983). Crandell's (1971) nomenclature is retained for the units he recognized. Given the textural differences in lahar and lahar-runout facies (Scott, 1988b, fig. 10), the older flow units are dated and correlated based on tephra units, radiocarbon dating, soil formation, and clast characteristics. Table 1 summarizes the prominent tephra units and other major postglacial volcanic events at Mount Rainier.

The dynamics of flows are integral to any discussion of flow behavior and hazards. Original flow-wave volumes are estimated from deposit volumes as discussed for specific flows. Ancient flow discharges are determined from flow velocities, as calculated from paleohydrologic techniques using vertical runup or superelevation around bends (see Costa, 1984, p. 304-305; Johnson, 1984, p. 305-309), and from cross-sectional areas derived from levels of flow deposits on valley-side slopes. Recently, discharges calculated using superelevation around bends were called into question by Webb and others (1989, p. 22, table 10), who noted large differences in cross-sectional areas calculated for flows in straight and curved reaches. We believe such discrepancies result because flow surfaces, particularly in very sharp bends, become markedly concave, as is well shown in photographs of 1990 debris flows at Jiangjia Ravine in Yunnan Province, China, by R.J. Janda and K.M. Scott (U.S. Geological Survey). Most cross sections at Mount Rainier (pl. 1) are not from comparably sharp bends, but the observation of Webb and others still stands as a cautionary note for any discharge calculated from a section in a bend (such as section T-1, pl. 1).

Post-flow valley erosion is generally small and, in dealing with flow depths of many tens of meters, is generally not more than several percent of the flow cross-section. The

Table 1. Tephra units and other indications of volcanic activity at Mount Rainier.

[Most data from Mullineaux (1974, 1986) and Crandell (1971). All events originated at Mount Rainier unless otherwise indicated]

Tephra set or layer, or other volcanic event	Age ¹	Remarks
Probable geothermal melting of South Tahoma Glacier...	Late 1960's	See Crandell (1971, p. 62).
Tephra from summit cone (layer X).....	Mid-19th century	
Set W (mainly layer W _n)	A.D. 1480 (layer W _n)	From Mount St. Helens. Dated by Yamaguchi (1983).
Pyroclastic surge	1,080	Identified locally on east side by R.P. Hoblitt, U.S. Geological Survey.
Lava flows forming summit cone.....	Post-layer C, pre-set W	Age estimated as from 2,100 to 1,200 absolute years by Crandell (1971, p. 14).
Layer C.....	2,200	
Block-and-ash flow in Puyallup River valley.	2,350	
Set P.....	2,500-3,000	From Mount St. Helens.
Set Y (mainly layer Y _n)	3,400 (layer Y _n)	From Mount St. Helens. Most prominent tephra deposit. Only layer common throughout Park.
Layer B.....	4,500	
Layer H.....	4,700	
Layer F (possible blast in part).....	5,000	See Mullineaux (1974, p. 19-20).
Bomb-bearing flows in White River valley.	5,700-6,600	See Crandell (1971, p. 23).
Layer S (possible blast).....	5,200	See Mullineaux (1974, p. 20). Also interpreted as possible blast by David Frank and Harry Glicken, U.S. Geological Survey, written commun., 1987.
Layers N, D, L, A.....	5,500-6,500	
Layer O.....	6,800	From Mount Mazama (Crater Lake). Latest data by Bacon (1983).
Layer R.....	>8,750	

¹Years before 1950 in radiocarbon years, except as otherwise indicated.

dated tephra layers (table 1) define the levels of valley bottoms at successive postglacial intervals, as well as the erosion of valley-side slopes through time. Cycles of aggradation and degradation related to Neoglacial advances and retreats are critical only in defining the cross-sectional areas of the relatively small glacial-outburst flows. In general, the accuracy of discharges determined with these techniques, proportional to the size of the flows, compares with that of other indirect-discharge determinations.

Some velocity measurements determined from runup and superelevation are suspect, however, because the techniques are unverified for debris flows and because of some locally high values (Costa, 1984), especially those above 30 m/s. Some high values measured for 1980 flows at Mount St. Helens (Fairchild, 1985; Pierson, 1985; Scott, 1988b) resulted from the lateral momentum provided by catastrophic ejection of wet debris that settled and flowed as a lahar. The most relevant velocities in this study are those determined near the points where flows left the confined valleys of the Cascade Range and inundated the Puget Sound lowland.

Some aspects of flow rheology can be inferred from texture and fabric comparisons with modern flows (Scott, 1988b). The texture of the deposits is determined from a combination of field measurements of the *b* axes of gravel-size (>2 mm) particles at a level or in a grid-defined area (Wolman, 1954), and laboratory measurements of the sand, silt, and clay fractions by sieve and pipet. This combination of techniques is statistically valid (Kellerhals

and Bray, 1971), and a technique for combining the two is described by Scott (1988b). The approach thus incorporates the complete spectrum of sizes in the deposit, whereas the size analyses of lahars reported in Crandell (1971) do not include sediment in the coarse cobble and boulder-size ranges. Crandell's approach could result in a reported clay content, for example, of twice the actual clay content for a lahar that contains 50 percent coarse cobbles and boulders. Differences in results were assessed by comparing his analyses with field counts of the coarser fractions at many localities. The analyses reported by Crandell (1971) are useful in showing the relative but not the absolute differences in clay content. The grain-size measures reported here are graphically determined, following the method of Folk (1980).

FLOWS OF HIGH MAGNITUDE AND LOW FREQUENCY (500 TO 1,000 YEARS)

Most of the lahars in this category originated directly from the large debris avalanches known as sector collapses (fig. 4). The major flows are listed in table 2, along with smaller flows of the same general origin. Many of the deposits were recognized and named by Crandell (1971). Size distribution measurements show that most are the deposits of cohesive debris flows, containing at least 3 to 5 percent clay. Consequently, most of the flows did not transform as they flowed downvalley for long distances.

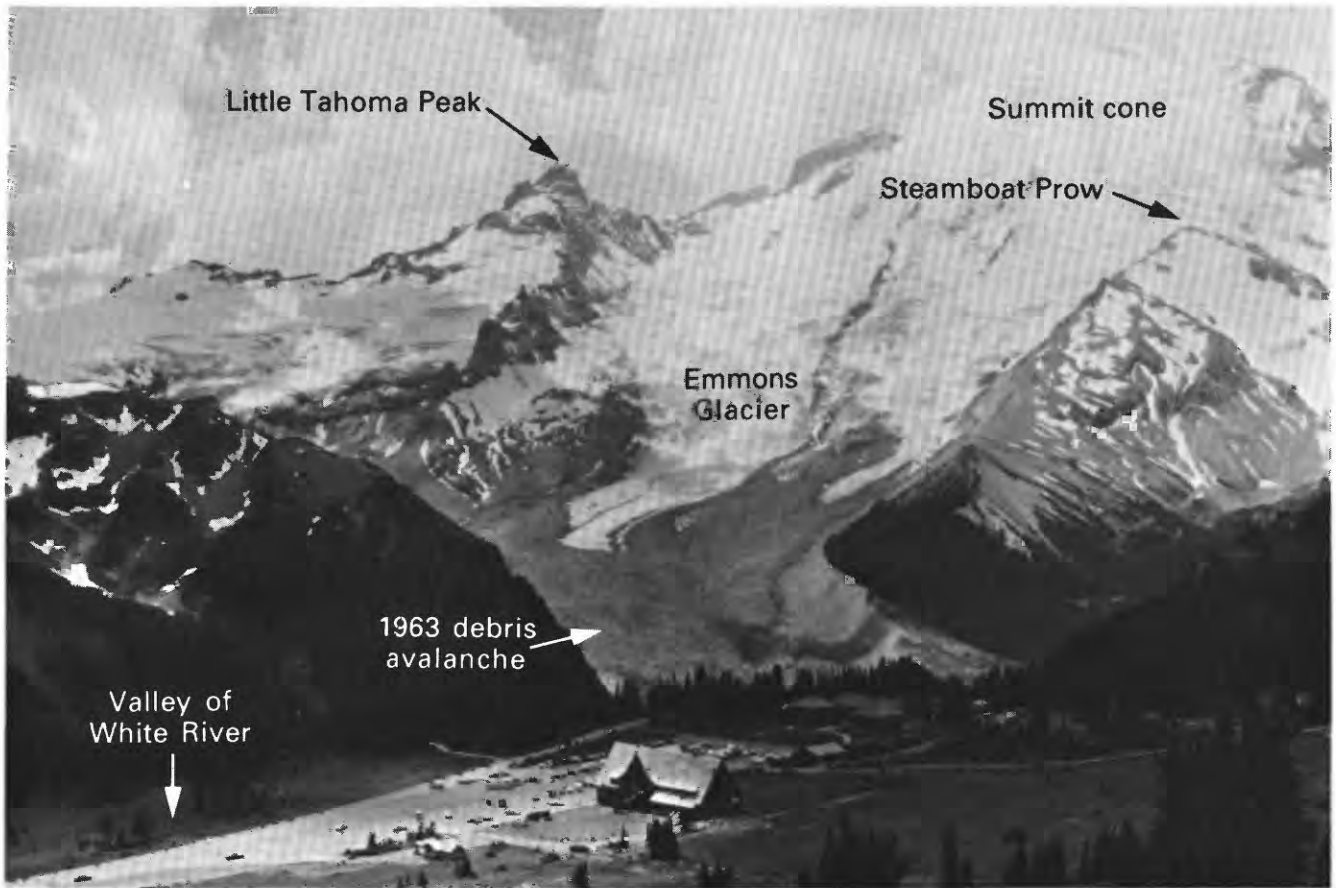


Figure 4. View of northeast side of Mount Rainier (right) and Little Tahoma Peak (left center). Note large embayment, now partly filled by the snow-clad summit crater, which yielded the sector collapse that formed the Osceola Mudflow. The flow diverged across Steamboat Prow, the apex of the partly barren triangle of rock at the right side of the photograph, into the main fork of the White River (center), now the site of the Emmons Glacier, and northward into the West Fork White River (to right of photo). Dark rubble on surface of the lower part of the Emmons Glacier is from the 1963 debris avalanche originating from Little Tahoma Peak.

Some do not correlate with known episodes of volcanic activity (table 1), which has implications for hazards planning, as discussed later in the report.

As noted above, Crandell (1971) concluded that the critical clay content defining flows of avalanche origin is approximately 5 percent, whereas Scott (1988b) found that the clay content defining this origin at Mount St. Helens, as well as the limit below which the flow behavior was noncohesive, is close to 3 percent. However, this difference results largely from differences in sampling and analysis procedures. Therefore, rather than modify Crandell's data, we describe the critical limit here generally as 3 to 5 percent. Probably no absolute limit exists, but the actual separation of behavior types at both Mounts Rainier and St. Helens correlates best with a clay content of about 3 percent. The observed behavior-limiting clay content will vary, depending on overall size distribution and clay mineralogy as well as analytical technique. Field "pebble counts" can be strongly influenced by the presence of a few large clasts, and

the results of laboratory analyses of cohesive deposits are extremely sensitive to technique.

An interesting correlation exists between flow volume, and thus avalanche volume, and the clay content of the resulting lahars. The larger the flow, the greater the clay content (fig. 5). The implication is that the larger the flow, the greater the penetration of the collapse into the hydrothermally altered core of Mount Rainier. Hydrothermal alteration and, consequently, clay content logically increase toward the center of the volcanic edifice. Clay mineralogy supports this conclusion (Frank, 1985, p. 144-145). Near-surface clay-rich areas can yield small cohesive flows, such as the modern debris avalanche on the Tahoma Glacier (Crandell, 1971, p. 17); that flow (of relatively small volume) would be an exception if plotted on figure 5. A practical use of the overall relation is that in a downstream sequence of Mount Rainier lahars, those with the highest clay content tentatively can be inferred to have been the largest. Much of the scatter in figure 5 is caused by

Table 2. Mainly cohesive debris flows of sector-collapse or avalanche origin at Mount Rainier.[Ranges in clay content include data from Crandell (1971). Leaders (- - -) indicate data unknown; km³ = cubic kilometers]

Flow	Clay (percent)	Age ¹	Drainage	Volume (km ³)	Extent
Broadly peaked flows that traveled a significant distance from the volcano					
Central part of Tahoma Lahar	3-4	Post-set W	Tahoma Creek; Nisqually River.	<0.15	Probably to Elbe.
Electron Mudflow	6-11	530-550	Puyallup River	0.26	Puget Sound lowland.
1,000-yr-old lahar	5-12	1,050-1,000	Puyallup River	Possibly >0.30	At least to Mowich River; possibly to Puget Sound lowland.
Unnamed lahar (possibly same as Round Pass Mudflow).	4-5	Same as below?	Puyallup River	- - -	Puget Sound lowland.
Round Pass Mudflow (main part).	4-5	2,170-2,710	Puyallup River	- - -	Puget Sound lowland.
Osceola Mudflow (probably includes Greenwater Lahar).	2-15	4,500-5,000	White River (main fork and West Fork).	3	Puget Sound lowland.
Greenwater Lahar (probably part of Osceola Mudflow).	< 3	- - -	Main fork White River	- - -	Puget Sound lowland.
More sharply peaked flows that attenuated rapidly on or beyond the volcano					
Lahar from main avalanche from Little Tahoma Peak.	< 2-4	A.D. 1963	White River	² 0.01	White River Campground.
Avalanche on Tahoma Glacier (small derivative debris flow).	- - -	³ A.D. 1910-1927	Puyallup River	⁴ 0.01	Below glacier terminus.
Round Pass Mudflow (part in Tahoma Creek).	2-8	2,610-2,790	Tahoma Creek; Nisqually River.	<0.1	Unrecognized below Tahoma Creek.
Pre-Y lahar at Round Pass	⁵ >3	>3,400	Puyallup River; Tahoma Creek.	- - -	Unknown.
Paradise Lahar (probably synchro- nous with Osceola Mudflow).	1-6	4,500-5,000	Paradise River; Nisqually River.	³ ~0.1	At least to National.

¹ Years before 1950 in radiocarbon years, except as otherwise indicated.² Avalanche volume, from Crandell and Fahnstock (1965).³ Slightly modified from Crandell's (1971) estimate of 1910-1930.⁴ Avalanche volume.⁵ Estimated.

the effects of scattered large clasts on the size distributions; clay content of only the matrix of each flow is more uniform.

In the following sections the flows relevant to hazard analysis are discussed in stratigraphic order of their deposits from oldest to youngest. The focus in each case is on aspects that are critical to analyzing risk: flow behavior, dynamics, and age. (Age is relevant chiefly for what it reveals about flow frequency.) Details of stratigraphy and exposure localities are not given here unless they have been changed or reinterpreted from Crandell (1971) on the basis of new exposures.

GREENWATER LAHAR AND OSCEOLA MUDFLOW

The Greenwater Lahar was described by Crandell (1971) as a hummocky, relatively low-clay lahar that filled the White River valley to levels not surpassed at most locations by the subsequent, high-clay Osceola Mudflow (pl. 1). Backwater deposits of the Greenwater Lahar form mounds in many tributary valleys in the river system as

mapped by Crandell (1971, fig. 6), and were described as undifferentiated lahar deposits by Frizzell and others (1984). The mounds are the surface expression of blocks of the volcanic edifice that were grounded or stranded in backwater areas. The unit has been interpreted as a debris avalanche (Siebert, 1984; Siebert and others, 1987). According to Crandell (1971), the Greenwater Lahar is overlain by the Osceola Mudflow and is differentiated from it by surficial mounds and a lower clay content of the matrix.

A deposit typical of the Greenwater Lahar contains 3 percent clay, without megaclasts included in the size distribution. Mean grain size (M_z of Folk, 1980) is -1.7ϕ (3.2 mm), sorting (σ_G of Folk, 1980) is 5.1ϕ , and skewness (Sk_G of Folk, 1980) is $+0.04$. The matrix of the Osceola is remarkably clayey; the composite deposit (matrix and coarse phases excluding megaclasts) contains 2 to 15 percent clay, with a mean of 7 percent (13 samples). Mean grain size is -0.3 to -5.7ϕ (1.2 to 51.0 mm), sorting is 4.6 to 6.2 ϕ , and skewness is -0.05 to $+0.48$, with all but one value positive, indicating the excess of fine material typical of lahars. Longitudinal change in size distribution is variable,

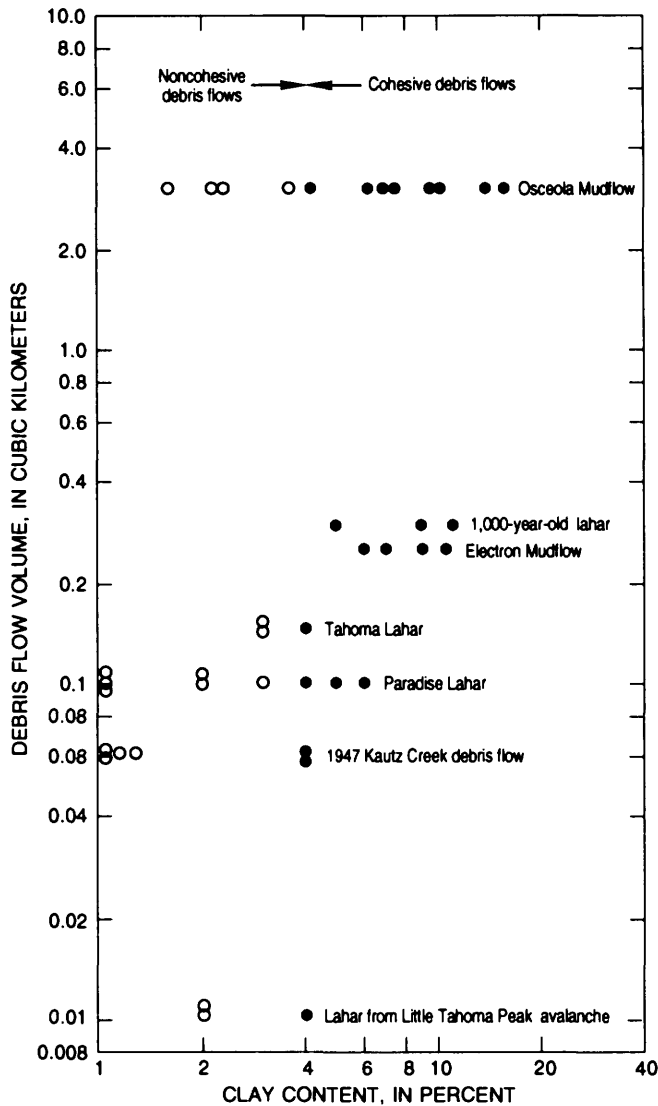


Figure 5. Flow volume versus clay content in several postglacial debris flows at Mount Rainier.

but a general downstream increase in mean grain size probably is the result of bulking of bed and bank materials coarser than clay, and from which the clay had largely been removed by hydraulic (or selective) sorting.

Four radiocarbon dates reported from the Osceola Mudflow by Crandell (1971) range from $4,700 \pm 250$ to $5,040 \pm 150$ radiocarbon years. Materials collected by us yield ages of $4,455 \pm 355$, $4,980 \pm 200$, and an older, age-limiting date of $5,230 \pm 235$ radiocarbon years. The locations and implications of the younger dates are discussed below; the older date is from charcoal fragments above layer O but at the base of two pre-Osceola lahars near Buck Creek (fig. 6A). Those two flows probably are part of the pre-Osceola lahar assemblage described by Crandell (1971, p. 23) from upstream exposures, mainly on the south valley bank of the White River near Fryingpan Creek. Charcoal

fragments from a third, older lahar, which is also near Buck Creek and is stratigraphically above layer O and below the Osceola, were $6,075 \pm 320$ radiocarbon years in age. Both of the dated pre-Osceola deposits are noncohesive; the youngest pre-Osceola deposit is cohesive. Pre-Osceola lahars are also present in the valley of the West Fork White River (fig. 6C).

A new interpretation of the Greenwater Lahar and Osceola Mudflow in the White River system is suggested, largely based on new exposures, especially those near the confluence of Huckleberry Creek with the White River. Much of what is mapped as the Greenwater Lahar (Crandell, 1971, fig. 6) may be a peak-flow facies of the Osceola Mudflow with a high megaclast concentration, as inferred from the following evidence: the deposits of both lahars are present at the same level at several localities, such as Crandell's cross section A-A' near Buck Creek (Crandell, 1971, pl. 2), but, at the localities where the base of the younger Osceola Mudflow is exposed, it most commonly overlies lahar-runout deposits and Pleistocene glacial drift rather than Greenwater deposits. If the Greenwater Lahar is a separate unit, much time must have elapsed for it to have been so extensively eroded before occurrence of the Osceola Mudflow. A cohesive lahar locally underlies the Osceola near Buck Creek and at a locality near the confluence with the West Fork White River where there is no evidence of a significant time break between the two lahars.

Two terraces north of the Mud Mountain Reservoir, near the point of discharge to the Puget Sound lowland, are underlain by a mounded lahar. Moreover, 90 percent of the mounds, which are as much as 15 m high and 60 m across, have cores composed of Mount Rainier rocks, indicating an origin from the slopes of the volcano. Less than 1 km upstream along Scatter Creek, a small tributary of the White River on the north side of the Mud Mountain Reservoir, the Osceola and underlying Pleistocene drift crop out nearly continuously without an intervening Greenwater equivalent, indicating that the mounded deposits downstream are Osceola rather than Greenwater. We infer that Osceola megaclasts were grounded here and formed mounds as peak discharge passed downstream, allowing the more fluid matrix to drain away. Other mound-bearing deposits along the West Fork of the White River must be Osceola because the Greenwater Lahar is thought to have flowed down only the main fork of the White River (Crandell, 1971, fig. 6). Two levels of mounded deposits downstream from the confluence of the west and main forks of the White River are explained by pre-existing topography or by slightly different arrival times of the peak from each fork at the confluence.

The textural difference between Greenwater and Osceola deposits corresponds to that between the lateral mound-bearing deposits and the clay-rich valley deposits of the Osceola into which the White River is incised. If these are deposits of the same flow, the textural variation is explained by figure 5. The clay-rich valley deposits

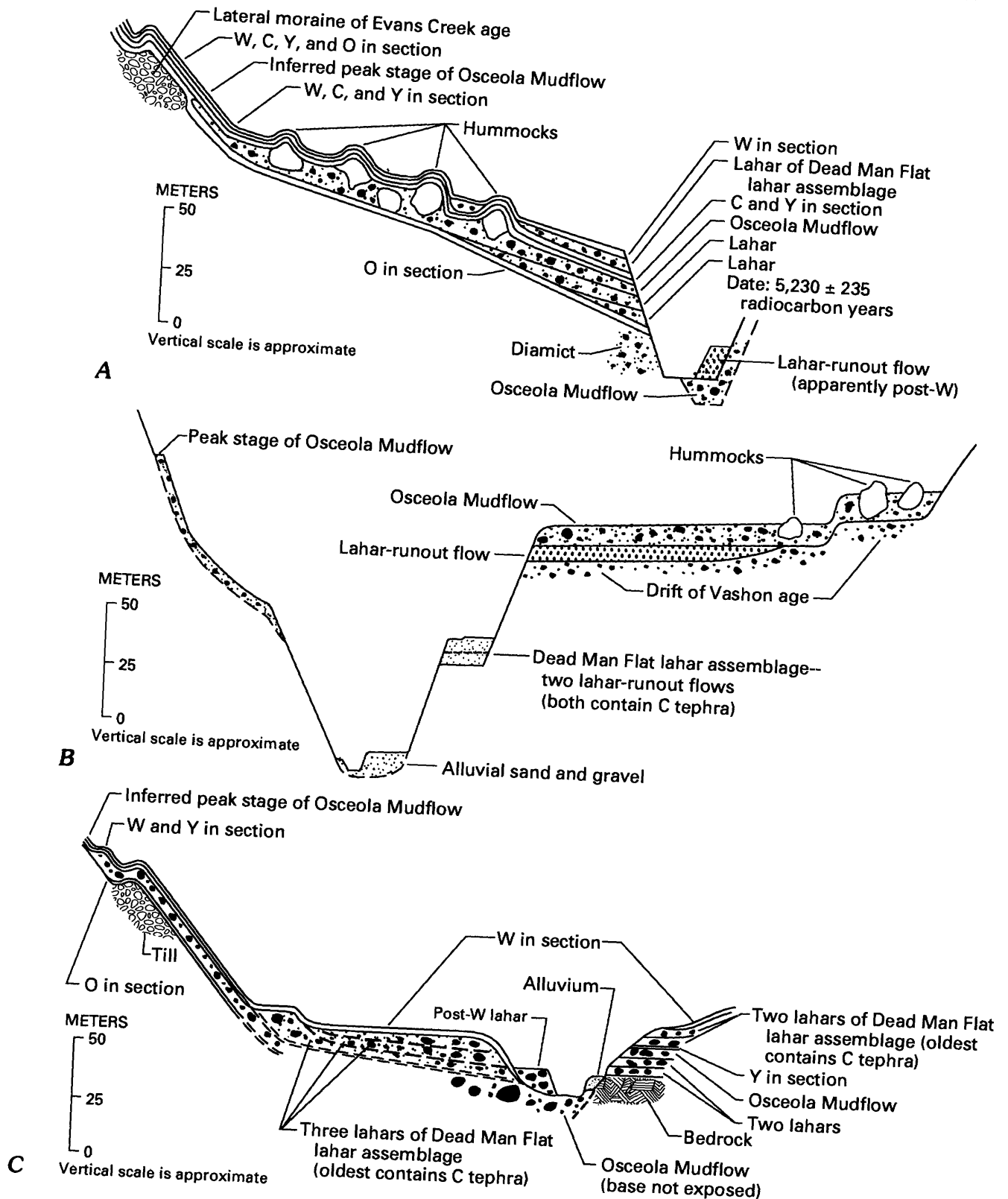
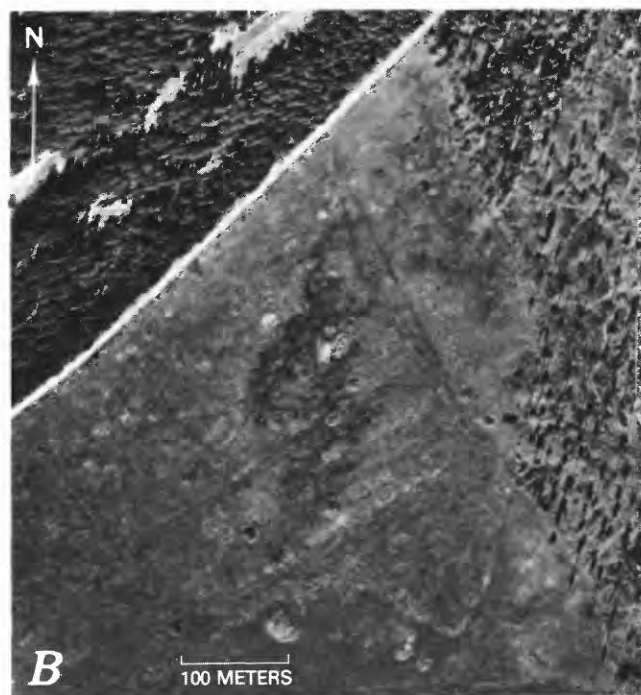


Figure 6. Diagrammatic composite sequence of valley-fill deposits in the White River valley (successive downstream sections). Vertical scale is shown to indicate approximate thicknesses. Horizontal scale is variable for better portrayal of stratigraphic relationships and is not shown. However, vertical exaggeration ranges approximately between 5x and 10x. *A*, White River between Buck and Huckleberry Creeks. *B*, White River at Mud Mountain Reservoir. *C*, West Fork White River between 25 km from Mount Rainier and confluence with main fork of White River.



Figure 7. Mound-studded surface of the Osceola Mudflow in the embayment formed by the tributary valley of Huckleberry Creek. *A*, View upstream across the cleared surface of the deposit. Note the gentle slope of the lateral deposit toward the White River, behind and to the left of the photographer. Largest mound visible, left of center, is approximately 3 m high. *B*, Aerial view of part of same area on April 20, 1982. Note that some masses that are possible megaclasts are not topographic mounds.



represent a late stage of flow, assuming the normal behavior of a lahar flood wave. Thus, these deposits were probably derived from fluidization of a deeper and more altered, clay-rich part of the volcano. This hypothesis is, in essence, not greatly different from the sequence of two flows proposed by Crandell (1971, p. 23) in which the first (Greenwater), formed from relatively unaltered surficial rock, exposed the underlying, altered part of the edifice for the sector collapse that produced the second (Osceola). Separate peaks in the same huge flow are possible, as in the sequence of slide blocks that produced the 1980 debris avalanche at Mount St. Helens (Glicken, 1986), but would yield deposits revealing their separation in time, however brief.

At the confluence of the White River and Huckleberry Creek, almost the entire backwater fill of mounded material, mapped as the Greenwater Lahar (Crandell, 1971, fig. 6), has been cleared of vegetation (fig. 7A). Aerial photographs of the clearing (fig. 7B) show, in addition to topographic mounds, abundant ghost-like shapes, some of which we interpret as disintegrated megaclasts. The disaggregation of blocks of relatively unaltered material, both during flow and after deposition, may partially explain the mounded, relatively low-clay backwater deposits and thus their contrast with the clay-rich deposits in the central valley. In addition, size analysis of material between megaclasts in an

extreme backwater position shows a prominent mode in the sand range, as in a typical noncohesive lahar, and it is likely that some of this sand originated by bulking during passage of the locally erosive peak of the flow. Calculation of the overall proportion of eroded sediment in the deposits at this point, by means of the lahar-bulking factor (LBF), shows that material derived by bulking of stream and valley sediment makes up at least 20 percent more of the sediment (excluding megaclasts) in the mounded deposit near the lateral margin than in the cohesive central-valley deposits. Our preferred hypothesis thus is that these two types of deposits (noncohesive with abundant megaclasts and

cohesive with fewer megaclasts) are facies resulting from a single large flow wave.

Also at Huckleberry Creek, newly exposed Osceola Mudflow deposits overlie a thick glaciofluvial section in a gravel pit within 180 m of the nearest mound that, along with many others, protrudes from a level identical with the surface of the Osceola Mudflow. Wood from the basal 50 cm of a 3.1-meter section of the Osceola Mudflow at the quarry yields the date of $4,455 \pm 310$ radiocarbon years, evidence that the deposit is not of pre-Osceola age (table 2). Wood from the upper meter of the quarry section yields the date of $4,980 \pm 200$ radiocarbon years, a date likewise conformable with an age of 4,500 to 5,000 radiocarbon years for the Osceola. Excavation of the mound nearest the quarry to a depth greater than 4 m shows it to be enclosed by typical deposits of the Osceola Mudflow. The existence of two flows or two separate peaks requires, therefore, the unlikely coincidence that mounded deposits of the Osceola filled the valley to exactly the same level as did mounded deposits of the Greenwater Lahar. The lateral, but not central or distal presence of the mounds is explained both by megaclast disintegration during flow, and by the similarity of a debris flow path to the path of a tractor tread: "The coarsest clasts remain in the front and are deposited along the sides of the moving flow, but the finer debris is recycled * * *," continuing downstream because "* * * debris at the center and top of a channel moves faster than debris along the sides and bottom * * *" (Johnson, 1984, p. 287).

This interpretation does not change Crandell's interpretations of the volume of the Osceola or of its distribution underlying the Puget Sound lowland. It does indicate, however, that mounds are not diagnostic of a debris avalanche in the Cascade Range. The other two notably mounded deposits, the 1980 rockslide-debris avalanche deposit at Mount St. Helens (Glicken, 1986) and the huge hummocky landslide north of Mount Shasta (Crandell and others, 1984; Crandell, 1988), are both debris avalanches. Overall, the mound-bearing deposits in the White River system, be they Osceola or two separate flows, are best characterized as those of a lahar. The fill of backwater areas with muddy, horizontally surfaced deposits (excluding the mounds) indicates fluidity and strength in the range typical of lahars. The flow originated by collapse of a hydrothermally altered, water-rich edifice. The contrast between the presumed Greenwater deposits, with the hummocky surfaces of a debris avalanche, and the Osceola Mudflow deposits is the contrast between relatively clay-poor sources with less water, and clay-rich sources with more water. The deposits represent, respectively, the initial part of the flow wave (the "Greenwater Lahar"), composed of surficial, relatively unaltered rocks, followed by flow derived from highly altered, deep-seated materials (the Osceola Mudflow). The Round Pass Mudflow, Electron Mudflow, and Tahoma Lahar, described below, also contain megaclasts expressed as mounds in lateral facies. Each of

these, like the Osceola, is a lahar inferred to have formed by mobilization of a debris avalanche.

The Osceola Mudflow contains weak megaclasts of unconsolidated, stratified gravel, sand, and silt that represent flood-plain deposits. Some such megaclasts were rotated from the horizontal; others were deformed. To document the proportion of eroded and disaggregated flood-plain sediment in the flow, we calculated the lahar-bulking factor from clast roundness, and we also compared the roundness and lithology of various clasts. The combination of LBF and rock type yields estimates of the proportion of material derived from the volcano, from valley-side slopes, and from the flood plain and channel.

The results for all or part of the size range of -3.0 to -5.0ϕ (8 to 32 mm) (fig. 8) indicate that bulking was substantial and progressive, but slightly less than indicated by the composition analysis of Glicken and Schultz (1980). This general degree of bulking is probably applicable to most of the gravel-size sediment (-1.0ϕ and coarser; 2.0 mm and coarser). Lesser but substantial amounts of bulking probably occurred in the sand (4.0 to -1.0ϕ ; 0.0625 to 2.0 mm) and silt (8.0 to 4.0ϕ ; 0.004 to 0.0625 mm) size ranges. Bulking did not add to the already high clay content of the flow; the bed material and channel deposits that compose most flood-plain sediment generally contain less than 1 percent clay. Variations in clast roundness with composition indicate substantial bulking from steep valley sides between the volcano and Greenwater, a distance of about 40 km. Farther downstream, the same comparisons indicate the increasing incorporation of more highly rounded valley-bottom sediment, especially on the drift plain of the Puget Sound lowland. The roundness of Mount Rainier rock types downstream indicates the incorporation of already rounded alluvial clasts. Bulking, although substantial, was not sufficient to increase the peak discharge of the lahar wave downstream. However, the flow volume obviously would have declined much more rapidly downstream had it not been for the effects of bulking, which accounted for at least 50 percent of sediment in the -3.0 to -5.0ϕ (8 to 32 mm) size range after 60 km of flow.

Clasts in the -3 to -5ϕ (8 to 32 mm) range with partially stream-rounded surfaces were examined for evidence of abrasion or breakage (cataclasis) during flow. Between 20 and 35 percent of the rounded clasts were broken, but only about half of these showed clear evidence that the breakage occurred during flow, rather than before or after. Coarse abrasion or grinding on clast faces was interpreted as the result of impacts with other particles during flow rather than glacial abrasion. Overall, cataclasis and grinding were nearly as abundant in the Osceola Mudflow as they were in the largest noncohesive lahar at Mount St. Helens (Scott, 1988a). This result occurred in spite of the probable cushioning effect of the more cohesive matrix in the clay-rich Osceola Mudflow.

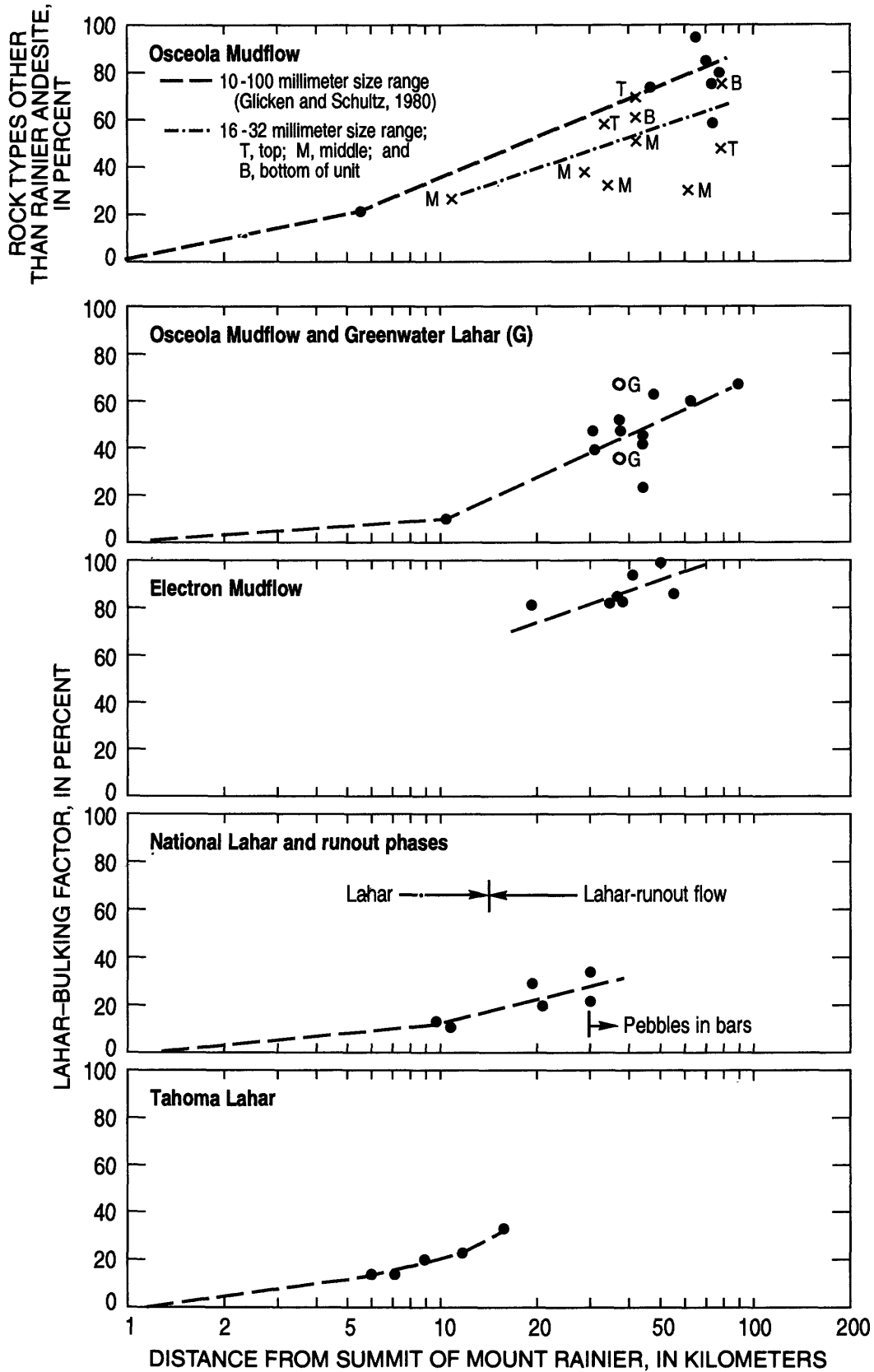


Figure 8. Lahar-bulking factors for four lahars at Mount Rainier, and composition changes in the Osceola Mudflow.

PARADISE LAHAR

An initially huge, mainly noncohesive lahar (fig. 5, table 2) originated on the upper flank of the volcano above Nisqually Glacier and overran Paradise Park, the subalpine meadow between the Nisqually and Paradise Rivers. This flow, the Paradise Lahar (Crandell, 1971), also spilled across the demarcating Mazama Ridge to enter the Cowlitz River system. Radiocarbon dates within the same range as those of the Osceola Mudflow (4,500 to 5,000 years) indicate that the Paradise Lahar probably reflects the same edifice collapse as the Osceola Mudflow. What was most unusual about the Paradise Lahar was that it attenuated rapidly and left only thin deposits, in spite of having reached depths of more than 300 m in canyons on the side of the volcano.

The Paradise Lahar contains from less than 1 to as much as 6 percent clay with an average of 2.5 percent (four new composite samples). Mean grain size ranges from 0.6 to -2.8ϕ (0.7 to 6.9 mm); sorting falls between 2.5 and 4.9 ϕ . Skewness is generally slightly positive, ranging between -0.03 and $+0.20$. Fine sediment is not as abundant as in more cohesive lahars like the Osceola.

The Paradise Lahar is noteworthy for several characteristics: (1) The size distributions are strongly influenced by the presence or absence of widely distributed, hydrothermally stained clasts, including large boulders 2 to 3 m in intermediate diameter, set in a thin (less than 1.0 m) layer. (2) Crandell's measurements (1971, p. 33) of very large flow depths on the flank of the volcano were substantiated; consequently, the ratio of deposit thickness to original flow depth is very low. (3) These flow depths declined rapidly downstream, and thus the rate of flow wave attenuation, as in the Round Pass Mudflow on Tahoma Creek, is uncommonly high. (4) The deposit is also remarkable for its occurrence directly above layer O, revealing its inability to erode this very thin layer (less than several centimeters) of fine-grained tephra and forest duff where flow depths were more than 100 m.

The above four features lead us to infer that the flow began, essentially as interpreted by Crandell (1971, p. 35, 36), as one or more huge avalanches. We interpret this as having been only a single avalanche, which had a degree of sudden, laterally directed momentum to create a sharply peaked flow wave in which the sediment was in part dispersed. Although these features could be explained by a large vertical drop (Crandell, 1971, p. 36), we infer that the Paradise Lahar is more likely to have been initiated by volcanic or phreatic explosive activity than the more broadly peaked flows originating as sector collapses. Such an origin also reconciles any difficulties in comparing the apparent flow volume and the volume of deposits (Crandell, 1971, p. 36). A similar explosive origin was proposed for some lahars originating with the 1980 lateral blast at Mount St. Helens (Major, 1984; Pierson, 1985; Scott, 1988b). The low clay

content of the Paradise Lahar may reflect loss of fines by the process of explosively induced sorting (Scott, 1988b) but could, of course, simply be evidence of formation from less altered, less clayey rock.

If the Paradise Lahar and Osceola Mudflow are the same age, their relations and origin are comparable to those of the 1980 lahars on the South Fork and North Fork Toutle Rivers, respectively (Scott, 1988b). In that case, a major sector collapse was associated with explosively initiated lahars in peripheral watersheds. The probable synchronicity of the Paradise Lahar with the Osceola Mudflow clearly suggests that both flows had a comparable explosive origin. Most likely, the Paradise Lahar resulted from concomitant failure of part of the rim of the crater formed by the sector collapse that produced the Osceola Mudflow.

The Paradise Lahar attained its maximum downstream depth of 240 m near the Ricksecker Point locality described by Crandell (1971, p. 36 and fig. 13), 1.2 km upstream from the confluence of the Nisqually and Paradise Rivers. Deposits at this locality contain charcoal yielding an age of $4,625 \pm 240$ radiocarbon years.

The depth of the Paradise Lahar declined rapidly downstream, but the flow was still at least 70 m deep near Longmire, where the deposit also overlies layer O, has only 1 percent clay, and is as much as 1.2 m thick. At that location, wood from just above layer O yields an age of $4,955 \pm 585$ radiocarbon years (fig. 9).

The Paradise Lahar is known to extend to Ashford (Crandell, 1971, plate 3), but it probably inundated the deeply incised flood plain of the Nisqually River beyond National. At least 1.0 m of a noncohesive lahar with hydrothermally stained clasts occurs below tephra set Y on the main valley floor at National (fig. 9); charcoal fragments in the upper part of the unit yield an age of $4,730 \pm 320$ radiocarbon years. This probable distal part of the Paradise Lahar is evidence of a flow volume near the upper limit of the range proposed by Crandell (1971, p. 36). Although the flow was generally noncohesive, a runout phase has not been identified, possibly because of the age of the flow and the consequent loss of the deposit by erosion or burial by later, post-set-Y aggradation.

No dates for the Paradise Lahar were reported by Crandell (1971) who noted, however, that the flow occurred between the times of tephra layers O and D, a range between about 6,800 and 6,000 radiocarbon years ago (table 1). The reason for the discrepancy with the three radiocarbon dates reported above was investigated. Interestingly, Crandell (1963a, p. 138; 1971, p. 35) originally thought the Paradise Lahar and Osceola Mudflow were the same age before the tephra evidence apparently negated the possibility. Our radiocarbon dates support Crandell's original inference; the new radiocarbon dates conform in near equivalence to the age of the Osceola, and conflict with the tephra evidence. One possible explanation for this conflict is that the

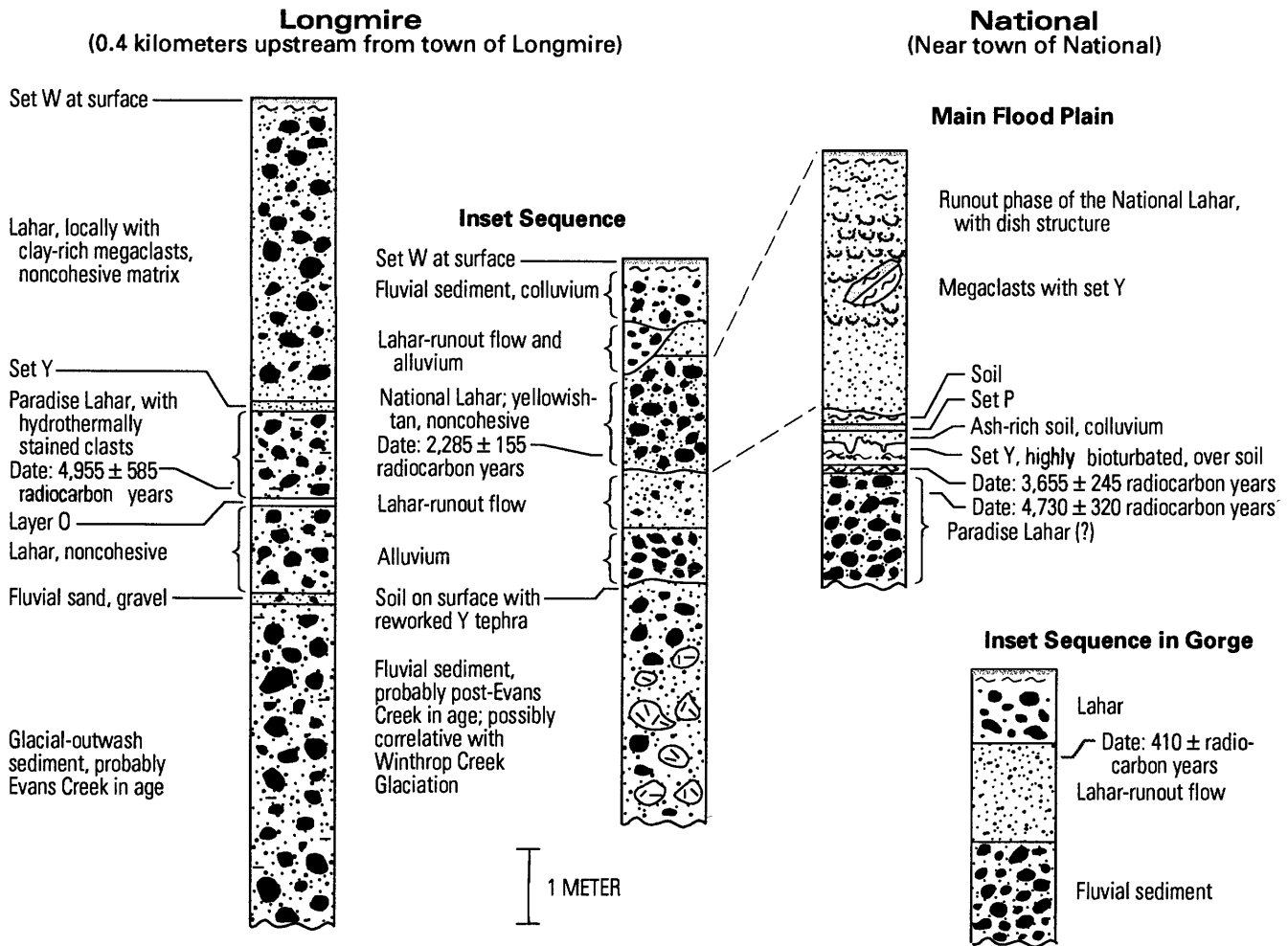


Figure 9. Composite columnar sections of lahars and associated deposits at Longmire and National in the upper Nisqually River drainage.

“Paradise Lahar” deposit on which Crandell based his tephra stratigraphy may actually be a nearly identical but somewhat older flow. He reports (1971, p. 33) a thin Paradise Lahar deposit underlying layer D on the east side of Paradise Valley near Sluiskin Falls. The tephra there confirm an older age, as does a date of $6,950 \pm 355$ radiocarbon years obtained by us from wood collected from the lahar at the site. Thus, the main Paradise Lahar is, as originally surmised by Crandell, close to or synchronous in age with the Osceola, and the tephra correctly date an older, smaller lahar near Sluiskin Falls.

ROUND PASS MUDFLOW (BRANCH ON TAHOMA CREEK)

A large lahar is exposed at Round Pass from which flow diverged into both the Puyallup and Nisqually River drainages, the latter by way of Tahoma Creek (fig. 1B). Crandell (1971) showed that the branch on Tahoma Creek attenuated rapidly, is post-set Y in age, and has a radiocarbon age of $2,610 \pm 350$ years. A date obtained by us from

wood in valley-bottom deposits was $2,790 \pm 130$ radiocarbon years.

The texture is highly variable at the three main exposures, ranging from cohesive to noncohesive as follows: Round Pass, 2–8 percent clay; valley bottom, unit 3 of Crandell’s section 9, 3–5 percent; and Indian Henrys Hunting Ground, 3 percent. Mean grain size is between $+0.5$ and -3.5ϕ (0.7 to 11.0 mm); sorting ranges from 3.5 to 5.0 ϕ (five samples). Skewness is not uniform in direction, varying between -0.10 and $+0.18$.

Rounded clasts, especially in the coarse fractions, characterize the unit at the type locality. A partial but less-than-satisfactory explanation is that valleys on both sides of Round Pass were filled with outwash gravel or debris-rich glacial ice to a higher level than they are now, and thus that the lahar was shallower than the present topography would suggest. In this event the lahar could have transported entrained material to the height of Round Pass. An early Neoglacial advance culminated in the time interval of 2,600 to 2,800 years ago (Porter and Denton, 1967), and

a synchronous advance probably occurred at Mount Rainier (Crandell and Miller, 1974). However, the lahar contacted the modern valley bottom only 3 km away from Round Pass, and Crandell (U.S. Geological Survey, written commun., 1989) does not believe that the Neoglacial advance could have filled the valleys significantly near Round Pass. Some rounded material in the lahar may have come from Evans Creek Drift in the vicinity (Crandell, 1969, pl. 1), and some undoubtedly came from local deposits of outwash gravel, which were probably more extensive and abundant than they are now.

The most likely origin of the flow was as a debris avalanche from the Sunset Amphitheater mainly confined to the watershed of the South Puyallup River. The part spilling over into the Tahoma Creek valley, although possibly more than 300 m deep in the headwaters of Tahoma Creek, apparently attenuated rapidly and was a sharply peaked tributary of the flow, subsidiary to the main part that traveled a longer distance in the Puyallup River valley. The pattern of erosion of tephra set Y by the Round Pass Mudflow clearly reveals the dynamics of the flow and shows that Crandell's (1971, fig. 25) interpretation of rapid attenuation is the most likely explanation of its limited extent along Tahoma Creek. The unit's most distal exposure in that valley is 3 km upstream from the mouth of Tahoma Creek, where it supported a forest inundated by the younger Tahoma Lahar.

ROUND PASS MUDFLOW (BRANCH ON PUYALLUP RIVER)

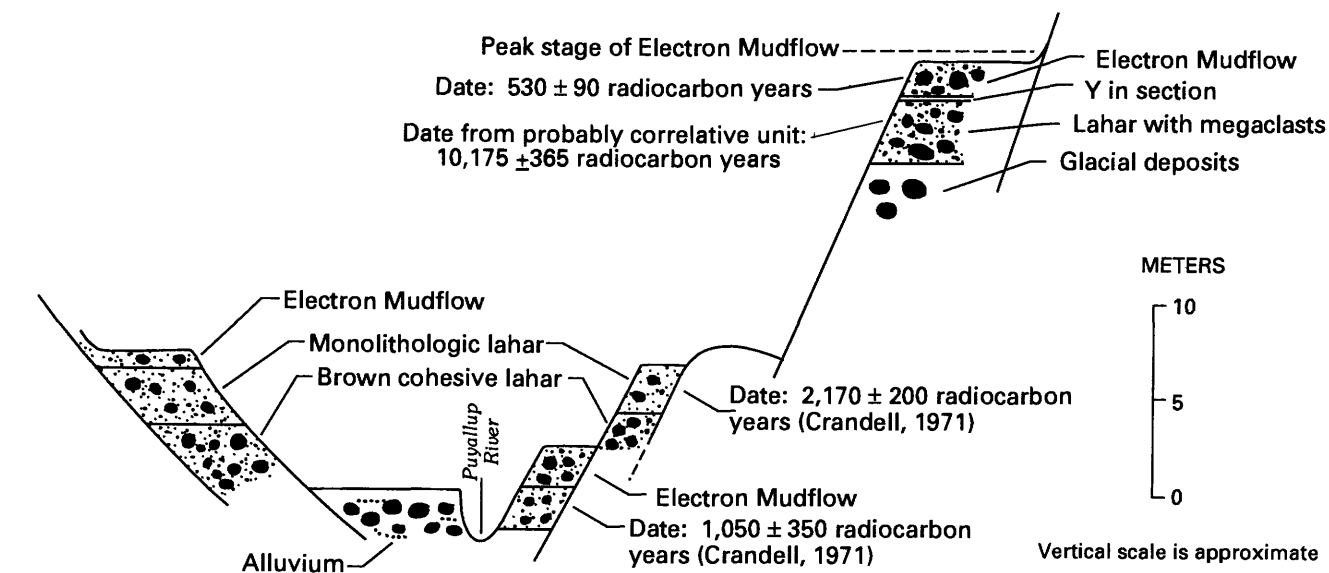
The behavior of the Round Pass mudflow in the Puyallup River system was substantially different from that of the sharply peaked tributary of the flow to the south. The initial flow was a broad lahar wave that probably reached the Puget Sound lowland. Ages of $2,710 \pm 250$ and $2,170 \pm 200$ radiocarbon years were obtained by Crandell (1971) from wood near the confluence with the Mowich River. A piece of wood collected by us at the same location yielded an age of $2,440 \pm 290$ radiocarbon years. The flow overran a forest 4.5 km upstream from the confluence of the North and South Puyallup Rivers, just outside the park boundary. The outermost 10 rings of a buried tree from that forest yielded an age of $2,600 \pm 155$ radiocarbon years. Three of the four dates are, therefore, consistent with the age of the tributary of the flow in the Tahoma Creek drainage.

Clay content is variable, as in the deposits along Tahoma Creek, but the Puyallup River deposits are mainly in the cohesive category if megaclasts are excluded from the size distributions. Two upstream samples contain 4 and 5 percent clay, and downstream the deposits become more cohesive. Mean grain size of the upstream samples is -1.6 and -1.3ϕ (3.0 and 2.4 mm), respectively, sorting is 4.2 and 4.9 ϕ , and skewness is slightly positive.

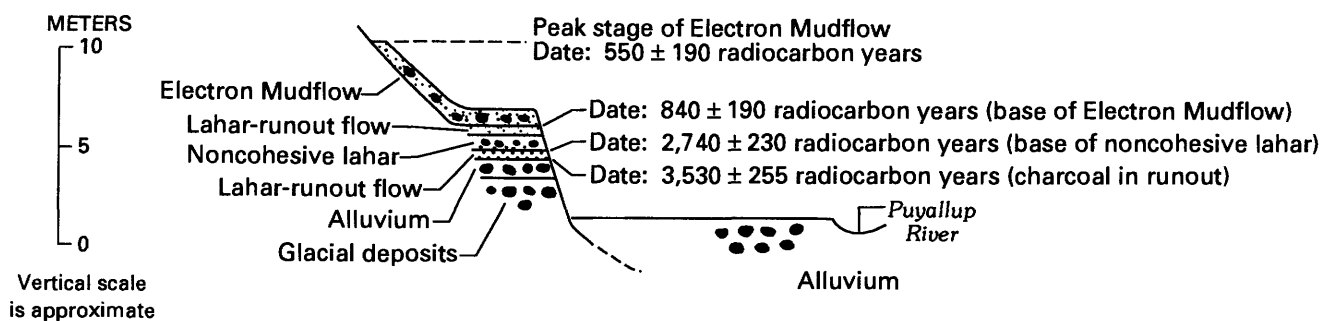
Where the unit is as much as 16 m thick near the confluence of the Mowich and Puyallup Rivers, large exposed megaclasts and the presence of many mounds farther upstream establish a slope-failure origin (as a debris avalanche) that is consistent with the generally cohesive downstream texture. That these mounded deposits probably are not those of an untransformed debris avalanche is indicated by their texture, both on Tahoma Creek and at the site of the buried forest mentioned above. At the latter locality the deposits between megaclasts have the character of a lahar, are generally cohesive in texture, and represent an upstream part of the flow distributed on the flank of the volcano as shown by Crandell (1971, fig. 25). The deposits in the upper Puyallup valley are more likely a mounded facies of a large lahar, similar in origin to the deposits mapped as the Greenwater Lahar.

Both flow depth and velocity were remarkable at the site of the buried forest near the park boundary. There the megaclast-bearing flow knocked down trees 240 m above the valley bottom on the south, outer side of a broad, northerly valley curve that begins upstream from Round Pass. The peak flow level is defined by a terrace with a mounded surface and a small, ephemeral lahar-margin lake. Estimates of minimum runup on lateral ridges strongly suggest a peak velocity of at least 40 m/s. Round Pass, only 3.0 km upstream from the buried forest, is 170 m above the valley bottom in a more confined reach; consequently, flow in the South Puyallup River valley was certainly deep enough to send a major tributary across Round Pass into Tahoma Creek as shown by Crandell (1971, fig. 25). Flow across divides farther upstream is even more likely. Concomitant with these findings is a probable hydraulic explanation of the high attenuation rate of the flow in the Tahoma Creek valley. Flow across the divides would have occurred only during the relatively brief passage of the peak of the high velocity flow, resulting in exactly the highly peaked, rapidly attenuating flow(s) recorded by the texturally variable deposits in Tahoma Creek valley.

A noncohesive lahar and lahar-runout deposit, which have bounding ages of 840 ± 190 and $2,740 \pm 230$ radiocarbon years, and an older runout deposit $3,530 \pm 255$ radiocarbon years in age, occur 6.0 km downstream from the boundary of the Puget Sound lowland (fig. 10B). The youngest two of the three units, described below, could be distal correlatives of the Round Pass Mudflow based on their ages. However, we believe that neither of the units is a likely correlative because of their noncohesive texture. A more probable origin was as meltwater surges resulting from volcanism as in the case of the younger two deposits exposed upstream, which formed near or following the time of the block-and-ash flow in the South Puyallup River valley. The deposit of the block-and-ash flow is noncohesive (with only 1 percent clay), and it is $2,350 \pm 250$ radiocarbon years old (Crandell, 1971). The Round Pass Mudflow probably extended to the Puget Sound lowland intact as a cohesive debris flow, untransformed to a hyperconcentrated runout.



A



B

Figure 10. Diagrammatic composite sequences of valley-fill deposits in the Puyallup River valley (successive downstream sections). Vertical scale is shown to indicate approximate thicknesses. Horizontal scale is variable for better portrayal of stratigraphic relationships and is not shown. However, vertical exaggeration ranges approximately between 5× and 10×. A, Puyallup River at Mowich River confluence. B, Puyallup River 6.0 km downstream from boundary of Puget Sound lowland.

UNNAMED PRE-ELECTRON DEPOSITS, PUYALLUP RIVER SYSTEM

The oldest postglacial lahar recognized during this study occurs above glacial drift and below set Y in the Puyallup River system (fig. 10A). The gray, generally noncohesive unit contains wood yielding an age of 10,175±365 radiocarbon years. Because tephra layers show that the valley configuration did not change greatly in postglacial time, the height to which the deposit extends above the present channel, about 100 m near the Mowich River confluence, indicates the flow was large.

Deposits of brown or gray cohesive diamicts of uncertain age and origin occur locally in the Puyallup River system (fig. 10A). Some exposures probably are of a non-megaclast-bearing facies of the Round Pass Mudflow;

others are pre-Y in age, and their correlation is not certain. In any case, the units record at least one cohesive pre-Y, postglacial lahar that attained levels approaching, but below, the peak stage of the younger Electron Mudflow. South of the Mowich-Puyallup confluence (fig. 10A), a brown cohesive diamict underlies a strikingly monolithologic and noncohesive debris flow deposit consisting of clasts of black vitric Rainier andesite. However, at the upstream site of the buried forest, a megaclast of an identical deposit is incorporated in the Round Pass Mudflow, the identification of which is verified by a nearby radiocarbon date. Thus, the brown unit below the black lahar near the confluence is probably not the Round Pass Mudflow but is most likely a pre-Y lahar.

The monolithologic lahar reaches at least 43 m above the valley bottom near the Mowich River confluence. The

lahar is granular and resembles a lithic pyroclastic flow, but it is distinct from the deposit of the block-and-ash flow exposed on the volcano (table 1). The unit very likely represents the cooled downstream continuation of such a flow, and it is closely similar to a pre-Osceola unit in the White River valley. The flow was probably larger than that producing the block-and-ash flow deposit seen on the volcano; that unit has not been traced downstream with certainty, although a granular, lithologically similar lahar with a pronounced content of prismatic jointed clasts is locally present beneath the Electron Mudflow in low, channel-bank exposures.

A large noncohesive lahar, untransformed to a runout phase, is recorded by deposits on the Puget Sound lowland in the Puyallup River system (table 3, fig. 10B). The age of the unit and its probable lack of correlation with the Round Pass Mudflow are discussed above in the section on the Round Pass Mudflow (Puyallup River branch). The lahar, which has an approximately 20-cm-thick, Type I sole layer (sandy, without a dispersed coarse phase), has inverse and normal grading identical to that of many granular lahars at Mount St. Helens (Scott, 1988b). The unit crops out at a level at least 6 m above the present river, 0.1 km upstream from the valley constriction at the first bridge upstream from Orting, and 6.0 km downstream from the lowland boundary. Clasts in the coarse mode are no larger than pebbles in size. The loss of coarser gravel and a locally intact framework indicate that transformation occurred not far downstream. Runout sands underlie and overlie the unit. The lack of weathering during the hiatus between the flows indicates that little time separated the lahar and the overlying runout deposit.

1,000-YEAR-OLD LAHAR

This clayey lahar extends down the Puyallup River system at least as far as a point 1.6 km below the mouth of the Mowich River (Crandell, 1971) but may have extended much farther. Wood yielding a radiocarbon date of 990 ± 130 years was collected from beneath a clayey lahar, which is exposed in a roadcut 1.0 km up Fox Creek on the Puget Sound lowland. This lahar flowed into a reentrant, Vashon-age (Crandell, 1963b) hanging valley about 1 km upstream from the lowland and then into Fox Creek before reentering the Puyallup River. Because the height of this deposit above the present river (37 m) is typical of Electron deposits at this point, it is more probably the Electron Mudflow than the 1,000-year-old lahar. The possibility exists, however, that a cohesive lahar extended to the lowland about 1,000 years ago.

ELECTRON MUDFLOW

This cohesive lahar in the Puyallup valley (table 2) is like the Osceola Mudflow, although it is smaller in volume.

Nevertheless, the Electron is still large, and its volume is more typical of the group of "large but infrequent" cohesive lahars that have formed at Mount Rainier in postglacial time. Like the Osceola, the Electron is relatively clay-rich (table 2, fig. 5) and has a significant LBF (fig. 8), which acted to reduce the rate of downstream attenuation and volume decline. The volume of deposits as measured by Crandell (1971, p. 57) on the Puget Sound lowland is accepted, but an additional volume representing an estimate of postdepositional erosion and dewatering losses is included in the value given in table 2. The lost volume was estimated by assuming an even, nearly horizontal original surface and then determining the volume represented by the difference between that surface and the present lower, dissected surface.

The clay content of the Electron Mudflow ranges from 6 to 11 percent with a mean of 8 percent (four samples). Its mean grain size is finer than that of the Osceola, in part because nearly all exposures are of thin deposits on steep valley side slopes; values range from $+1.7$ to -2.2ϕ (0.3 to 4.5 mm). Sorting ranges from 4.2 to 5.1 ϕ , and skewness values are positive, from $+0.06$ to $+0.38$. The unit contains only a few scattered megaclasts, forming mounds on lateral deposits in upstream reaches; the deposits are notable for a relative scarcity of mounds compared to those of other flows believed to have had the same origin of sector collapse and mobilization of the consequent debris avalanche. Crandell (1971) described large coherent boulders on the lowland, as opposed to the less coherent mound-forming megaclasts representing pieces of the failed edifice, and similar boulders were observed upstream.

A wood sample obtained by Crandell (1971) near Electron yielded an age of 530 ± 200 radiocarbon years. A sample collected by us downstream, 4.0 km below the town of Electron, yielded a date of 550 ± 190 radiocarbon years (fig. 10B). Forest duff at the base of the deposit, 5.5 km downstream from Electron, yielded a date of 840 ± 190 radiocarbon years. As noted by Crandell (1971), no volcanic activity has been recorded at Mount Rainier near the time the Electron Mudflow occurred.

Although set W is not well developed in the Puyallup River valley (Mullineaux, 1974, fig. 18), we have tentatively identified a distal version of the tephra, which overlies the Electron on the surface of the terrace described by Crandell (1971, p. 57) near the mouth of St. Andrews Creek. This stratigraphy corresponds to the most probable absolute ages of the events. These ages are critical because of the closeness in time of both events to the Tahoma Lahar, a smaller flow in the valley of Tahoma Creek (described subsequently) which is clearly of debris-avalanche origin. Set W was deposited just before that flow and can be documented to underlie it in new exposures. The Tahoma Lahar correlates with unit 9 of Crandell's measured section 9 (1971, p. 58), where he recognized set W at the base of the deposit.

Table 3. Mainly noncohesive debris flows and their runout phases at Mount Rainier.

[Many small flows excluded]

Drainage and flows	Age ¹	Extent (as flow large enough to inundate flood plain)
White River (including West Fork)		
Large gravel-rich debris flow and flood gravel extensively aggraded present channel; nonvolcanic in origin.	~A.D. 1550	At least to Mud Mountain Reservoir.
At least one lahar-runout flow in both main and West Fork, the latter valley-wide below park boundary.	Post-W	At least 5 to 10 km outside park boundary.
Lahar in West Fork 5 km above confluence of the forks	Post-C, pre-W	Unknown; at least to confluence of forks.
Transition facies in West Fork, 6 km above confluence	Post-C, pre-W	Unknown; possibly to Puget Sound lowland.
Dead Man Flat lahar assemblage--transition facies filled valley from near Fryingpan Creek to Buck Creek; runout flow farther downstream.	Post-C, pre-W	At least 11 km on Puget Sound lowland as large runout flows from both main fork and West Fork; flows probably reached Puget Sound.
At least five lahar-runout flows inset in channel incised in Osceola, near confluence of forks of White River.	Post-Osceola, pre-W.	Most flows in this group probably reached the margin of the Puget Sound lowland.
At least two lahar-runout flows, near Buck Creek, Greenwater, and also near Mud Mountain Reservoir.	Pre-Osceola	Puget Sound lowland.
Cowlitz River		
At least two runout flows	Post-W	At least 10 km downstream from Packwood.
Lahar-runout flow	Post-C, pre-W	Packwood.
At least three lahars	Probably post-Y, pre-W.	At least to park boundary in Muddy Fork.
Nisqually River		
Debris flow and runout flow of glacial-outburst origin in Kautz Creek	A.D. 1947	Only locally overbank below confluence with Nisqually River.
Lahar and lahar-runout flow	Post-W	At least to Elbe.
Lateral parts of Tahoma Lahar	Post-W	At least to Elbe.
Lahar-runout flow	Post-P, pre-W	At least to National.
Lahar-runout flow	Probably post-P.	To Elbe.
National Lahar (runout phase inundated all valley bottoms above Alder Reservoir to a depth of at least 3 m).	Post-C, pre-W	Puget Sound.
Lahar-runout flow	Post-Y, pre-W	At least to Ashford.
Large lahar and lahar-runout flow	pre-Y	Probably to Puget Sound lowland.
Puyallup River		
Lahar-runout flow	Post-Y, pre-Electron. ²	Puget Sound lowland.
Lahar	Post-Y, pre-Electron. ²	Puget Sound lowland, untransformed to runout flow.
Lahar-runout flow	Immediately pre-Y.	Puget Sound lowland.
Carbon River		
Lahar-runout flow	Post-W,	At least 5 km below glacier terminus.
Lahar-runout flow	Pre-W	8 to 10 km below glacier terminus.

¹ Ages of tephra shown in tables 1 and 2.² Flows closely related in time.

A cohesive diamict caps a terrace along a logging road on the north side of the Mowich River about 2 km upstream from its mouth. The unit was mapped as Round Pass Mudflow by Crandell (1971). A log at the base of the unit yielded a radiocarbon date of 530 ± 90 years (fig. 10A), indicating that the unit is the Electron Mudflow, which was more than 25 m deep near this locality.

The Electron Mudflow, as interpreted by Crandell (1963b, p. 69), dammed the drainage of Kapowsin Creek to form Lake Kapowsin. The lake has a maximum depth of 9 m (Crandell, 1963b), which is deep for a lahar-margin lake (Scott, 1989) and suggests that the strength of the flow was significant (Johnson, 1984, equation 8.6c). The original flow margin may or may not have had that much relief, however;

according to local residents, the lake level has risen substantially in the last century due to outlet blockage, either natural or constructed.

OTHER LAHARS AND POSSIBLE LAHARS

Other cohesive lahar deposits were reported by Crandell (1971) or observed by us. These observations were mainly at single localities on the volcano, but because the deposits are cohesive, it is possible that some of the flows were large enough to have extended long distances. Some were early in postglacial time, and their deposits on downstream valley-side slopes may have been eroded.

The deposits listed here were observed at altitudes or with thicknesses indicating that the flows were of significant size. Deposits noted by Crandell (1971) include unnamed deposits along the South Puyallup River (pre-Y in age); the relatively young unit 3 in section 10 of Crandell (1971); deposits at Round Pass (pre-Y in age); a lahar at Van Trump Park (pre-O in age); and a lahar older than the Paradise Lahar at Paradise Park. Additional clay-rich lahars discovered during this study include a post-Paradise, pre-Y lahar on Mazama Ridge above Reflection Lakes; a post-O, pre-Osceola Mudflow lahar locally preserved near Buck Creek and Greenwater; and a post-Osceola Mudflow, pre-Y lahar along the White River near Fryingpan-Creek.

The pre-Y lahar on the South Fork Puyallup River may record a flow approaching 180 m in depth in that tributary (Crandell, 1971). A possible correlative consists of slumped, clay-rich deposits near Electron that yielded wood fragments with a date of $3,760 \pm 350$ radiocarbon years. This deposit suggests that yet another cohesive lahar in the Puyallup valley reached the Puget Sound lowland, but it may also be interpreted as a slumped glacial deposit that incorporated younger wood.

SYNTHESIS OF THE RECORD OF LARGE, LOW-FREQUENCY LAHARS

At least six lahars can be documented to have inundated parts of the Puget Sound lowland or can reasonably be inferred to have done so. A seventh, the Greenwater Lahar, is not interpreted as a separate flow. These lahars occurred after deposition of layer O, 6,800 radiocarbon years ago. At least seven other postglacial flows were cohesive and, therefore, possibly large enough to have reached the lowland. The recurrence interval of these largest debris flows therefore is in the range of 500 to 1,000 years.

FLOWS OF INTERMEDIATE MAGNITUDE AND FREQUENCY (100 TO 500 YEARS)

Debris flows in this intermediate range were analyzed for the time following the deposition of tephra layer Yn (3,400 radiocarbon years) or C (2,200 radiocarbon years),

depending on drainage. Erosion or burial by the inset deposits of younger flows prevents a complete analysis of the intermediate-size flows older than these tephras. This span of 2,200–3,400 years is a sufficient period of record for these flows because the types of debris flows that occur at Rainier have not changed significantly in postglacial time. Intermediate-size flows are dominated by noncohesive lahars and their runouts (table 3). The runout phases consisted primarily of hyperconcentrated streamflow, which extended to the Puget Sound lowland or to a large downstream flood plain at least several times in all drainages except the Carbon River.

WHITE RIVER SYSTEM

Sequences of noncohesive lahars and their runout phases occurred at the following times: before the Osceola Mudflow; after the Osceola and before set C; between sets C and W; and after set W (table 3). Pre-Osceola flow deposits are seen only at the few places where the base of the Osceola Mudflow is exposed. All of these sequences are exposed near the Mud Mountain Dam and, therefore, at least locally inundated the downstream Puget Sound lowland.

The largest flows are between tephra sets C and W in age. They probably resulted from the volcanism that was responsible for construction of the summit cone during part of this time interval (table 1). Because the flows were dominantly noncohesive, most of them probably originated as meltwater flood surges that bulked with sediment on the side of the volcano and then debulked, in most cases beginning near the base of the volcano. The melting may have been the result of lava flows, pyroclastic flows and surges (both mainly lithic in composition), steam eruptions, or extensive geothermal heating.

Where approximately synchronous flows occurred in more than one watershed, they are probable evidence of significant episodes of volcanic or geothermal activity. Tephra-producing eruptions were not a general cause of the flows. Only pumice of tephra set C, which was erupted about 2,200 radiocarbon years ago, is found in significant amounts in any flow deposit, and radiocarbon dating shows that this pumice was mainly entrained through erosion. Some flows originated from shallow landslides, indicated by a high content of lithologically similar, hydrothermally stained clasts.

The largest noncohesive flows in the White, Nisqually, and Puyallup River systems probably formed about the same time, if not synchronously, from summit-cone volcanism. Crandell (1971) did not describe the runout phases of lahars, but he noted that the extensive aggradation in the White and Nisqually River systems, which resulted largely from runout flows, could be ascribed to summit-cone volcanism. That volcanism may have begun near the time of the block-and-ash flow in the South Puyallup River valley, 2,350 radiocarbon years ago (Crandell, 1971).

Table 4. Radiocarbon dates from hyperconcentrated-flow and normal streamflow deposits in the Mount Rainier area.

[Data mainly from lahar runout-flow deposits, but may include deposits of runout flows from debris flows not of volcanic origin]

Location	Stratigraphy and significance	Age ¹
White River (including West Fork)		
4.8 km upstream from confluence of Buck Creek and White River.	Trees killed by burial by flood deposit of nonvolcanic origin	400 ± 75
2.3 km upstream from White River Campground	Wood in upper part of lahar-runout deposit, 1.0 m thick	810 ± 75
Confluence of Fryingpan Creek and White River	Wood in Dead Man Flat lahar assemblage; unit includes layer-C pumice.	1,120 ± 80
In West Fork, 6 km upstream from confluence with White River.	Stump on large lahar-runout flow deposit, more than 1.8 m thick; overlain by 7 layers of flood deposits.	1,255 ± 130
1.6 km upstream in Clearwater River	Wood below lahar-runout flow from Mount Rainier; a maximum age.	3,005 ± 230
1.3 km upstream from confluence of Buck Creek and White River.	Charcoal fragments from base of noncohesive lahar beneath Osceola Mudflow.	5,230 ± 235
1.3 km upstream from confluence of Buck Creek and White River.	Charcoal fragments from noncohesive lahar underlying above unit and overlying layer O.	6,075 ± 320
Cowlitz River		
South bank of active channel 1.8 km upstream from Randle (river mile 104.3 on Randle 15-minute quadrangle).	Wood in lowest of four silty sand overbank deposits, 0.2 to 0.5 m thick, representing floods occurring after youngest lahar-runout flow.	325 ± 180
North side active flood plain 10 km downstream from Randle (river mile 117.5).	Wood from base of 0.5 m silt layer over lahar-runout flow with layer-C pumice; dates major flood.	440 ± 70
South bank of abandoned meander 5.5 km upstream from Randle (near river mile 108.0).	Charred wood bioturbated with set W, in upper part of lahar-runout deposit, below 1.0 m of silt representing large post-W flood.	815 ± 120
Nisqually River		
12.5 km upstream from main bridge crossing river near Yelm.	Bark from silt-rich unit burying cedar forest; dates flow that killed flood-plain forest.	220 ± 70
1.2 km upstream from boundary of Nisqually Indian Reservation.	Wood from same unit as above	240 ± 60
0.5 km downstream from National	Wood from lahar-runout flow younger than National; inset sequence in gorge cut in valley bottom.	410 ± 75
1.4 km upstream from boundary of Nisqually Indian Reservation.	Outermost wood of 250- to 350-yr-old cedar buried by two silt-rich flood deposits; tree grew on deposit correlated with the National Lahar.	585 ± 125
6.2 km downstream from Alder Reservoir	Wood within upper part of 3 m of hyperconcentrated-flow deposits correlated with the National Lahar.	790 ± 205
1.6 km downstream from bridge crossing Nisqually River in National Park.	Wood from top of fluvial unit underlying transition facies of National Lahar; maximum date of that flow.	2,285 ± 155
Puyallup River		
0.1 km upstream from main highway bridge below Electron.	Charcoal fragments from contact between lahar-runout flow and underlying large cohesive lahar.	840 ± 190
Do.....	Charcoal fragments from contact between lahar-runout flow and overlying large noncohesive lahar.	2,740 ± 230
Do.....	Charcoal fragments in lahar-runout flow under large non-cohesive lahar.	3,530 ± 255
Carbon River		
4.8 km downstream from glacier terminus	Probable lahar-runout deposit in low terrace (2–4 m above active channel).	650 ± 120

¹ Years before 1950 in radiocarbon years.

The largest post-C, pre-W noncohesive flows in the White River system are informally designated as the Dead Man Flat lahar assemblage (fig. 6), believed to consist of several nearly synchronous flows, at least one from each fork of the White River. The flows of the assemblage are lahar-runout flows over most of their longitudinal extent. Wood from the flow in the main fork at Fryingpan Creek yields a date of 1,120±80 radiocarbon years (table 4).

Although layer-C pumice is abundant in this flow deposit, the date, from a limb segment with bark that was completely contained within the deposit, is probably an accurate measure of flow age. The flow deposit is immediately overlain by a unit interpreted as a blast deposit, with a radiocarbon age of 1,080±25 years (table 1) determined by R.P. Hoblitt (U.S. Geological Survey, oral commun., 1994). The flow apparently came down the main fork and did not

originate in Fryingpan Creek. Downstream from the National Park boundary near Buck Creek, the transition facies of this flow locally overtopped the mound-bearing Osceola surface as much as 60 m above the White River (fig. 6A). Downstream from the confluence with the West Fork, the runout deposits of the flow are interbedded with those of a similar flow, also containing set-C pumice, which probably originated in the West Fork White River at about the same time. The outermost wood of a small stump on a large runout deposit along the West Fork yielded a date of $1,255 \pm 130$ radiocarbon years (table 4). Even though the tree was 55 years old, its corrected age ($1,310 \pm 130$) still overlaps with the radiocarbon date ($1,120 \pm 80$) for the Dead Man Flat assemblage on the main fork. Total thickness of the assemblage, bounded by sets Y and W, is locally more than 3 m. From 6 km below Greenwater to the Mud Mountain Dam (fig. 6B), deposits of the assemblage occur at least 30 m above the White River. Even 11 km beyond the Cascade Range front, the flows reached nearly 20 m above the present river.

The dated occurrences of noncohesive flows show a concentration near but well beyond the end of the period of summit cone volcanism. This period was interpreted by Crandell (1971, p. 14) to be between 2,100 and 1,200 absolute years ago, about the same as the range in radiocarbon years (Stuiver and Becker, 1986). Dating of the noncohesive flows in the White and other river systems indicates that the lahar-producing volcanism continued to at least 800 years ago. Wood fragments from deposits of a small flow upstream from the White River Campground yielded a date of 810 ± 75 radiocarbon years (table 4). A flood deposit that extensively aggraded the present White River channel and killed many trees contains wood yielding an age of 400 ± 75 radiocarbon years. The deposit was only locally emplaced as a debris flow and is dominated by non-Rainier and reworked Rainier rock types. It is probably of nonvolcanic origin.

COWLITZ RIVER SYSTEM

Typical lahar-runout flow deposits occur throughout the Cowlitz River system, from the headwaters of the Ohanapecosh River to cutbanks in the flood plain near Packwood. The watershed was notably less affected by lahars and lahar-runout flows than either the White River system to the north or the Nisqually River system to the west. This difference probably reflects the lack of major, deeply incised valleys in the sector of the volcano drained by the Cowlitz River. Although the three separate flows observed (table 3) were overbank, they were not markedly greater than historical floods in the watershed. An overbank thickness of about 0.5 m is typical for the lahar-runout deposits upstream and downstream from Packwood and is comparable to the thicknesses of interbedded flood deposits

(table 4). The lahars observed in the upper Muddy Fork (table 3) average about a meter in thickness, a value also comparable to the thickness of younger flood deposits in that area.

Except for one locality, radiocarbon dates could be obtained only from flood deposits overlying the runout flows. A date from wood within a runout deposit was 815 ± 120 radiocarbon years (table 4). Other minimum ages of runout flows, and the probable actual radiocarbon ages of major-flood deposits occurring above them, are 440 ± 70 and 325 ± 180 radiocarbon years. The dated runout deposit is consistent in age with others in the White, Nisqually, and Puyallup River systems (table 4).

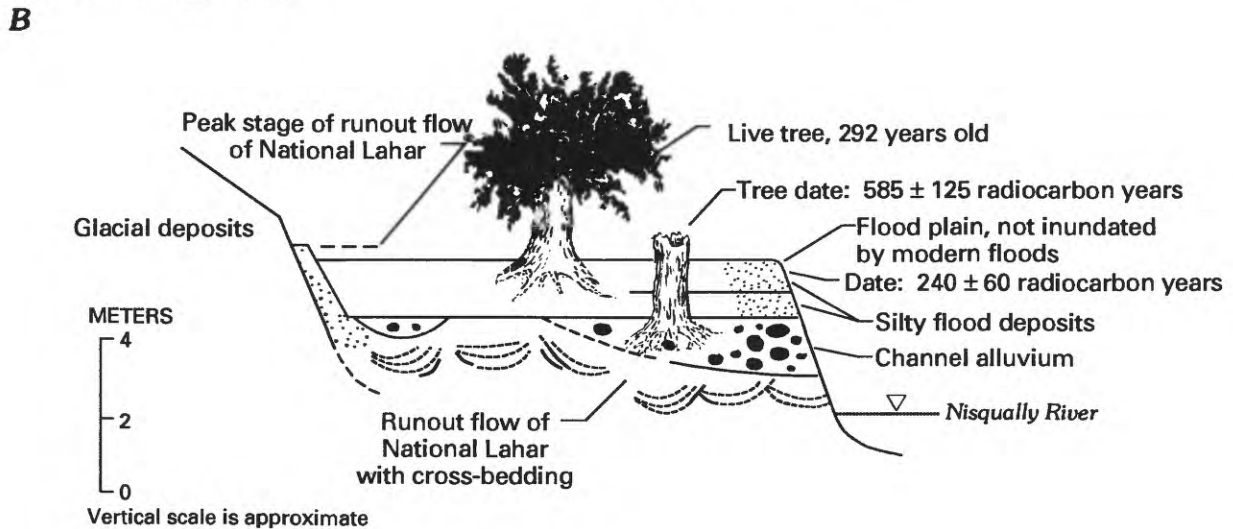
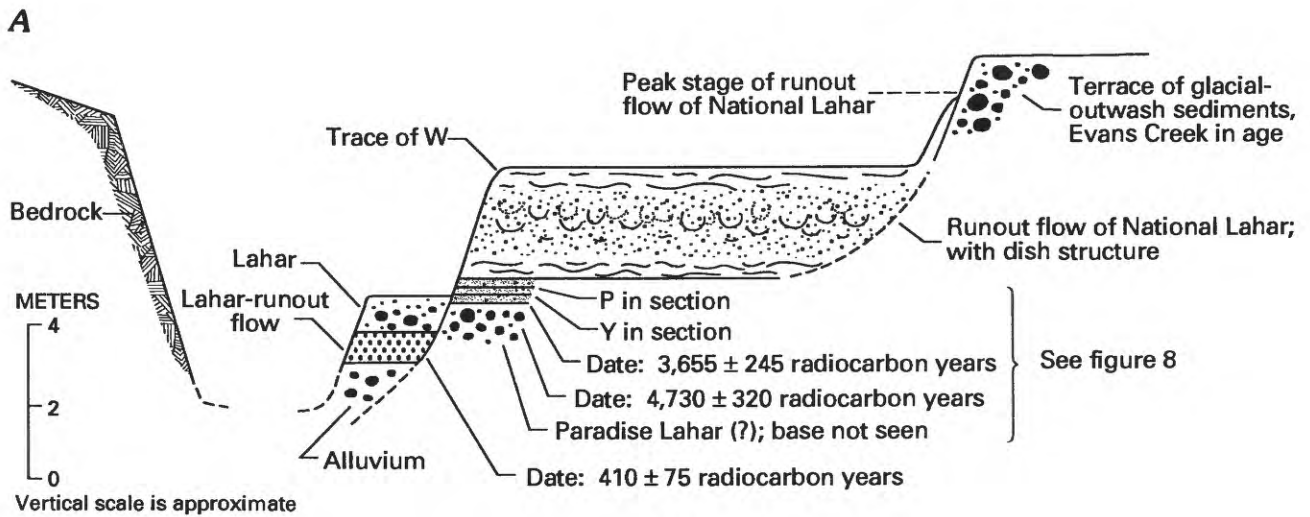
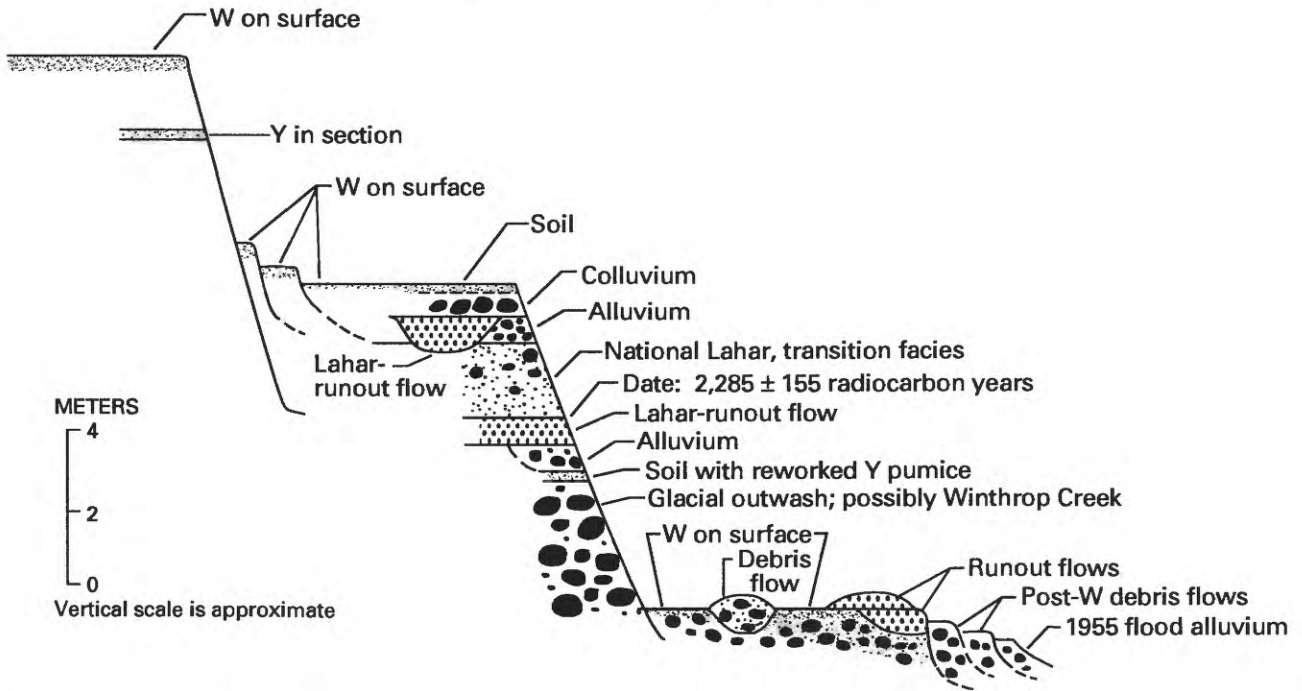
NISQUALLY RIVER SYSTEM

The oldest noncohesive lahar and runout flow to be recorded at multiple locations is pre-Y in age. It occurs at scattered exposures upstream of Longmire, indicating an origin from the part of the watershed headed by the Nisqually Glacier. Although not seen in direct contact with the Paradise Lahar, it is probably younger. Other pre-Y flows certainly existed, but their deposits were seen at only a single locality and could not be correlated. Characteristics used to correlate flow deposits in the absence of age information include soil development, matrix color, alteration products on and in clasts, and deposit texture.

A series of noncohesive lahars and lahar-runout flows occurred between the deposition of tephra sets Y and W (table 3). The flows were part of the aggradational cycle that resulted from summit-cone volcanism, as described above for the White River system. At some localities, set P (3,000 to 2,500 radiocarbon years in age) can be distinguished for further age refinement (figs. 9 and 11B). Because none of the Rainier tephra are present on the west side of the volcano, which faces prevailing winds, further tephra-based dating was not possible.

The best exposed lahar of this series, comparable in size with those in the White River system, can be traced to Puget Sound and is here informally named the National Lahar after the town of National (figs. 9 and 11B), a designation incorporating the runout phase. The National Lahar and its runout phase have textures typical of a noncohesive lahar and its hyperconcentrated runout-flow deposits (fig. 2). Mean grain size of the lahar is -1.2ϕ (2.3 mm); sorting is a

Figure 11 (facing page). Diagrammatic composite sequences of valley-fill deposits in the Nisqually River valley (successive downstream sections). Vertical scale is shown to indicate approximate thicknesses. Horizontal scale is variable for better portrayal of stratigraphic relationships and is not shown. However, vertical exaggeration ranges approximately between 5× and 10×. A, Nisqually River upstream from Longmire. B, Nisqually River between Ashford and National. C, Nisqually River downstream from Yelm.



C

relatively low 2.0ϕ , barely within the range characteristic of flows with sufficient strength to support dispersed coarse clasts (Scott, 1988b). Mean grain size of the runout deposits is $+0.5 \phi$ (0.7 mm); sorting is 1.3ϕ , within the range common to runout flow deposits (1.1 to 1.6ϕ ; Scott, 1988b) and reflecting the progressive downstream loss of strength. The lahar transformed to hyperconcentrated flow near the National Park boundary, as indicated by flow deposits consisting of the transition facies (Scott, 1988b, fig. 10) above Longmire. The flow may have originated in more than one tributary of the Nisqually River, but a significant part of the flow was derived from the headwaters of the main stream. The inclusion of erosionally derived clasts of tephra layer C, which was distributed mainly to the east of the volcano but also into the upper Nisqually River watershed (Mullineaux, 1974, fig. 24), supports this probability. Downstream from the National Park boundary, the deposits are largely those of hyperconcentrated flow. The further transformation to normal streamflow is marked by the appearance of well-defined stratification and of sorting below 1.1ϕ . Mean grain size of the deposits near Yelm is 3.1ϕ (0.1 mm); sorting is 0.6ϕ .

A noteworthy feature of the runout phase of the National Lahar is the presence of dewatering structures (fig.

12). Dish structure, named by Wentworth (1967) and correctly interpreted by Lowe and LoPiccolo (1974), is well developed in the longitudinal interval representing the upper part of the hyperconcentrated range of sediment content. This interval corresponds to the approximately 30 km of flow downstream from the distal end of the transition facies, the point at which the transformation from debris flow to hyperconcentrated flow was complete. Dish structure in the runout deposits of the National Lahar consists of concave-upward, strata-like concentrations of darker, commonly finer sediment that truncate each other laterally and locally resemble cross strata. Concavity increases upward within 2- to 3-m sections of the runout deposits, locally producing closed, concretionary forms near the top of the unit. The structure clearly is not antidune cross-bedding as interpreted by Wentworth. The basic mechanism is, as interpreted by Lowe and LoPiccolo, expulsion of water from the deposit shortly after deposition. However, the more pronounced development of the structure in older runout flows, such as that of the National Lahar, indicates additional progressive development with time as phreatic processes further concentrated fine sediment at the interfaces. Pillar structure (Lowe and LoPiccolo, 1974) is present along with the dish structure in some runout

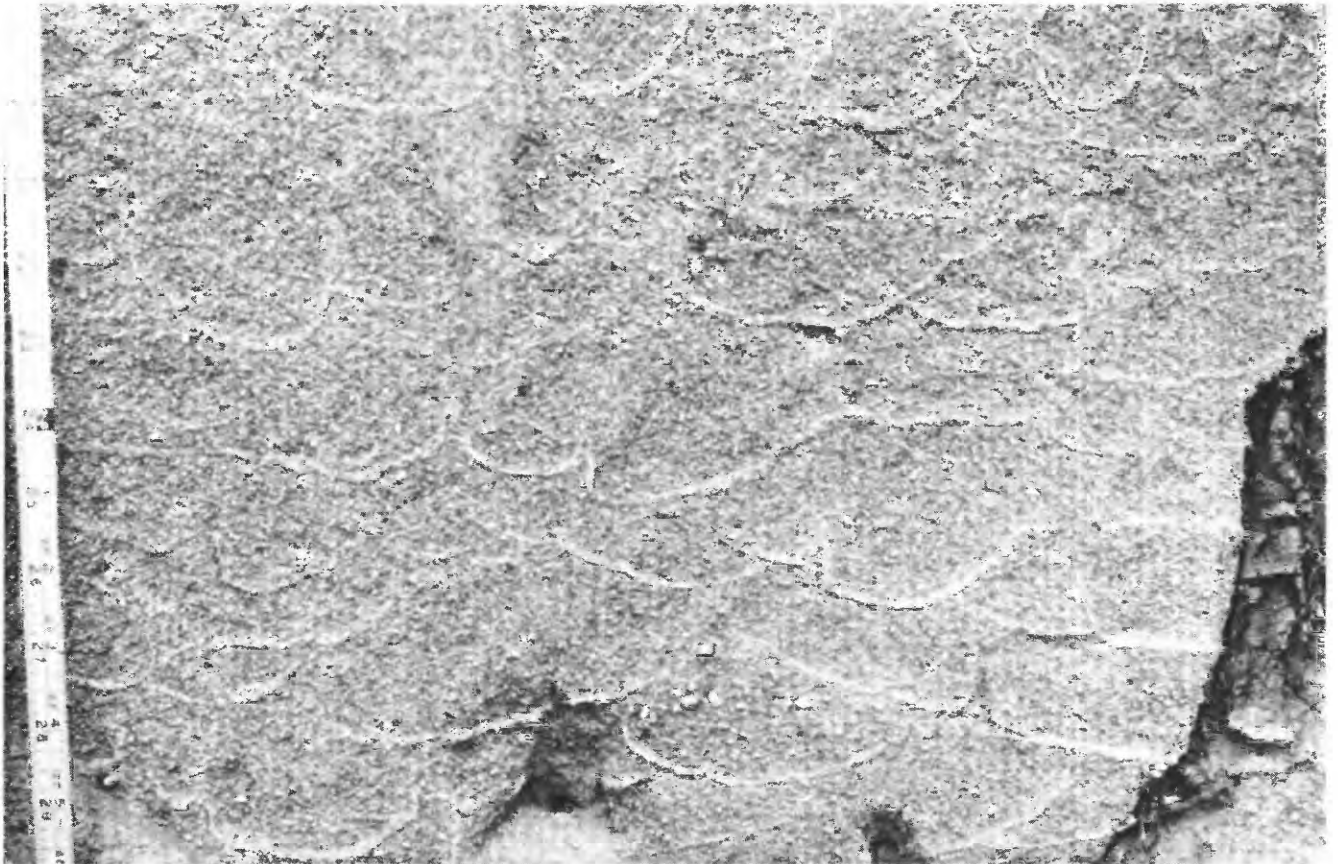


Figure 12. Dish structure in deposits of National Lahar at the type locality. Note that the concavity of the “dishes” increases upward in the section. Structures shown are about 1 m below the top of a 3-m section. Scale at left is in inches.

deposits, but is less common than in the deep-water marine sequences from which both structures have been previously recorded.

The type section of the flow deposit consists mainly of the lahar-runout phase in a quarry near National (fig. 9). Most attempts to date "wood" fragments in the unit yielded ages either too old (inconsistent with ages of underlying deposits, as well as known tephra ages) or too young (inconsistent with the age of trees growing on the surface). Some of the fragments that resemble carbonized wood were found to be inorganic during analysis; others are low-grade coal derived from Tertiary bedrock. Two dates establish a probable age, however. Wood within the upper, possibly reworked part of the unit below Alder Dam (table 4) yielded a radiocarbon age of 790 ± 205 years. Near the end of the river system, a cedar tree growing on the correlative deposit died 585 ± 125 radiocarbon years ago. This date is from its outermost wood and corresponds to an absolute age of about 550 to 650 years (Stuiver and Becker, 1986). Inasmuch as the tree was 250 to 350 years old when it died, the age of the deposit is at least 800 to 1,000 years. Upstream, trees growing on the sequence containing the flow deposits are at least 800 years old (Crandell, 1971, p. 42). In the White River valley, the most likely correlative surface is probably at least 1,000 years old (Sigafos and Hendricks, 1961, p. 16). The National Lahar may be a close or synchronous correlative of the Dead Man Flat lahar assemblage in the White River. The lahar of that assemblage in the main fork of the White River has a radiocarbon age of $1,120 \pm 80$ years. Both the National Lahar and the Dead Man Flat lahar assemblage contain abundant clasts of erosionally derived layer-C pumice.

The carbon content of the National Lahar is high, indicating that it occurred after a large forest fire. Evidence from other parts of the Mount Rainier area shows that at least one such fire did occur in the interval between tephra sets Y and W. Crandell (1971, p. 57) found forest-fire debris in a bank of Tahoma Creek, and he tentatively correlated it with the block-and-ash flow, 2,350 radiocarbon years in age, in the South Puyallup River valley. A remarkable layer of forest-fire debris was found in the banks of Kautz Creek upstream from the Wonderland Trail bridge, and wood from this layer yielded a date of $1,625 \pm 70$ radiocarbon years. The National Lahar, if associated with a fire, expectedly would contain carbonized wood, but none was found. This suggests either that the flow occurred much later than the fire, after flushing of charred wood from the watershed, or earlier than the fire. The presence of carbon-impregnated rock suggests the former possibility.

The maximum age of the National Lahar is limited by included clasts of tephra layer C, with an age of 2,200 radiocarbon years; set P, which underlies the unit and has an age of 3,000 to 2,500 radiocarbon years; and a date of $2,285 \pm 155$ radiocarbon years from wood below the unit upstream from Longmire. The maximum possible age is

more closely bracketed by samples from beneath the unit, which yield ages of $1,820 \pm 300$ and $1,970 \pm 250$ radiocarbon years (R.P. Hoblitt, U.S. Geological Survey, oral commun., 1994).

Another noteworthy feature of the runout phase of the National Lahar is the distance over which the flow was hyperconcentrated, a total of more than 40 km from near National to downstream of Alder Reservoir. Long distances of hyperconcentrated flow were common to most lahar runouts at Mount Rainier.

Younger noncohesive lahars, debris flows, and their runout phases in the Nisqually system (table 3) include: (1) flows occurring shortly before and after the National Lahar (fig. 11A, B); (2) lahar-runout-flow deposits interbedded with flood-plain gravel near the National Park headquarters between Ashford and Elbe; (3) a lahar-runout flow exposed in the gorge upstream from National; and (4) the runout phase of the largest of the 1947 debris flows, which originated as glacial-outburst floods in response to precipitation. This last flow, although recent, is a probable example of a flow with an intermediate magnitude and recurrence interval (100 to 500 years). This conclusion is based on its inundation area (it locally overlies set W and inundated a valley width of 0.9 km at the highway crossing) as well as the magnitude of its discharge (fig. 13) and deposit volume. In terms of estimated peak discharge, the flow was at least 10 times larger than any other 20th-century flow in Kautz or Tahoma Creeks.

The 1947 flow was the largest of a series of flood and debris flow surges that occurred mainly on October 2–3 in response to an intense cloudburst that caused the lower 1.6 km of the Kautz Glacier to collapse. Areas of stagnant ice resulting from long-term Neoglacial recession are major factors contributing to the formation of these modern flows, which are discussed more fully in the section on smaller, more frequent flows. Inasmuch as the 1947 flows are well described by Grater (1948a and 1948b), Erdmann and Johnson (1953), Richardson (1968), and Crandell (1971), only a general description is given here, along with any new details relevant to our topic.

Each 1947 debris flow was clearly noncohesive; Erdmann and Johnson (1953) recorded a "more or less complete absence of clay." Two composite samples of complete flow units contained 1 percent or less of clay. Crandell (1971) reported 4 percent clay in two matrix samples. A well-developed runout flow evolved from the largest 1947 debris flow; its deposit near the confluence of Kautz Creek and the Nisqually River is now a source of sand and granule gravel for aggregate, as are many other runout-flow deposits. Downstream, the flow was overbank only locally but can be traced to the western park boundary, 4.5 km downstream. Farther downstream at the gaging station at National, the flood wave had transformed from hyperconcentrated flow to normal streamflow; at that point the flow had attenuated to only $42 \text{ m}^3/\text{s}$ above base flow (Nelson, 1987).

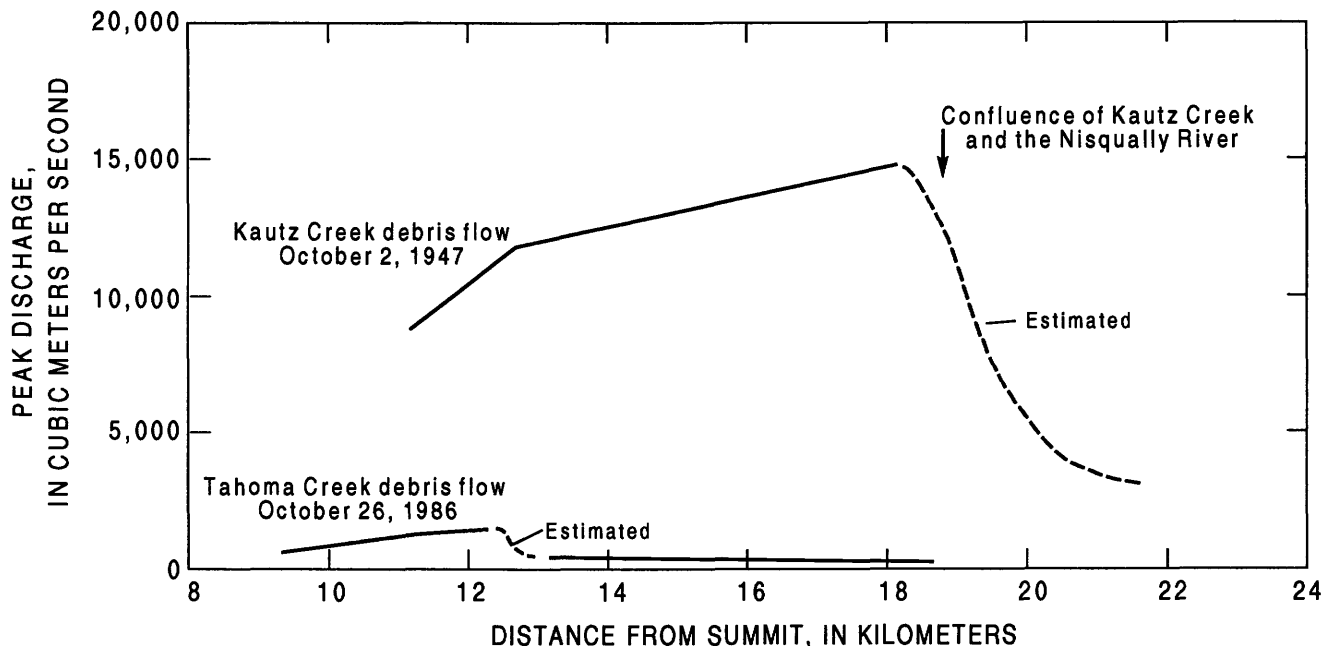


Figure 13. Discharge versus distance for two debris flows resulting from glacial outburst or collapse. Rapid decline of discharge downstream reflects debulking of sediment in response to valley expansion, slope reduction, or confluence with streamflow.

The 1947 runout deposits are easily distinguished from older lahar-runout deposits of volcanic origin by their darker color, contrasting with the lighter, generally more yellow colors, typical of volcanic alteration, of the flows originating as lahars. The darker color is ascribed to the dominance of morainal streambed sediment as the main 1947 source materials. This sediment originated as ice-shattered debris scoured and eroded from the surfaces of relatively unaltered lava flows. Headwalls above Kautz Glacier expose flows (frontispiece) less altered than those above Tahoma Glacier in the Sunset Amphitheater, source of several flows in the Tahoma Creek valley. As much as 18.3 m of net channel erosion accompanied formation of the flows, deposits of which totaled 38 million m³ in volume along Kautz Creek (Grater, 1948a).

The 1947 runout deposits have size distributions typical of hyperconcentrated streamflow derived by direct transformation from debris flow, as shown in figure 2 for the National Lahar and its runout flow. The main debris flow deposit has a bimodal size distribution, mean grain size of -2.1ϕ (4.2 mm), and sorting of 3.8ϕ . More than 80 percent of grains in two samples of the runout flow are in the sand size range; the mean grain sizes in these samples are 1.0 and 0.9 ϕ (0.5 mm), and their sorting values are 1.3 and 1.6 ϕ , respectively.

The behavior of the main 1947 flow was similar to that of smaller, more frequent flows. Its peak discharge attenuated rapidly at places of rapid energy loss as sediment debulked from the flow (fig. 13), transforming the debris flow surges to hyperconcentrated streamflow. Unlike the smaller modern flows on both Kautz and Tahoma Creeks,

however, the place where debulking was most rapid was not at the main slope inflection at the base of the volcano, but near the confluence with the Nisqually River. The energy loss was in response to a great increase in valley width and spreading of the flow across the maturely forested fan. The hazard implications of the rapid attenuation and debulking of noncohesive flows are discussed in the section on risk analysis.

PUYALLUP RIVER SYSTEM

Flows in this drainage are dominated by large, mainly cohesive lahars, the valley-bottom deposits of which would have buried most runout deposits of the generally smaller, noncohesive flows. Several deposits of noncohesive flows were seen, including the large noncohesive lahar described in the section on large, infrequent flows. That flow extended as debris flow for at least 6.0 km beyond the lowland boundary and is the most far-reaching noncohesive lahar known from Mount Rainier. It is directly overlain and directly underlain by lahar-runout-flow deposits (tables 3 and 4), and the younger, overlying runout unit is evidence of an upstream lahar nearly synchronous with the large noncohesive lahar.

CARBON RIVER SYSTEM

Most of this river system consists of a deeply incised bedrock gorge from which any volcanoclastic flow deposits have been eroded. A ridge extending north of the summit may have diverted some noncohesive flows originating at

the summit to the White or Puyallup River systems (Crandell, 1971). Crandell observed a lahar in the headwaters, and we noted two valley-wide lahar-runout deposits that are pre- and post-W in age. Set W was not found by Mullineaux (1974, fig. 18) to extend significantly into the watershed, but a distal facies of that tephra is locally recognizable. Layer Yn is more widespread (Mullineaux, 1974, fig. 16). Its preservation at the surface on low valley-side slopes shows that no large flows have originated in the river system in the last 3,400 radiocarbon years. However, neither the diversionary effect of the ridge noted above nor the paucity of previous debris flows in the watershed changes its susceptibility to a future cohesive lahar originating as a sector collapse (Frank, 1985).

FLOWS OF LOW MAGNITUDE AND HIGH FREQUENCY (LESS THAN 100 YEARS)

The smallest, most frequent debris flows and their derivative runout flows are common in a few river systems at Mount Rainier, but rare in others. These flows have several general characteristics: (1) They tend to occur in clusters within periods of several years (such as those that occurred in the periods of 1967–70 and 1986–92), and decades may separate the clusters; (2) the debris flows that originate as glacial-outburst surges have been historically most common in late summer and fall; (3) the flows are uniformly noncohesive, forming from flood surges and in most cases transforming downstream through hyperconcentrated flow to normal streamflow; (4) this transformation is rapid, occurring at the base of the volcano, and so the flows attenuate rapidly (fig. 13) and are typically contained within stream channels beyond that point; and (5) the flows have a variety of glacier-related origins and interactions; the largest flows occur during or just after periods of precipitation, which may trigger collapse of the stagnant terminal ice resulting from Neoglacial recession. Walder and Driedger (1994) have prepared a detailed analysis of the effects of outburst floods and the debris flows formed by them.

Lakes dammed by terminal Neoglacial moraines are not a large hazard at Mount Rainier. Unlike the numerous moraine-dammed lakes on some Oregon volcanoes (Laenen and others, 1987, 1992), the lakes on Mount Rainier either are cirque lakes with bedrock sills or are dammed by old moraines and have highly stable outlets, having broken out long ago. However, a landslide into a lake, as has occurred at Lake George in the Tahoma Creek watershed, could catastrophically displace enough water to create a significant surge that may bulk to debris flow.

A second and more hazardous type of frequent flow is a debris avalanche, which is not likely to extend far from the volcano, unlike the large debris avalanches that most commonly transform to lahars. This flow type and its

possible mobilization to a lahar are discussed in a later section.

RECURRENCE INTERVAL OF SMALL DEBRIS FLOWS

Many small streamflow surges originate on the volcano. They have occurred at a rate of at least one per year between 1986 and 1992 (Walder and Driedger, 1993). Most are glacier-related, either as subglacial outbursts or supraglacial outbursts of ponds dammed by saturated modern moraines. Others are the result of temporary impoundment of streams by landslides, commonly in Neoglacial lateral moraines. Some of the surges are not large enough to erode the coarse bed material and thus do not bulk to debris flows.

The larger surges of this type, especially those triggered by precipitation, are competent to erode all bed material, including boulders several meters in diameter. These surges bulk to debris flows and may be divided into precipitation-induced events and clear-weather events (fig. 14). The best-known examples are along the Nisqually River and its tributaries, Tahoma and Kautz Creeks. At least 20 such events between 1925 and 1990 were of sufficient size to inundate areas of inactive flood plain in those watersheds and pose a local hazard to hikers. (Flows for which only the year is known are not shown in figure 14.) Walder and Driedger (1993) have prepared a guide to their hazards and occurrences for park visitors.

Between 1986 and 1988 there were eight major flows from Mount Rainier—five on Tahoma Creek and three on Kautz Creek—and at least two smaller flows (on Tahoma Creek in late August 1987). A similar cluster of flows between 1967 and 1970 on Tahoma Creek was ascribed by Crandell (1971, p. 60) to possible geothermal activity. Although no increase in geothermal activity was known to accompany the latest cluster, Frank (1985) reported the presence of heated ground and sub-boiling-point fumaroles on the South Tahoma and Kautz Glacier headwalls. Study of the Tahoma Creek deposits before the initial 1986 flow verified that the lapse in reported flows between 1970 and 1986 represents a true lack of significant flows in that drainage, not just a lack of observations.

Some flows of this type have occurred unseen and unrecorded in other drainages, even since construction of the Wonderland Trail, which circumnavigates the volcano near its base. Deposits are covered or eroded by those of later flows of similar noncohesive texture. The record of 20 significant, flood-plain-inundating debris flows since 1925 is clearly a minimum in the Nisqually River headwaters. An appropriate composite recurrence interval for planning purposes in those watersheds is approximately two years. At present (1994), however, even though the cluster of flows on Tahoma Creek that began in 1986 may be tapering off, it is reasonable to assume that at least one flow can be anticipated

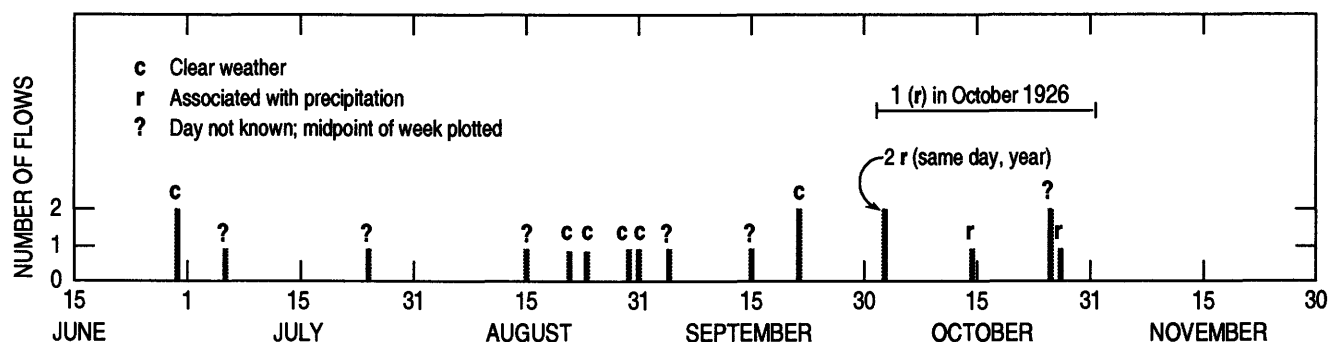


Figure 14. Seasonal distribution of debris flows, hyperconcentrated flows, and floods in glacier-fed tributaries of the Nisqually River from 1925 to 1990. Only flows with known dates are shown; many others, smaller or of unknown date, are not shown. Some data from Crandell (1971); Erdmann and Johnson (1953); Richardson (1968); J. J. Major (U.S. Geological Survey, written commun., 1985); and M. Carney, S. V. Scott, and D. J. Sharlow (National Park Service, oral commun., 1986–1987).

each year. Each flow's area of inundation is likely to extend only locally outside that of the previous members of the cluster. However, a detailed study focusing on origins and valley responses of these flows concludes that long-term predictions of flow frequency in the watershed are not possible (Walder and Driedger, 1994).

SEASONAL DISTRIBUTION

A significant factor mitigating the hazards of these flows is that they tend to occur in late summer and fall (fig. 14) after most back-country tourist use. The mean date of the known flows in figure 14 is September 7. In addition, the largest flows recorded historically in each of the three major valleys in the Nisqually headwaters have occurred in October—October 2 for Kautz Creek, the 25th for the upper Nisqually River, and either the 15th (highest volume) or 26th (highest discharge) for Tahoma Creek. Each of those flows began as a precipitation-induced surge, and two were amplified by the collapse of areas of stagnant ice. Although these surges probably were amplified by subglacial water, the glaciers served mainly as conduits and temporary reservoirs of storm runoff.

Many clear-weather flows are logically ascribed to subglacial storage of meltwater. These flows tend to occur earlier in the year than the precipitation-induced flows (fig. 14). The previous cluster of flows, from 1967 to 1970, occurred in the relatively narrow time interval of August 20 to September 23 (Crandell, 1971). This time of occurrence suggests an origin as glacial-outburst floods induced by warm-weather melting. Other evidence cited by Crandell (1971) suggests a geothermal origin, and we assume that possibility exists.

FLOW TEXTURE AND FORMATIVE TRANSFORMATIONS

Whether their origin is from precipitation or meltwater, the flows bulk rapidly through hyperconcentrated flow to

debris flow. These transformations have occurred on the moraine-covered surface of the glacier for surges that exited above the terminus (fig. 15), or in the unvegetated, proglacial valleys for subglacial surges that emerged at the terminus. The proglacial valleys contain vast amounts of reworked sediment of morainal and volcanoclastic origin. This sediment readily bulks, mainly by mobilization of unstable bed and bank material, into the surges from the glaciers to yield debris flows that are uniformly noncohesive in texture and contain 1 percent or less of clay in 10 examples, including the 1947 flows on Kautz Creek.

FLOW DYNAMICS AND TRANSFORMATIONS

Two flows in the Tahoma Creek valley were studied as models to analyze the dynamics and transformations of a precipitation-induced flow and a clear-weather flow: the former occurred October 26, 1986, and the latter, June 29, 1987. By chance, the watershed and stream channel had been studied immediately before each event, and they were restudied afterwards. Both flows were noncohesive, although the deposits of the clear-weather flow contain slightly more clay. The mean grain size and sorting of the flow matrixes are shown in figure 3.

A significant part of the October 1986 flow originated from a sinkhole-like collapse near the active glacier terminus, which is presently just below a crevassed ice fall at an altitude of about 1,830 m (6,000 ft) to 2,260 m (7,400 ft). The dimensions of the collapse were estimated from an aircraft as 9 by 15 m (R. Dunnagan, National Park Service, oral commun., 1986). The precipitation-induced surge bulked as it flowed across the top of the stagnant, moraine-covered lower portion of the glacier. Part of the flow may have entered a small sinkhole (fig. 16A), and the remainder was apparently dammed temporarily on the surface before cutting a channel along the west side of the glacier. The flow probably was already a debris flow at that point, as indicated by boulder levees and deposit texture on



Figure 15. Active front of the South Tahoma Glacier 5 days before (A) and 1 day after (B) the clear-weather glacial-outburst flood and debris flow of June 29, 1987. Arrow in B points to dark areas of collapse, source of at least part of the flow.

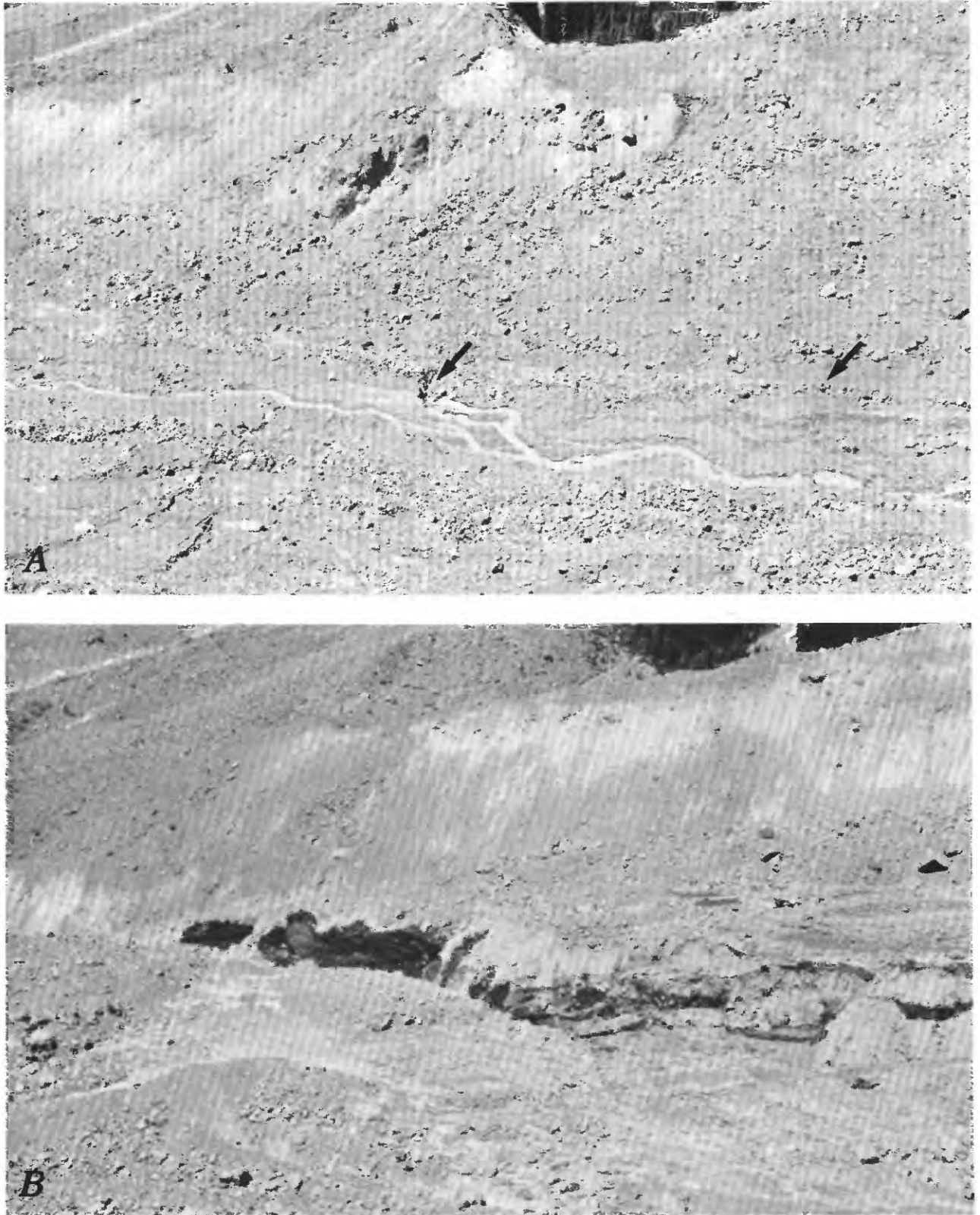


Figure 16. Area of stagnant, moraine-covered lower part of South Tahoma Glacier 5 days before (A) and 1 day after (B) the flow of June 29, 1987. Location 0.9 km downstream from active front of glacier shown in figure 15. In A, note flow of part of supraglacial stream into sinkhole (left arrow) and fresh scarps and fractures in alluvium (extending from lower left toward sinkhole), corresponding to crevasses in underlying stagnant ice. Boulder berms delineate flow of October 26, 1986 (right arrow). B shows incision into the debris-rich stagnant ice by the June 29 flow.

the glacier surface (fig. 16A). As the two distributaries (subglacial and supraglacial) rejoined below the stagnant-ice terminus at 1,510 m (4,960 ft) altitude, bulking continued to enlarge the flow in the channel incised in the Neoglacial moraine. Bulking was amplified by the collapse of debris-rich ice at the front of the stagnant part of the glacier, and the resulting material may have dammed the main channel.

The 1986 flow had the highest discharge of any flow in the 1986–88 period (fig. 13). The flow volume, however, was exceeded by the flow or series of flows that occurred on October 15, 1988. The deposits of that flow (or flows) inundated the entire valley floor, 0.2 km in width at the site of the former picnic area, and occurred in greatest volume at a point farther downstream than any other flow in the 1986–88 group. This observation suggests a correlation between flow size and the distance of the locus of deposition from the mountain, which is also suggested by the data shown in figure 13. Although peak discharge was higher on October 26, 1986, the volume of sediment transported on October 15, 1988, was greater, accomplished by either a broader flow wave or by multiple flows.

The June 1987 flow originated from the base of the icefall (fig. 15B), at the end of a week of completely clear weather that marked the beginning of a severe drought period. (This drought also resulted in small debris flows along Tahoma Creek on August 28 and 31 and one of moderate size on September 23.) Lateral deposits of the June flow were silt-rich as the surge issued from the ice fall, and bulking to debris flow occurred on the surface of the stagnant ice above the site of the previously existing sinkhole. Lateral erosion of stagnant ice triggered an ice-block avalanche into the channel, and blocks of mixed ice and rock several meters in diameter were transported. Figure 16 shows the channel several days before and the day after the flow. Below the lateral ice avalanche, the flow triggered a spectacular collapse of the stagnant glacier surface from above the sinkhole to the terminus. Rapid incision into the debris-rich ice then led to further bulking and enlargement of the flow wave.

The depositional patterns of the 1986 and 1987 flows were nearly identical. The deposits were thickest within 0.5 km of the inundated picnic area (a campground before inundation in 1967) along Tahoma Creek. Boulder fronts as much as 3.5 m high (eroded or buried in 1988) represented the “frozen” termini of convex lobes of the coarse front of the flow. As movement of each lobe ceased, its deposits diverted flow from the following segment of the wave to one side. Each new surge successively stopped, diverting the following portion of the wave, and so on in a chain reaction. Distal surges in the flow were thereby created from a single flood wave, as shown by the existence of only a single berm of deposits upstream. The coarsest boulder fronts of each flow contained as much as 10 percent clasts of ice and frozen ground (fig. 17).



Figure 17. Ice clast, more than 1 m in maximum dimension, included with andesite clasts of similar size in lobate boulder front of flow of October 26, 1986, Tahoma Creek drainage.

Each flow front was lower and finer grained than the preceding lobe. At a point in this progressive longitudinal “sampling” of both the 1986 and 1987 flows, the transformation to hyperconcentrated flow was reached, and the successive deposition of debris flow lobes ended. The point in each case was about 0.5 km downstream from the former picnic area. The pattern documents the progressive fining, improvement in sorting, and decline in strength (shown by loss of dispersed large clasts) longitudinally within the flow wave (fig. 18).

The tail of the flow wave clearly consisted of hyperconcentrated flow. Deposits having the texture characteristic of that flow type accreted to the sides of the debris flow channels and distributaries at levels lower than those achieved by the debris flow levees. Both the continuity in the successively finer and lower debris flow fronts and the textural transformation to hyperconcentrated flow indicate fractionation of a single flow wave. Some of these events have been interpreted as a series of separate flows because the differences in flow within a single flood wave, as well as the creation of distal surges, were not recognized. With the exception of the 1947 Kautz Creek flows, which were clearly separated, most of the flows in this category of magnitude and frequency began as single flood waves. The distal surges described above are variants of the surges resulting from temporary damming of a confined channel by the coarse boulder front of a flow. (See Pierson, 1980; and Costa, 1984.)

For both the 1986 and 1987 flows, the hyperconcentrated flow deposits of the receding flood wave overlie the sole layers of distributary debris flow channels (fig. 19).

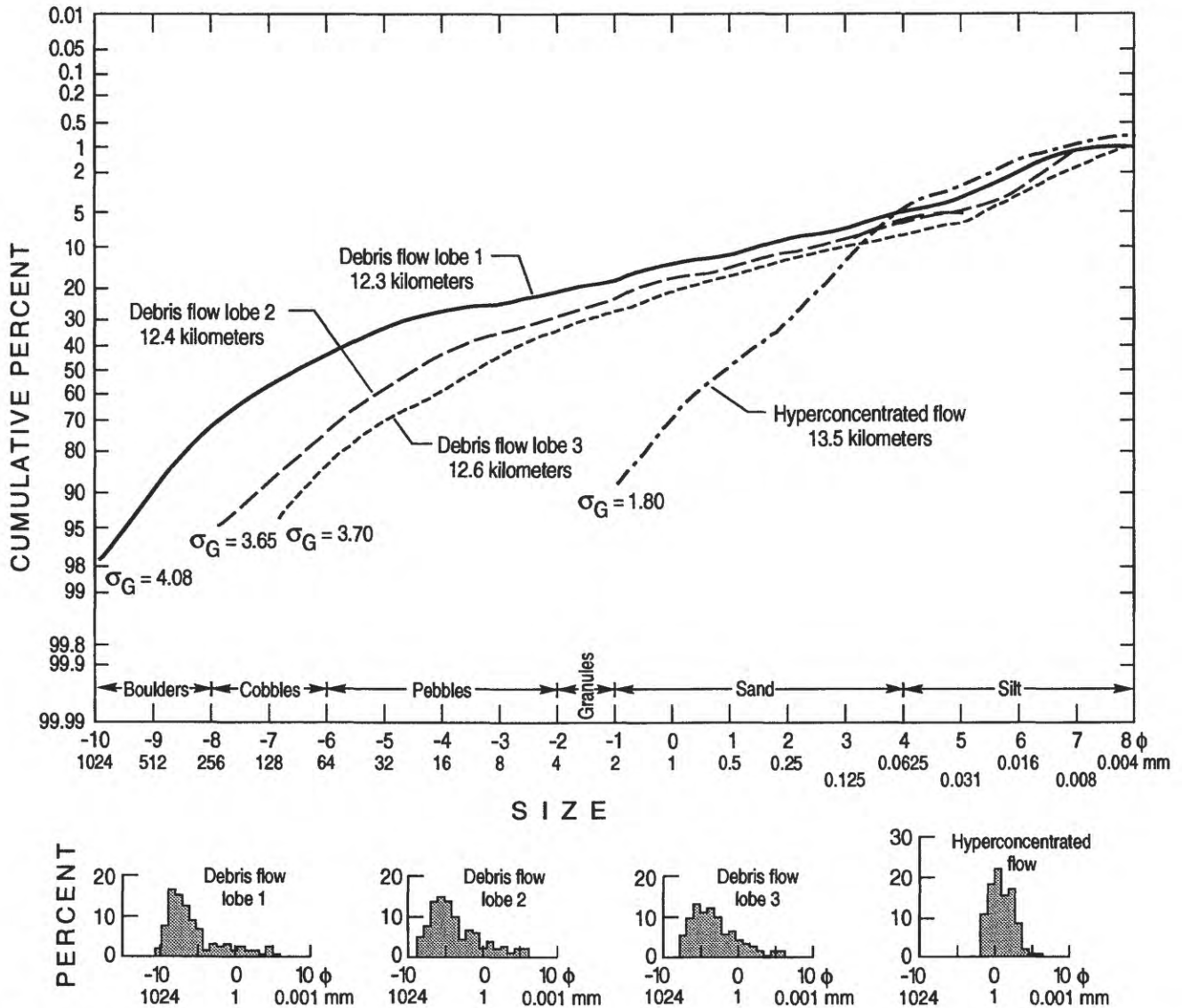


Figure 18. Cumulative curves of particle sizes within successive boulder fronts and hyperconcentrated-flow deposits formed during transformation of the Tahoma Creek debris flow of October 26, 1986. After deposition of the lobate fronts, only the hyperconcentrated tail of the flow continued downstream. Down-channel distance from the peak of Mount Rainier is shown for each deposit.

These highly compacted layers of pebbles dispersed in a silty sand matrix are identical to the Type II sole layers at the bases of lahars formed in 1980 at Mount St. Helens (Scott, 1988b).

After the hyperconcentrated tail of the main flow wave had passed, a small secondary debris flow was formed through dewatering of the coarse debris-flow deposits. Pore fluid draining from the coarse flow fronts contained sufficient silt (15 percent of deposits) and clay (2 percent of deposits) to yield a 1-cm-thick deposit in downstream channel thalwegs. The elevated deposit margins indicate strength in the range of debris flow. Most of the deposit is sand (75 percent, fig. 20) and, like a sole layer in a subsequently active channel, is unlikely to be preserved. This deposit is a smaller version of the large lahar formed

from the 1980 debris avalanche in the North Fork Toutle River at Mount St. Helens; it is likewise similar to the lahar formed from the main 1963 debris avalanche from Little Tahoma Peak into the White River drainage (fig. 20).

The deposit textures of the 1963 debris avalanche, the 1987 debris flow, and the flows derived from each by dewatering are illustrated in figure 20. The slope of the cumulative curve of each derivative flow is very similar to that of the finer part of the source flow. The dewatering process thus removes part of the matrix of the primary deposit but, unlike the more common direct transformation of the debris flows to hyperconcentrated flows, produces another, relatively small debris flow. The ability of the dewatering process to produce large flows is documented by the 1980 lahar in the North Fork Toutle River at Mount St.

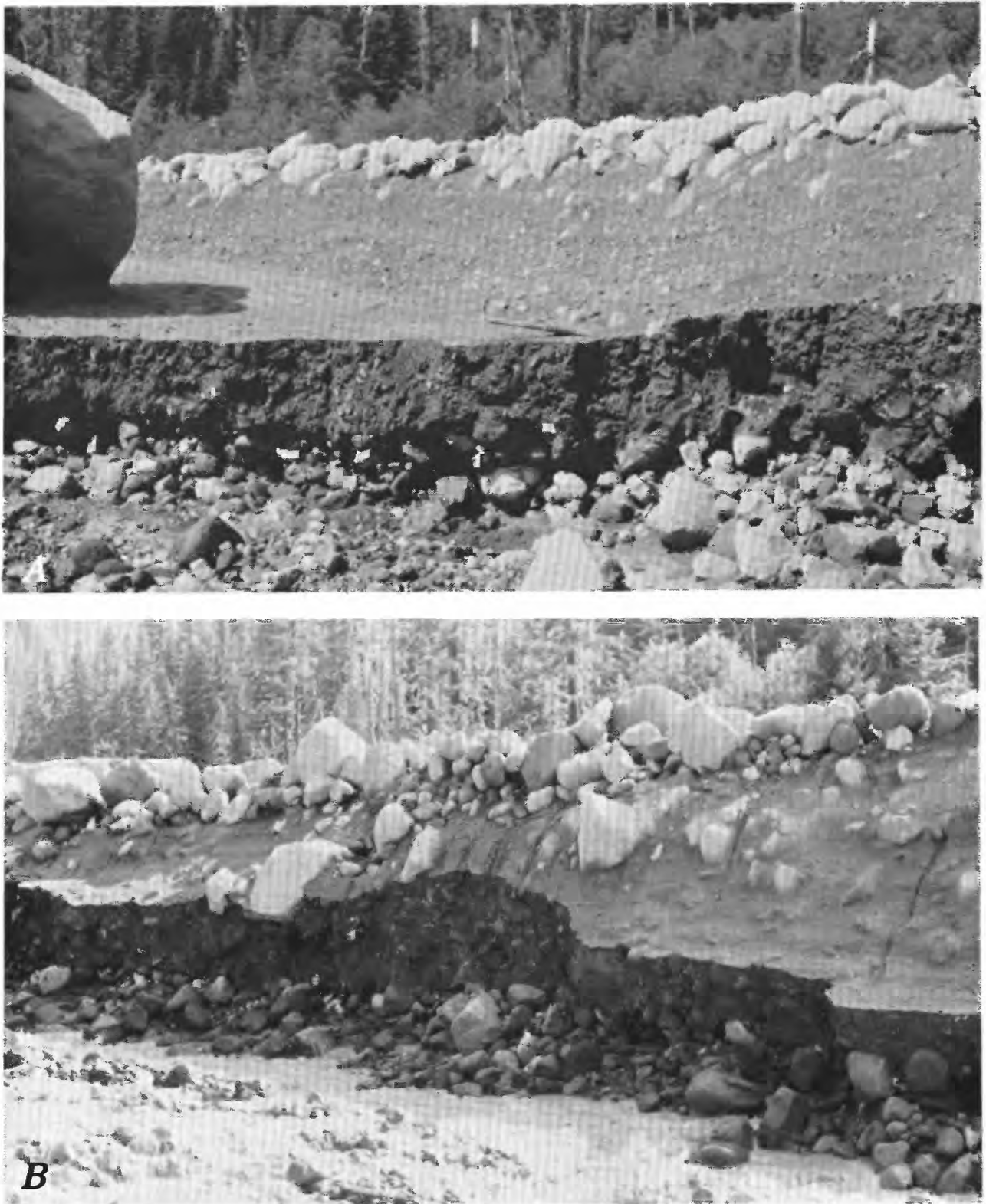


Figure 19. Debris-flow levees and underlying sole layers from recent flows along Tahoma Creek. *A*, Distributary channel of the October 1986 debris flow as it appeared in May 1987. Darker, compacted sole layer, in middle, overlies lighter channel bed material. Sole layer is 30–50 cm thick. Flow lines formed by recessional hyperconcentrated flow are visible just below the coarse debris at the tops of the levees. *B*, Main channel of the June 1987 debris flow at same site in July 1987. Sole layer, accreted to channel sides, is being eroded. Bank topped by levee is 3.5 m high.

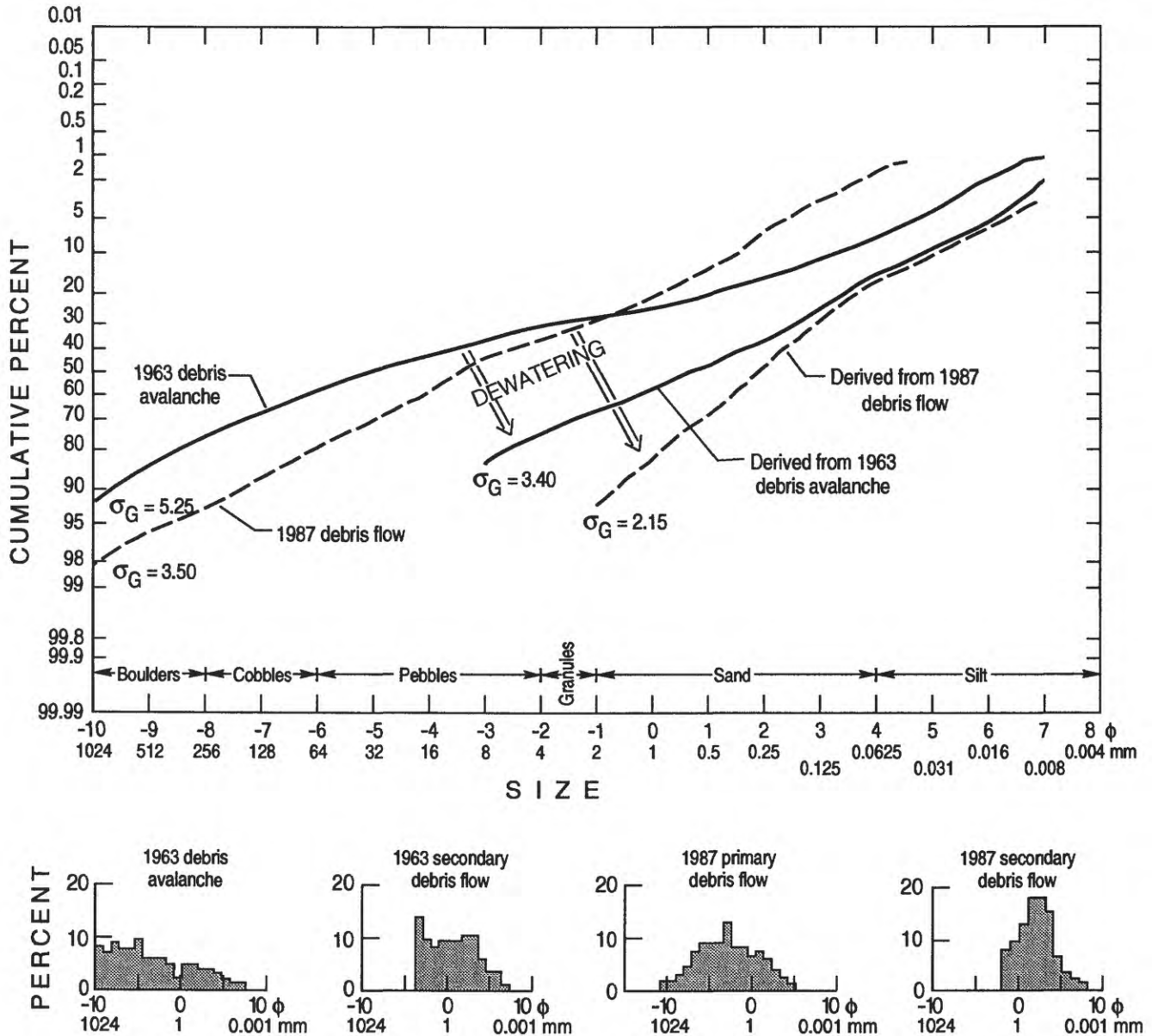


Figure 20. Cumulative curves of particle sizes of debris flows derived by dewatering from the main 1963 debris avalanche in the White River valley and the June 1987 debris flow in Tahoma Creek, compared with cumulative curves of the primary deposits.

Helens. No such origin, however, can be established at Mount Rainier for any debris flow larger than the relatively small 1963 example. This conclusion confirms our belief (and that of Crandell, 1971) that the large sector collapses at Mount Rainier continued directly as debris flows for long distances, rather than yielding thick, hummocky masses immobilized nearer the volcano.

DEBRIS AVALANCHES AND THE TAHOMA LAHAR

A small debris avalanche derived from a shallow slope failure is a second type of flow that is best included in the final general category, that of the smallest but most frequent

flows and avalanches. Although less frequent than glacial-outburst debris flows, several historical debris avalanches have occurred. The two largest examples traveled (1) from the Sunset Amphitheater onto the Tahoma Glacier in the early 20th century (fig. 21) and (2) from Little Tahoma Peak onto and beyond the Emmons Glacier in 1963 (fig. 4). Smaller debris avalanches fell onto the Winthrop Glacier in 1974 (Frank, 1985, p. 138), onto the Cowlitz Glacier in 1975 (Frank, 1985, p. 138-139), and onto the Winthrop Glacier in 1989.

The most recently documented debris avalanche originated August 16, 1989, from upper Curtis Ridge, as did the 1974 flow, and descended from 3,600 to 3,700 m (11,800 to 12,100 ft) to 1,950 m (6,400 ft) in altitude. Runout occurred over a horizontal distance of 4.1 km. The flow



Figure 21. Debris avalanche on the surface of the Tahoma Glacier, at the head of the South Puyallup River. Note the lighter, hydrothermally altered debris originating in the Sunset Amphitheater, contrasting with the darker morainal sediment, foreground, on and lateral to the Tahoma Glacier. The origin of this flow was similar to that of the Case III flow, the Tahoma Lahar.

deposits were noncohesive in texture; deposit thickness is surprisingly thin, as are the thicknesses of the deposits of the debris avalanches on the Tahoma and Emmons Glaciers. The total volume of the flow is probably in the range of 0.1 to 0.5 million m³, based on an average thickness of about 20 cm. The main seismic record of the avalanche consisted of complex, high-amplitude signals at 1706, 1714, 1715, and 1721 hours UTC on August 16, with the 1721 event lasting for 9 minutes (Norris, in press). The length of the signal is too great to reflect the velocity of the flow and probably reflects either continuing failure or the continued rolling of house-size boulders.

Multiple rock avalanches originated in pre-Rainier rocks that form the ridge known as Mount Wow and inundated the bottom of the Tahoma Creek valley with several lobes of debris, and another extended from the east end of the ridge of pre-Rainier terrane known as Mother Mountain almost to the Carbon River. The Mount Wow avalanches might have been triggered by the April 13, 1949, Olympia earthquake (*M* 7.1), as suggested by the decomposition stage of killed trees (decay sequence in Franklin and others, 1981).

These avalanches warrant serious attention because of their extremely rapid, catastrophic emplacement and their

known frequency and hazard at Mount Rainier and many other stratovolcanoes. Therefore, we focus on one large avalanche-derived flow that is typical of several young flows known at Mount Rainier. The Tahoma Lahar is the case history most suitable for planning within Park boundaries. It is distinct from the large sector-collapse debris avalanches and landslides but like those flows, also mobilized to a downstream lahar. Based on the record of all known flows, the smaller avalanches will not pose a large hazard outside the Park.

The Tahoma Lahar is interpreted as a variably disaggregated debris avalanche mainly transformed to a lahar (tables 2, 3). Its deposits form a distinctive unit in the Tahoma Creek watershed; they are mainly cohesive but are locally noncohesive in some lateral exposures. Like the Paradise Lahar, the unit is characterized by a yellow color and hydrothermally stained clasts. It is post-set W in age and thus much younger than the Paradise Lahar. The Tahoma Lahar, named here, is 0.5 to 2.0 m thick on valley-side slopes; more than 20 m thick in cross section near the base of Neoglacial deposits about 0.5 km upstream from the Wonderland Trail bridge across Tahoma Creek; and at least 4.3 m thick in the valley bottom as seen in exposures only 4.8 km upstream from the Highway 706 bridge. Most

deposition probably occurred in this area, filling the expanding lower valley of Tahoma Creek, where deposits are now covered by those of glacial-outburst floods. Clay content is variable but is characteristic of cohesive debris flow in most exposures. Because of further disaggregation of megaclasts in the flow and a more clayey recession phase (as we also propose for the Osceola Mudflow and other cohesive lahars), clay content is highest downstream where deposits were seen locally near the center of the valley.

The flow deposits overlie set W and compose the uppermost unit of most stratigraphic sections downstream from the Neoglacial terminus (about 100 m upstream from the trail bridge), as reported by Crandell (1971, p. 58) and verified in new exposures. The older Round Pass Mudflow supports trees as much as 700 to 800 years old, some of which were killed by the Tahoma Lahar and others which were killed at least 100 years ago by flows from Mount Wow. Significant attenuation of the Tahoma Lahar began as the flow left the confined channel upstream from the former picnic area. Although deposition was pronounced between the ex-picnic area and a point about 3 km downstream, the distal configuration is estimated (pl. 1) based on levels revealed by peak-stage deposits on valley-side slopes where they are not covered by younger deposits.

The stratigraphic relation of the Tahoma Lahar to Neoglacial morainal deposits and the estimate of tree ages on the lahar surface by Crandell (1971, p. 58) establish the time of the flow as shortly following the A.D. 1480 deposition of layer Wn, or about 400–500 years ago. Radiocarbon dates are variable, however. The outermost 25 rings of a tree that grew on the Round Pass Mudflow and that possibly was killed by the Tahoma Lahar provided an age of 560 ± 75 radiocarbon years. A radiocarbon date from the outermost wood from an apparently similar tree near the site of the picnic ground was 200 ± 50 years. That date is in a time interval for which the correlation between radiocarbon and calendar years is poor, and it could correlate with a calendar age of A.D. 1665 to 1955 (Stuiver and Becker, 1986). No volcanic activity is recorded from Mount Rainier near the probable time of the lahar.

The coloring of the surficial unit, which might be taken to indicate soil formation, instead reflects an origin as a mobilized debris avalanche of hydrothermally altered rock from the Sunset Amphitheater. The source is probably a different sector of the Sunset Amphitheater than that yielding the modern clay-rich debris avalanche on the Tahoma Glacier (fig. 21; see Crandell, 1971, p. 17). The trend of the distinctively colored Tahoma deposits within the Neoglacial moraine (incised by the branch of Tahoma Creek draining South Tahoma Glacier) suggests an origin above the Tahoma Glacier rather than from the South Tahoma Glacier. A debris avalanche above the Tahoma Glacier, however, should have created a correlative lahar in the South Puyallup River downstream from the Tahoma Glacier, and no such unit has yet been indisputably

identified. A highly likely correlative, however, is unit 4 of Crandell's measured section 8 (1971, p. 57), which is younger than the Electron Mudflow, as is the Tahoma Lahar, and is texturally similar to the Tahoma Lahar.

The Tahoma Lahar locally has a hummocky surface. Megaclasts form mounds in forested backwater areas of the fanhead downstream from the former picnic ground. The megaclasts are similar in composition (but with less clay) and color of alteration products to those in the modern debris avalanche on the surface of Tahoma Glacier. Many mound-forming megaclasts were eroded or buried by the glacial-outburst flood and debris flow of October 15, 1988. The strength of the Tahoma Lahar is indicated by a lake dammed by the lateral levee of the peak flow about 0.5 km upstream from the trail head. The lake had a maximum depth of about 2 m, a width of 30 m, and a length of approximately 100 m in 1989.

The peak flow of the Tahoma Lahar probably was too cohesive for a runout phase to have formed. A lahar-runout deposit of similar age occurs in the Nisqually River near National (fig. 9, tables 3, 4). That deposit contains wood with an age of 410 ± 75 radiocarbon years, corresponding to a true age of about 540 years (before 1994). It is more likely that the debris avalanche did not transform beyond a lahar and that the runout flow is a separate event.

HISTORICAL FLOODS COMPARED WITH DEBRIS FLOWS

Glacial-outburst debris flows and some smaller examples of both cohesive and noncohesive lahars are all likely to be less destructive than some historical floods have been. The largest floods of record were caused by intense precipitation on snow during prolonged warm periods, and they are described for comparison with the smallest, most frequent volcanic flows. Historical floods in the Nisqually River have been analyzed by Nelson (1987); peak annual discharges in the Puyallup River at Puyallup from 1915 to 1986 were compiled by Prych (1987, table 2).

Probably the largest post-settlement flood occurred in 1867 (described by Summers, 1978, p. 235). In early December, much of a heavy snowpack on Mount Rainier was melted by four days of warm rain, causing a major flood in at least the Cowlitz River system. The city of Monticello at the mouth of the Cowlitz was completely destroyed on December 17. Upstream flooding was not reported, because settlement there had not begun. However, several other large floods between 1886 and 1911 probably inundated the entire valley bottom of the upper Cowlitz River. The valley downstream from Packwood, which is as much as 3 km wide, was apparently inundated in March 1907 and possibly again in 1909 (Packwood History Committee, 1954; Superintendent's Reports, Mount Rainier National Park, 1907 and 1910; U.S. Geological Survey stream-gaging

Table 5. Summary of origins and transformations of debris flows at Mount Rainier.

Flow No. ¹	Origin	Example	Transformation ²	Planning or design case
Cohesive debris flows (>3–5 percent clay)				
1	Mobilization of deep-seated debris avalanche (sector collapse).	Osceola Mudflow, Electron Mudflow.	Commonly none; type C possible.	Case I.
Noncohesive debris flows (<3–5 percent clay)				
2	Melting of snow or ice by pyroclasts (flow, surge, fall) or lava, or by geothermal heat, steam eruptions.	National Lahar and many similar flows.	Type A common	Case II.
3	Mobilization of shallow debris avalanches	Tahoma Lahar (lateral part)	Type A probably common; type C possible.	Case III.
4	Relatively small, shallow debris avalanches that do not disaggregate to lahars.	1963 Little Tahoma Peak	Type C possible	None. ³
5	Mobilization of debris avalanche possibly caused by explosion.	Paradise Lahar	Type A probable	None. ³
6	Glacial-outburst floods bulked to debris flows:			
	(a) Precipitation-induced flows	1947 Kautz Creek	Type B common; type C probable.	Hazard zonation. ⁴
	(b) Clear-weather flows	1987 Tahoma Creekdo.....	Do. ⁴

¹Numbers used for comparison with table 6.

²Transformation types: A, Direct, progressive transformation of wave front to hyperconcentrated flow.
 B, Deposition of successive flow fronts; bypassed by dilute tail of hyperconcentrated flow.
 C, Dewatering of coarse deposits to yield secondary debris flow.

³Risk is much lower than in the three described planning cases.

⁴Site-specific hazard-zone mapping based on techniques described in the text.

records). Subsequent high flows occurred on the Cowlitz River at Packwood in 1933, 1959, and 1977, but cannot be directly compared. Inundation of the Cowlitz valley to a depth of approximately 2 m is described in several undated early accounts. The Nisqually River drainage was also flooded early in 1910, when flood waters from a drainage to the south overflowed into that river (Bretz, 1913, p. 27). In general, historical flood inundation has been similar in depth to that by the most recent lahar-runout flows (table 4).

Historical flood data for the Nisqually River near and downstream from Longmire (Nelson, 1987) show that floods having recurrence intervals of 25 to 500 yr generally have smaller areas of inundation than do lahars with similar recurrence intervals. This is especially true as recurrence intervals reach and exceed 100 years, because the more frequent volcanic and glacial-outburst debris flows attenuate rapidly at the base of the volcano (fig. 13), whereas rainfall floods amplify downstream with increased tributary inflow. A 500-yr flood will locally affect flood plains outside the active channel (Nelson, 1987, pls. 1 and 2), whereas a 500-yr volcaniclastic flow, like the National or even the Tahoma Lahar, could be catastrophic at a location like Longmire.

While dating the younger noncohesive lahars and their runout phases, we also dated some flood deposits and groups of such deposits (table 4). Some were probably local; others were the deposits of floods affecting all drainages of the mountain. Yet others may have been the distal flood waves evolved from upstream lahar-runout flows. In assessing risk, no presumption of a debris flow is made from fluvial

sediment unless a direct correlation is possible. The distal streamflow deposits of the National Lahar (fig. 11C) are an example of such a correlation.

SUMMARY OF FLOW ORIGINS AND TRANSFORMATIONS

In order to rank the flows according to magnitude and frequency, the preceding discussion focused on the relative sizes of the various flow types and the evidence for their ages. To assess risk, the size and frequency of flows must be known, but other factors, such as the probability of a warning (Costa, 1985), are also important. Table 5 extracts the general flow origins that can be recognized, as well as the transformations that occur with each type. For simplicity, the formation of a secondary debris flow from the surface or interstices of a primary debris flow is treated as a transformation (type C in table 5), but the original concept of flow transformations invoked a fundamental change in flow behavior (Fisher, 1983). Because the change is from debris flow to debris flow, albeit accompanied by a change in texture, there is no change in rheology.

Unlike cohesive debris flows, noncohesive flows undergo the complete transformation of the entire flood wave to hyperconcentrated streamflow, which then evolves to normal streamflow with sediment content below hyperconcentration. Both these distal transformations involve fundamental changes in flow behavior and grain interaction

(Scott, 1988b, table 9; Pierson and Costa, 1987). Each also involves the progressive loss of sediment, which, combined with the commonly more peaked flood wave of the noncohesive flows, can produce greater attenuation. Conversely, during the formative transformations to debris flow, as sediment bulks into the flow, the flow wave may be amplified in volume many times. These differences between cohesive and noncohesive debris flows are tendencies, not laws of behavior. For example, a cohesive flow can be more peaked, and can lose sediment rapidly by deposition on a wide flood plain. However, the overall tendencies are consistent with flow type.

Three types of flow transformations are represented in figures 2, 18, and 20. At Mount Rainier, the first (fig. 2) is the complete, progressive transformation of the entire flood wave (Scott, 1988b, fig. 37). The second (fig. 18) is the repeated, successive deposition of the flow front as a series of lobes, until only the hyperconcentrated tail of the flow remains to flow downstream. The third (fig. 20) is the creation of a secondary debris flow by dewatering and slumping of the surface of a debris avalanche, or by drainage of the matrix from coarse, clast-supported debris flow deposits. Avalanche dewatering has produced significant lahars elsewhere, but is not known to have produced any but small flows at Mount Rainier. Although large cohesive lahars have occurred in the post-Y time period, we found no upstream debris avalanches that corresponded in size and age and from which they could have been derived secondarily.

RISK ANALYSIS

Risk analysis is a generic term for methods that support decision-making by quantifying consequences (magnitude and extent of lahars, for example) and the probabilities of their occurrence (frequency of lahars) (National Research Council, 1988). Which of the types of flows in table 5 pose sufficient risk to influence downstream hazards planning? An initial premise is that volcanic debris flows and their transformations can be treated like other hydrologic hazards. That is, flow events of equivalent frequency require the same planning awareness, whether the flow wave consists of sediment moving interstitial water (debris flow, and the upper range of hyperconcentrated streamflow) or water moving sediment (floods, and the lower range of hyperconcentrated flow). Floods and volcanically induced flows can be treated as separate components of a mixed population with a minor overlap in their scales of magnitude: that is, the high end of the flood scale overlaps the low end of the volcanic flow scale. Pragmatically, the risks are additive. The chief practical differences between inundation by floods and inundation by lahars are the destructive impact forces of a lahar and the long-term effects of its deposits as contrasted with the ephemeral inundation by a flood.

"Hazard" refers both to the agent and to the potential for harm posed by that agent. Also, risk can be said to exist when something of value is at jeopardy. Thus, in the general case of volcanic hazards (Dibble and others, 1985):

$$(1) \text{ RISK} = \text{HAZARD} \times \text{VALUE} \times \text{VULNERABILITY},$$

where HAZARD is an event of known probability, VALUE is the economic assessment of loss, and VULNERABILITY reflects susceptibility for harm, which may vary for different things affected by the same hazard. The inclusion of the latter term is extremely valuable in assessing volcanic flow hazards.

A similar approach to the dangers of volcanic flows is:

$$(2) \text{ RISK} = \text{FLOW MAGNITUDE} \times \text{FLOW FREQUENCY} \times \text{VALUE} \times \text{VULNERABILITY},$$

where each flow subpopulation can be treated separately and ranked by the risk it poses. Although the results (table 6) are qualitative, they clearly separate the differing risk of each flow type and provide a logical basis for the quantitative analysis of individual case histories of flows that represent the flow types that pose the greatest risk (pl. 1). In this initial ranking, MAGNITUDE is replaced by a convenient surrogate, area of inundation, which is based on the extent of the flows as established by their deposits (tables 2, 3). FREQUENCY is the probability of each flow type, or the inverse of the recurrence interval. VALUE is also proportional to inundation area, but its inclusion is necessary to assess the relative risks of different size flows. At Mount Rainier, population and property values increase downstream in each watershed, approximately exponentially, but with a large increase as flow reaches the Puget Sound lowland (data from Pierce and Thurston Counties, Washington). Consequently, including a VALUE term correctly emphasizes the catastrophic potential of the larger flows.

The VULNERABILITY factor in equation 2 significantly affects the danger of certain flow types. That is, vulnerability to a flow type is reduced if there is the probability of a warning in the form of volcanic activity precursory to the flows. People and movable objects in the path of rapid debris avalanches at Mount Rainier are far more vulnerable than those near the attenuating debris flows of glacial-outwash or rainfall origin. Vulnerability also depends on probable reservoir levels and whether they can be drawn down in the event of a warning. For example, vulnerability is reduced by the fact that Mud Mountain Reservoir on the White River is solely a flood-control structure and is thus normally empty.

No single flow type and origin will pose the greatest hazard throughout an entire river system. On the highly populated Puget Sound lowland, the huge sector-collapse debris avalanches mobilized as lahars (flow 1, table 6) pose

Table 6. Ranking of debris flows described in table 5 by magnitude, frequency, and risk.

Rank from greatest to least		
Magnitude (Inundation area)	Frequency	Risk
Flow 1	Flow 6	Flow 1
Flow 2	Flow 4	Flow 2
Flow 4	Flow 3	Flow 3
Flow 5	Flow 2	Flow 5
Flow 3	Flow 5	Flow 4
Flow 6	Flow 1	Flow 6

the greatest danger. In valleys on and immediately adjacent to the volcano, noncohesive lahars (flows 2, 3, or 5, table 6) and debris avalanches (flow 4, table 6) pose the greatest danger. And, for hikers along proglacial streams on the volcano, a debris flow formed from a glacial-outburst flood (flow 6, table 6) is the greatest statistical risk.

FLOW FREQUENCY AND RISK AT MOUNT RAINIER

This discussion focuses on flows of the frequencies most commonly used in long-term hydrologic planning—100 and 500 years (Brice, 1981). These recurrence intervals correspond to probabilities of 1 percent and 0.2 percent per year. By contrast, Latter and others (1981) believe it is “desirable” to incorporate events with recurrence intervals of 1,000 and perhaps 10,000 years when assessing volcanic risk. Although practice is variable, design frequency for bridges on primary roads is commonly 50 years, with some states using a 50-yr flood for the bridge superstructure and a 100-yr flood for the substructure (Brice, 1981). Flow frequencies for structures such as reservoirs and power plants are commonly lower (that is, return periods are higher) than these values and are commonly controlled by economic factors (Linsley and others, 1958).

In occurrence, lahars at Mount Rainier differ from those at Mount St. Helens in an important way. The latter have a significant tendency to cluster in groups, and their time distribution can be analyzed both in an eruptive period, as at present, or over any other time interval. At Mount Rainier, in contrast, both volcanism and lahars are scattered throughout postglacial time (tables 2–4). Therefore, the occurrence of one large lahar does not increase the odds of a second, as it does during the modern eruptive period at Mount St. Helens. The assumption of basically random occurrence, as in flood analysis, is probably valid at Rainier.

All recurrence intervals discussed here are based on mountain-wide occurrences over undivided intervals of postglacial time. This dispersion of risk, rather than its definition within each river system, reflects the uncertainty in knowing what river system or systems will experience the

next major lahar. For example, the Carbon River system records the lowest frequency of lahars. However, considering the modern topography and structure of the volcano, that river system may have substantial risk of conveying part or most of a huge, sector-collapse lahar. The river system also contains a large volume of glacial ice that, although covered with insulating rockslide debris, is subject to melting and thus to the formation of noncohesive lahars. The example illustrates the need to reassess risk once the location of any precursor intrusive activity is evident. For example, volcanic activity affecting the Carbon River sector will pose an extreme risk of large debris flows.

Conversely, the White River system illustrates the possible temporary reduction in risk of a second large lahar following a significant sector collapse and before edifice reconstruction. The crater remaining after the Osceola Mudflow is now largely infilled, however, and the original failure plane could facilitate renewed failure. Correlations between changes in risk and the occurrence of flows are complicated, perhaps hopelessly so, by the lack of knowledge of hydrothermal alteration and structure within the edifice. Supporting evidence of a temporary risk reduction is not definitive and, at Rainier, cohesive flows have recurred in the same drainage.

Other factors also support a volcano-wide risk assessment: (1) large cohesive flows have recurred from a single drainage; (2) a single flow has affected more than one drainage (Osceola and Round Pass Mudflows); (3) three of the river systems, the White, Puyallup, and Carbon Rivers, join downstream within range of Rainier lahars; and (4) a major explosive eruption like that at Mount St. Helens in 1980 would produce lahars in all of the main drainages. The situation is largely analogous to arid-zone flood-hazard mapping where, although only one sector of an alluvial fan will probably be affected by any given flood, all parts must be considered potentially prone to inundation (Scott and others, 1987; Scott, 1992).

The length of time needed to evaluate frequency depends on flow size—the smaller the flow type, the shorter the time span needed to establish recurrence interval statistically. The time intervals selected, such as the post-Y time interval used for the definition of noncohesive lahars, are in part a function of geological convenience, but each is sufficient to define flow probability. Even if older and smaller flows are eroded or obscured (a possibility given the number of postglacial episodes of aggradation and degradation in entire river systems), the analysis is not affected substantially.

Lahars are far more numerous than episodes of known volcanic activity (producing juvenile eruptive products) at Mount Rainier. Neither cohesive nor noncohesive lahars correlate well with volcanism, and many of the latter probably resulted from geothermal heat flux and steam eruptions. The noncohesive lahars that formed by bulking of meltwater surges are not obviously linked to the most clearly

recorded eruptions, those producing tephra. Prevailing west winds have distributed Rainier tephra on the east side of the volcano (Mullineaux, 1974), yet the Cowlitz River (east side) has a sparser record of lahars than all other Rainier drainages except the Carbon River (northwest side), and the large number of flows in the Nisqually River (southwest side) is similar to that in the White River (northeast side). The lack of a clearly recorded association of the large cohesive lahars with known volcanism is discussed by Crandell (1971), and his conclusion is reinforced by the ages of the additional cohesive lahars reported here.

DEBRIS FLOWS AND SUMMIT-CONE VOLCANISM

Along with the small glacial-outburst flows, a previously unrecognized grouping of lahars is an exception to the general lack of time-clustering of flows at Mount Rainier. Noncohesive lahars and derivative lahar-runout flows (tables 3 and 4) occurred throughout the post-Y time interval, as described in the section on flows of intermediate size and frequency. The deposits of these flows form much of the fill in the White and Nisqually River valleys recognized by Crandell (1971) and then believed to have had a normal fluvial origin. The last such flow occurred in 1947. There is, however, a clear concentration of flows late within the post-C, pre-W time interval. The radiocarbon dates in table 4 define flow activity that peaked between about 2,200 and 800 radiocarbon years ago, and particularly in the last 500–600 radiocarbon years of that interval. The interval is bounded by calendar ages of about 2,250 to 710 years (Stuiver and Becker, 1986).

This interval of flow activity does not coincide with an eruptive period as defined at Mount St. Helens (Mullineaux, 1986). Rather, it overlaps the assumed end of lava and pyroclastic flow activity during building of the summit cone above the east rim of the volcano (fig. 4; Fiske and others, 1963, p. 80). Summit-cone lava flows are believed to have occurred between about 2,100 and 1,200 calendar years ago (Crandell, 1971, p. 14). Either lahar-producing activity associated with the construction of the summit cone continued later than believed, or later pulses of geothermal heat or steam eruptions created major meltwater surges. Geothermal activity at the modern summit (Frank and Friedman, 1974) produces only local melting.

DESIGN OR PLANNING CASES AND HAZARD ZONATION

DEFINITION OF CASES

The dynamics of debris flows are described here in hydrologic and hydraulic terms, because that nomenclature

is appropriate, and because it is familiar to land-use planners and civil engineers dealing with structures subject to inundation. What we believe is the best example of each of the flow types that pose risk (table 6) is described in this section, its dynamics are presented (table 7), and its flow cross sections are portrayed (pl. 1). There is no substitute for the description of real-world flow behavior, through the case-history approach when dealing with engineering problems involving complex phenomena. No rheologic model deals with the spectrum of debris flow behavior at Mount Rainier.

MEASUREMENTS AND ESTIMATES OF FLOW DYNAMICS

Velocities (table 7) are based on measurements of runup on obstacles to flow, or on superelevation of flow around bends. Johnson (1970), Costa (1984), Fairchild (1985), Pierson (1985), and Scott (1988b) have analyzed or commented on field applications of this method and the accuracy of the results. The behavior of the large cohesive lahars near the boundary of the Puget Sound lowland is critical, so special attention was given to the measurements near that point. Several sets of measurements defined flow above 15 m/s and approaching 20 m/s. No runup measurement was ideal, as in the case of a steep bare surface (a frictionless surface is assumed) normal to flow. We believe that 20 m/s is a conservative minimum velocity for the cohesive lahars at the lowland boundary. A velocity in the range of 25 to 30 m/s was obtained from runup of the branch of the Osceola Mudflow in the West Fork White River where it entered the White River valley at a high angle, and the estimate of velocity of at least 40 m/s for the Round Pass Mudflow near the base of the volcano was noted in the section on that lahar. In general, runup measurements were more readily obtained than measurements of superelevation in bends for both cohesive and noncohesive lahars.

Cross sections were defined by the distribution of deposits. Unlike floods, debris flows leave deposits accreting on valley sides to the level of peak flow. Delineation of the highest peak flow deposit, equivalent to the high water mark of a flood, was commonly confirmed at multiple points, and the cross sections of flows were measured only where the valley-bottom deposit of the same flow was known. In a few instances, the thickness of valley fill of a flow was extrapolated longitudinally. As noted above (under "Flow magnitude and frequency"), markedly concave flow surfaces in sharp bends may have the effect of exaggerating both cross-sectional areas and the discharges calculated from them (Webb and others 1989, p. 22, table 10). However, of the sites used for calculating the discharges shown in table 7, none has a radius of curvature sufficient to cause this effect.

Flow wave volumes were estimated from the volumes of their deposits. The volume was in most cases not increased

Table 7. Characteristics of design- or planning-case lahars.

[Characteristics determined as described in text; N.A. = not applicable]

Characteristic	Maximum lahar	Case I	Case II	Case III
Debris flow type	Cohesive	Cohesive	Noncohesive	Usually cohesive. ¹
Recurrence interval (yrs)	~10,000	500–1,000	100–500	<100
Volume at lowland boundary (x10 ⁶ m ³).	>3,000	230	60 (Puyallup R.) 65 (Carbon R.)	N.A.
Mean flow velocity (m/s):				
Base of volcano	² >40	² >30	10	² >30
Lowland boundary	>20	~20	~7	N.A.
1 km on lowland	~10	~8	~3–4	N.A.
Cross-sectional area of flow at lowland boundary (m ²).	~90,000	~16,000	1,000 (Puyallup R.) 1,200 (Carbon R.)	N.A.
Peak discharge at lowland boundary (m ³ /s).	>1,800,000	~320,000	7,700 (Puyallup R.) 8,400 (Carbon R.)	N.A.
Flow depth (m):				
Base of volcano	~200	~50	15	55
Lowland boundary	~100	22	8	N.A.
1 km on lowland	≤30	~10	1–3	N.A.
Sediment concentration at lowland boundary (percent by volume). ³	>60	>60	~40 (Puyallup R.) ~45 (Carbon R.)	N.A.
Extent (or inundation area)	To Puget Sound or Columbia R. (in Cowlitz R. drainage).	Inundation of 36 km ² (Electron) to ~50 km ² (modern recurrence of same flow).	All active flood plains (except Cowlitz R.) above reservoirs, if present; otherwise upstream of Puyallup.	Runout phases of noncohesive lahar could extend an additional 10 km.

¹Some may be partly or entirely noncohesive depending on source area.²Estimated by comparison with similar flows at other volcanoes.³Estimated using the linear relation observed between sorting and concentration at Mount St. Helens (Scott, 1988b).

to account for loss of water because, in the case of the cohesive debris flows, a large proportion of the deposits probably remained saturated, and in the case of the noncohesive debris flows, the water content of the flow wave was largely interstitial between grains in nearly continuous contact. Volumetric comparisons worked well for the Electron Mudflow where the distal end is defined and the deposits were extensively augered (Crandell, 1971). It is less exact where flows continued into Puget Sound or, in the case of the runout phases of the noncohesive lahars, where the flow wave was diluted eventually to streamflow. Corrections for loss of deposits by erosion are an additional source of error, but reconstructions of the original depositional surfaces were possible for some flows.

MAXIMUM LAHAR

The term “maximum lahar” is substituted for the “worst-case flow” of hydrologic analysis, because there can always be a flow worse than that defined as the worst case. We also prefer the term to “most-extreme lahar,” used for a moraine-dammed-lake breakout in which the most-extreme case is displacement of an entire lake by a snow or debris avalanche (Laenen and others, 1992). The true “worst-case” or “most-extreme” analog at Rainier is the improbable removal of the entire edifice. “Maximum lahar” is analogous to the “maximum mudflow” or “maximum

credible mudflow” used in forecasts of lahars at Mount St. Helens (for example, U.S. Army Corps of Engineers, 1985). The term is intended to imply that, although larger flows are possible, they are so unlikely they need not be considered.

The Osceola Mudflow (Crandell, 1971), is the maximum lahar at Mount Rainier. Cross sections of this flow are shown on plate 1, and its dynamics are described in table 7. The inundation area of the actual flow is easily discernible on the Puget Sound lowland (Crandell, 1963b, 1971), although the flow was difficult to define upstream (noted in sections O–1 and O–2, pl. 1). The inundation area of a modern cohesive lahar of the same size could extend to Puget Sound, through Tacoma along the Puyallup River and through Seattle by way of the Green River system and the Duwamish Waterway. The lower resistance to flow of the modern unforested river valleys would allow a recurrence of this flow to go farther and faster than did the original flow approximately 5,000 radiocarbon years ago. Relative sea level in the Duwamish Embayment of Puget Sound was higher at that time, and the flow entered the sound farther upstream. In a well 6 km northwest of Auburn, deposits of the flow occur 85 m beneath present sea level and are 7 m thick (Luzier, 1969, p. 14); submarine deposition is probable.

The Osceola Mudflow had a volume many times that of the next largest cohesive lahar. We accept Crandell's (1971) estimate of 2–3 km³ for the present volume, but the original volume may have been as much as twice that amount if

subsequent erosion and a possibly larger original submarine extent are taken into account. A lahar this size has occurred only once in postglacial time, within the last 10,000 years. When compared with all other large cohesive lahars, it is a statistical outlier. It is tentatively assigned a recurrence interval of 10,000 years. Thus, for illustrative purposes, its probability approximates that of a return of glaciation to the Puget Sound lowland. One or more events of at least this size have a 1 percent chance of occurring within a century (Reich, 1973). An event of this frequency is not normally considered in hazards planning, but Latter and others (1981) propose that it should be. In modern risk analysis, such an event is described as one of "low probability and high consequences," with the implication that the risk may be unacceptable at even very small probabilities.

The record at Mount Rainier indicates that the most probable recurrence of a maximum lahar will be a debris avalanche that transforms directly to a lahar on or near the volcano. Primary transformation is not a certainty, however, and Crandell (1988, fig. 18) calculates the probable runout distances in each river system at Mount Rainier of untransformed debris avalanches with a volume of at least 1 km^3 . The hazards of untransformed debris avalanches are discussed by many (including Crandell, 1988; Scheidegger, 1973; Siebert and others, 1987; and Francis and Self, 1987); the risks from debris avalanches are generally greater than those from lahars, mainly because of higher flow velocities. A debris avalanche from Mount Rainier would probably be at least partially saturated; such a flow would have the potential to yield a large secondary lahar as did the 1980 example at Mount St. Helens. If a primary debris avalanche occurs, downstream warnings of a subsequent lahar would be necessary. The lag time at Mount St. Helens from avalanche emplacement to lahar initiation was about five hours. This sequence of events can be regarded as a much less probable variant of both the maximum lahar and Case I, below.

DESIGN OR PLANNING CASE I

Case I is a large cohesive debris flow having a recurrence interval of 500 to 1,000 years and is the appropriate case for long-term planning in the watersheds draining Mount Rainier. Even one event (or more) equal to or greater than a flow with a 1,000-yr recurrence interval has a 9.5 percent probability of occurring at least once in the next century (Reich, 1973).

If the Osceola Mudflow is excluded on the grounds that it is a statistical outlier of this flow type, several smaller cohesive lahars form a discrete population. The most recent and best defined of these flows is the Electron Mudflow. The importance of this flow to hazard analysis has long been recognized (Crandell, 1971; Cullen, 1977; and Cullen Tanaka, 1983). The lahar is here assigned a magnitude and

frequency, and its dynamics are specified at the margin of the Puget Sound lowland, where risk increases greatly (table 7, pl. 1).

The volume of the Electron Mudflow deposits on the Puget Sound lowland was satisfactorily determined by Crandell (1971, p. 57) as slightly more than 183 million m^3 . The flow deposit is overlain by reworked deposits of the flow. Its original volume (table 7) is estimated by assuming deposition near the levels of the highest medial flow deposits. This assumption is based on the downstream behavior of the cohesive lahar originating in the North Fork Toutle River at Mount St. Helens in 1980.

The risk of this type of flow surpasses that of all smaller but more frequent flows. Moreover, the risk is increased by the lack of a clear association with major episodes of volcanic activity which could provide a warning (Crandell, 1971; Scott and Janda, 1987). Such flows may be triggered by nonmagmatic seismicity, by steam eruptions, or just by gravity in places where a failure plane has been lubricated by clay and geothermal pore fluids. No assumption of precursor volcanic activity can be made in planning for these flows. This is a conservative approach that is consistent with the available evidence.

Sector collapses of the size that produce cohesive lahars can occur on any side of the volcano (Frank, 1985, p. 181). Given the lack of evidence that one flow of this type will stabilize the affected sector of the volcano thereafter, this is the best assumption. Potential effects on downstream areas differ only slightly among watersheds. The main complicating factor is the presence of reservoirs in three of the five major watersheds.

A modern recurrence of a large cohesive lahar will inundate a larger area of the Puget Sound lowland than did the prehistoric flows because of the greatly reduced friction on deforested flood plains. The distribution of a modern flow can be predicted by estimating the deposit thickness on unforested flood plains and distributing the design volume at the mountain front over the corresponding area. On the basis of the behavior of the 1980 cohesive lahar at Mount St. Helens, which traversed clearcut and forested flood plains, the modern thickness would be close to 70 percent of the prehistoric thickness. Some additional bulking of the flow on the cleared flood plains will reduce its natural rate of attenuation, but erosion will probably be concentrated in active channels as it was under forested conditions. Thus the inundation area of a modern flow of the same type and same original volume as the Electron Mudflow could increase to approximately 50 km^2 (compared to the 36-km^2 area of the Electron). A similar but somewhat larger volume will just be spread over a larger area.

The flow record indicates that the most probable recurrence of Case I will be a debris avalanche that transforms to a lahar on or near the volcano. As noted for the "maximum lahar," this origin is not a certainty. Untransformed debris avalanches (Crandell, 1971, fig. 18)

can be regarded as a much less probable variant of Case I. Because such flows have not occurred at Mount Rainier, it is impossible to specify probable magnitudes or frequencies except by means of examples at other volcanoes, as Crandell has done.

DESIGN OR PLANNING CASE II

Case II is a noncohesive flow represented by the National Lahar, which with its runout phases is a suitable example of this category that can be extrapolated to all watersheds. The recurrence interval of noncohesive flows in the size range of the National is near the lower end of the 100- to 500-yr range and thus is analogous to the 100-yr flood, one widely considered for structure design and flood-plain management. Flow cross sections (pl. 1) can be applied upstream from reservoirs.

Comparison shows that this design debris flow will be larger than design water floods in upstream reaches, but will be smaller downstream. This difference is explained by the continuous attenuation of a lahar or lahar-runout flow, as compared with the typical amplification of a meteorologic flood as tributary inflows increase downstream. Measured flood-carrying capacities of the Puyallup, White, and Carbon Rivers on the Puget Sound lowland illustrate this trend (Prych, 1987). Nonetheless, the noncohesive debris flows increase the risk of flood-plain inundation throughout a river system without reservoirs. Upstream, the lahar subpopulation presents more risk than meteorologic floods. Inundation levels can be estimated by adjusting the cross-sectional areas (pl. 1) for the attenuation, as shown, due to distance from the volcano.

The flow wave in this design and planning case consists of hyperconcentrated flow during much of the flow interval beyond the base of the volcano. Hyperconcentrated flow probably will persist to the boundary of the Puget Sound lowland, but will transform to normal streamflow rapidly beyond that point because of rapid loss of sediment from the flow wave on flood-plain surfaces. The runout phases of the National Lahar (figs. 2, 11B, and 11C) are representative of changes expected in future noncohesive flows.

If Case I presents the greatest total risk, should Case II be considered as well as Case I in any part of a drainage? The answer here is affirmative, because of the distinction between planning for the longest term that is cost-effective, as in a land-use evaluation contingent on Case I, and designing for a flow with a high degree of probability during the life of an individual structure. For example, a flow equal to or greater than the event with a recurrence interval of 100 years has a 64 percent probability of occurring at least once in the next century (Reich, 1973).

An additional rationale for the application of Case II is its probably greater association with precursory volcanic activity than Case I. In the event of impending eruptive

activity forecast by a monitoring network, Case II is the minimal flow event that logically can be expected. Each river system contains enough glacial ice to provide meltwater capable of producing a noncohesive lahar of this size.

DESIGN OR PLANNING CASE III

Case III is a relatively small debris avalanche, originating as a landslide, that probably will transform to a debris flow. Two moderate-sized and several small debris and rock avalanches have occurred since 1900. The largest of these came within a kilometer of the White River Campground in 1963, albeit at a time (December) when the campground was closed (Crandell and Fahnstock, 1965). Neither moderate-sized flow transformed directly to a lahar, but both produced small debris flows by dewatering and slumping of their surfaces.

The origin of the Case III flow is the same as that of both Case I and the maximum lahar, but the smaller Case III examples occur much more frequently on the volcano. They probably will recur without warning and certainly will move at high velocity. As the case history best exemplifying this flow, the debris avalanche yielding the Tahoma Lahar (pl. 1) is the most appropriate example. At least part of that debris avalanche transformed to a hummocky lahar with a flow depth of as much as 55 m in confined canyons on the volcano and 20 m shortly beyond the base of the volcano. Subsequent attenuation was rapid.

Greatly adding to the risk from these flows is their high velocities, almost certainly well in excess of 30 m/s (67 mph). The velocity of the largest avalanche from Little Tahoma Peak was at least 35 to 40 m/s (Crandell and Fahnstock, 1965). A velocity of about 50 m/s, which was increasing at the point of measurement, was reported for the 1980 debris avalanche at Mount St. Helens (Voight and others, 1981).

The best outcome of planning for such a rapid flow can only be to minimize exposure. Risk associated with a runout flow like that possibly developed from the Tahoma Lahar will be much less than that of Case II. Within the Park, however, consideration can be given to siting new campgrounds and facilities above the flow depths of the Tahoma flow wave (pl. 1), and in other drainages, above its extrapolated cross-sectional area adjusted for distance from the summit.

HAZARD ZONATION

Hazard-zone analysis is another approach to assessing the composite risk of all flows, including those smaller and more frequent than the above cases. The approach involves the determination of past inundation levels from tephra

layers, vegetation, and fan and flood-plain morphology. The combination of criteria yields areas of inundation over several time intervals useful for land-use planning. Hazard zones delineated by deposits and dendrochronology have effectively defined the risks of small, high-frequency flows at Mount Shasta (Osterkamp and others, 1985). A similar analysis can be useful in siting individual facilities in Mount Rainier National Park. Hazard zones, however, are not calculated or presented in this report. The zones can be determined, as needed, for specific locations according to the following guidelines.

ZONE I

Tephra set W, deposited over most of the National Park, can be treated as a paleohydrologic crest-stage gage by measuring the height to which the layer has been truncated by flow against valley side slopes. Set W consists of two layers, deposited in A.D. 1480 and 1482 (Yamaguchi, 1983 and 1985). The first of the two layers predominates at Mount Rainier. Its eroded lower margin records the highest level of flow since deposition in at least the upper part of each drainage surrounding the mountain. Where a drainage did not convey a significant flow like the Tahoma Lahar in the last 500 years, the level to which set W is eroded provides an estimate of the inundation potential without a major eruption or sector collapse. Zone I is thus defined. Because zone I defines only the most recent time interval, preference in planning should be given to the planning and design case histories selected with the perspective of longer time periods.

ZONE II

The area inundated since the beginning of the 20th century can be established by the historical record and by dendrochronology; such data can provide a good approximation of the level to which flow has extended in the last century. In most cases, glacial-outwash flow patterns subsequent to the start of Neoglacial recession about 60 to 200 years ago (Sigafoos and Hendricks, 1961 and 1972; Burbank, 1981) are discernible from vegetation patterns on aerial photographs.

ZONE III

This area encompasses the modern alluvial fans at the base of the volcano, active flood plains, and marginal areas subject to lateral erosion. The boundaries would seem obvious except on the alluvial fans, whose surfaces are broad and convex and locally support a mature forest. The fans record debris flow deposition triggered by the decreasing slope and expansion in reaches at the base of the volcano. Debulking

is rapid in such areas, which explains why the smaller flows attenuate rapidly (fig. 13).

LATERAL EROSION ASSOCIATED WITH HAZARD ZONE III

Lateral (or bank) erosion is an additional hazard downstream along the streams with normal flood plains. The high terrace bordering the Nisqually River upstream from Longmire (figs. 9 and 11A; set W on surface) is being cut by normal fluvial erosion, requiring some resiting of trails. Progressive lateral erosion tends to be localized and is controlled by factors such as channel pattern (Brice and Blodgett, 1978, chap. 4), bank material (Schumm, 1960, 1961), and vegetation (Scott, 1981).

Channel pattern normally will be the determining factor in localizing erosion at banks cut against a terrace. A meandering pattern will result in erosion at the outsides of bends, for example. Braided streams in the proglacial environments may regularly impinge against bedrock valley walls, and where streams are confined by steep-sided Neoglacial moraines, erosion can be large, episodic, and unpredictable in location. Trails and climbing routes along crests of Neoglacial moraines are subject to mass failures triggered by lateral erosion at the base of the moraine. Most of the major streams fall in the category of "streams wider at bends," which, according to Brice and Blodgett (1978), have greater lateral instability than either equiwidth streams or those with random variation.

The White River shows the effects of a cohesive valley fill, the deposits of the Osceola Mudflow, in reducing lateral erosion. Where the active channel is incised into the valley fill, an uncommonly low width/depth ratio results (in the range of 4-7 at locations downstream from the national park). This low ratio is a function (inverse) of the high silt and clay content of the central-valley facies of the Osceola and is consistent with the findings of Schumm (1960) elsewhere.

PROBABILITY OF PRECURSOR VOLCANIC ACTIVITY

Detectable volcanic activity may precede the largest cohesive and noncohesive lahars, but this is not a premise on which the planning process can rely. As demonstrated by the flow record over the last thousand years (a period including lahars that exemplify each of the planning cases), no flows correspond to the single known episode of major activity during that time (tables 1 through 4). A correlation with precursor events is suggested by the concentration of large flows, such as the Osceola Mudflow and Paradise Lahar, during the mid-Holocene when many tephra-producing

events occurred. This association, noted by Crandell (1971) and Mullineaux (1974, p. 17), does not relate the flows directly to volcanism but is evidence of a linkage that may lack better definition only because of the confidence limits on radiocarbon dating.

The potential nonvolcanic causes of both the cohesive and noncohesive debris flows and of the relatively small debris avalanches at Mount Rainier include (1) regional, nonmagmatic seismicity; (2) edifice effects; and (3) several phreatic effects of the active hydrothermal system, including rapid ice or snow melting, steam eruptions, failure in response to increased pore pressure, and lubrication of potential slip surfaces such as those of previous deep-seated failures again buried by edifice construction. The first two effects are discussed further here.

Mount Rainier is the site of occasional small earthquakes, the largest two of which may have been due to a strike-slip fault on the south side of the volcano (Crosson and Frank, 1975; Crosson and Lin, 1975). Nevertheless, the general areal distribution of historical earthquakes, such as a cluster of seven earthquakes in 1987 with magnitudes of 0.8 to 2.1 at depths less than 5 km, shows a clear association with the volcano (University of Washington Geophysics Program, written commun., 1988). These earthquakes may be the result of edifice effects. Like many subduction-related stratovolcanoes, Mount Rainier is noteworthy for the large mass of layered material at high altitude, leading to gravitational stresses such as those described as edifice effects in a study of Hawaiian volcanoes (Fiske and Jackson, 1972). Some microearthquake activity at Rainier was ascribed to these crustal-loading effects (Unger and Decker, 1970), a view later modified (Unger and Mills, 1972). Some low-frequency tremors recorded at Longmire may result from glacier or debris flow movement in the Tahoma Creek, Kautz Creek, or upper Nisqually River drainages.

The Rainier area is subject to large regional earthquakes (Gower, 1978). If the Cascadia subduction zone offshore is storing the elastic energy characteristic of other subduction zones, several great earthquakes are necessary to fill the seismic gap represented by the zone (Heaton and Hartzell, 1987). The deep, plate-boundary earthquakes of 1949 (M 7.1) and 1965 (M 6.5), both with epicenters on the east side of Puget Sound, caused local incidences of rock-falls, slope failures, and flood-plain liquefaction throughout much of western Washington (Schuster and Chleborad, 1989). As many as five great earthquakes have occurred in the last 3,100 years, the latest about 300 years ago, as suggested by the stratigraphy of buried wetlands in southwest Washington (Atwater, 1988). Major slope failures can occur, however, in response to minor seismic accelerations at times of high susceptibility; for example, the largest historic landslide in Canada was probably triggered by a small (M 3.1) seismic event (Evans, 1989).

Many similar volcanoes have experienced collapses yielding large debris avalanches; Mount Rainier is appar-

ently unusual because the large collapses have transformed directly to lahars, but more detailed study may show this also has occurred at some other volcanoes. Major sectors of the mountain are composed of steep, outward-dipping lava flows (frontispiece) between which hydrothermal water has infused and altered material to clay-rich zones that are potential slip surfaces (fig. 22). Where exposed at the surface, these zones range from 0.2 to several meters in thickness. At depth, hydrothermal alteration is doubtless more intense.

Consequently, volcanoclastic flows beginning as large debris avalanches from Mount Rainier may have little correlation with the warning signs of an eruption. Only one of the modes of collapse described by Francis and Self (1987) requires precursory activity. Moreover, Siebert (1984) found a uniform relation between the height of origin and the runout distance of debris avalanches, regardless of whether the initial slope failure was induced by an explosion or merely by gravity, indicating that the energy from an explosive initiation does not increase the runout distance and thus does not increase the hazard.

TRAVEL TIMES OF LAHARS AND POTENTIAL RESERVOIR EFFECTS

The Puyallup and Carbon River systems presently (1994) have no reservoirs. The White and Nisqually River systems each have one reservoir, and the Cowlitz has two of greatly differing capacities. All but one of the reservoirs are far enough from the volcano that they are not at direct risk of a debris avalanche, except for secondary or transformation phases. All are at some risk from a Case I lahar; the travel time of such a flow from the volcano to the upstream end of each reservoir would be no more than several hours. Other possible reservoir impacts include the beneficial, hazard-reducing effects of impounding or attenuating volcanic flows.

The importance of a warning of dam failure is dramatically illustrated by the much greater numbers of survivors where warning was received (Costa, 1985). The importance of a warning system is equally applicable to Case I and Case II lahars whether or not a reservoir is involved. So rapid and localized are Case III flows that only advance planning and minimizing exposure will be effective.

TRAVEL TIMES OF LAHARS

The time it takes a debris flow wave to travel from point to point involves uncertainties, but a range of values can be estimated. A major source of uncertainty is the difference between mean flow velocity (table 7) and the flow-wave velocity (celerities in table 8). The first of these is the observed (or estimated) forward speed of mud and water in



Figure 22. Megaclast at surface of the 1963 debris avalanche below the Emmons Glacier in the main fork of the White River. Note the lighter colored zone of hydrothermal alteration (outlined) developed along a flow contact or fracture zone in volcanic breccia. The zone is about 1 m thick and is typical of flow contacts (frontispiece), fractures, and fault zones at Mount Rainier.

the flow; the latter is the rate at which the form of the flow wave progresses down the channel (celerity). A pronounced difference is apparent from a comparison of the velocity data of Fairchild (1985) and the celerity data of Cummins (1981) for the same 1980 lahars at Mount St. Helens. In general, the velocity of the material in the flow at the time of peak stage was faster than the speed with which the flow wave moved. For example, the average peak flow velocity of the 1980 North Fork lahar was about 9 m/s (Fairchild, 1985, fig. 4.4) over a channel interval where celerity of the maximum stage was only 2.1 m/s (Cummins, 1981, p. 485). The factors causing this difference are summarized below.

The 1980 North Fork lahar was texturally similar in behavior to the Case I lahar, and each was derived from a debris avalanche. The 1980 lahar originated by slumping of the surface of the 1980 avalanche, whereas the Case I example was mobilized directly from such a flow.

The behavior of the two cohesive lahars was probably similar with the exception that the 1980 flow probably was more broadly peaked at the point of origin. Thus, the celerity of the Case I lahar was likewise less than the actual flow velocity. Although a flood wave of water commonly travels

Table 8. Celerities and travel times of the maximum lahar, Case I lahar, and Case II lahar from Mount Rainier to the nearest downstream reservoir or the Puget Sound lowland.

[Maximum and minimum values of celerity calculated as described in text; R., River; Res., Reservoir]

Property	Maximum lahar	Case I lahar	Case II lahar
Lahar type	Cohesive	Cohesive	Noncohesive
Celerity of peak stage ¹ (m/s):			
Approximate maximum ²	25	22	8
Approximate minimum	6	5	3
Range of possible travel times ³ (hours):			
White R. to Mud Mtn. Res. (56 km)	0.6-2.6	0.7-3.1	1.9-5.2
Cowlitz R. to Riffe Lake (77 km)	0.9-3.6	1.0-4.3	2.7-7.1
Nisqually R. to Alder Res. (45 km) ...	0.5-2.1	0.6-2.5	1.6-4.2
Puyallup R. to lowland (38 km)	0.4-1.8	0.5-2.1	1.3-3.5
Carbon R. to lowland (38 km)	0.4-1.8	0.5-2.1	1.3-3.5

¹ Probably equivalent to peak discharge.

² Equal to estimated mean peak velocity between the volcano and either the first reservoir or the Puget Sound lowland.

³ Values in parentheses show distance along valley axis from volcano to head of reservoir or to boundary of Puget Sound lowland.

faster than its constituent water and sediment particles, this is not possible in a debris flow. The highest possible celerity of a lahar is the peak flow velocity. The minimum celerity may be estimated by the relation of celerity to peak flow velocity for the 1980 North Fork lahar. That ratio is 0.23. By such reasoning, the celerity of the Case I lahar varies from a minimum of 5 m/s to a maximum of about 22 m/s. This range of possible values is used to estimate travel times of the Case I lahar to the reservoirs (or the Puget Sound lowland) in river systems draining the volcano (table 8). Because the actual behavior of comparable flows is utilized, values intermediate within this range but tending nearer the longer travel times (lower celerities) can be considered for planning emergency response. Using an intermediate value, rather than the longest travel time, will adjust for the more rapid arrival of the leading edge of the flow. For example, though the possible travel times for the Case I lahar down the Puyallup or Carbon Rivers to the lowland range from 0.5 to 2.1 hours (table 8), a probable range for planning purposes would be 1.0 to 1.5 hours. The remaining uncertainties, however, require that these figures be treated as approximations.

By similar reasoning, the behavior of the noncohesive South Fork lahar at Mount St. Helens was probably similar to that of the noncohesive Case II flow. The ratio of celerity to peak flow velocity over a 40-km interval for the 1980 lahar was about 0.35 (Cummins, 1981; Fairchild, 1985). Consequently, the possible values of Case II celerity could range from a minimum of about 3 m/s to a maximum of about 8 m/s. These values are used to compute possible travel times (table 8).

Several factors contribute to this apparent discrepancy between the peak flow velocity and the wave celerity of debris flows: (1) the velocity measurements use relations unverified for debris flows and may be too high (Costa, 1984); (2) material may be continuously recycled through the peak to a point of temporary storage lateral to or beneath the flow, and that material then may re-enter the flow by draining back after passage of the peak, again to move forward into the peak (the caterpillar-track-path analogy; Johnson, 1984, p. 287); (3) velocity-measurement sites may be concentrated in narrow reaches where flow is faster than the average rate over many reaches; and (4) the flow waves commonly broaden during movement (Fairchild, 1985; Pierson and others, 1990), increasing the distance between the leading edge and the peak stage of the flow, and thereby reducing peak stage celerity.

RESERVOIR EFFECTS

WHITE RIVER

The Mud Mountain Dam (fig. 1), near the boundary of the Cascade Range and the Puget Sound lowland, is entirely a flood-control structure and is normally drawn down to

negligible storage. The maximum-impoundment level extends to within 56 km downvalley from the summit of Mount Rainier. Capacity above dead storage is 131 million m³, about 57 percent of the Case I volume (table 7). The actual proportion of the Case I volume retained would be greater because the depositional surface of the debris flow deposits would approach the slope of the stream channel, whereas the calculated reservoir capacity assumes a horizontal water surface. In addition, the backwater effects of the debris flow deposits could trigger an additional, unknown volume of upstream deposition.

The dam is a rock-and-earthfill structure with a rolled impervious core and probably could safely contain at least its capacity, so that any flow but the maximum lahar would be significantly attenuated. No wave of translation is likely to be generated by a lahar entering the reservoir, and any volcanically induced flow across the spillway would be debris flow. A concern is spillway abrasion by intralahar impact forces, described by Scott (1989). Runouts of Case II and III flows would be contained by the reservoir. Probable routing of any uncontained flow, as interpreted by Crandell (1971), would be within the White River valley unless (1) valley walls near Buckley were overtopped, sending part of the flow into the Carbon River drainage, or (2) flow extended to Auburn and crossed into the Green River drainage.

COWLITZ RIVER

The large, concrete-arch Mossyrock Dam (Riffe Lake, fig. 1) is a multipurpose impoundment. The upstream end of the reservoir at capacity is 77 km downvalley from the summit of Mount Rainier. Usable storage capacity is 1,600 million m³, a value 7 times the volume of the Case I example but only half that of the maximum lahar (table 7). Not all of this capacity is available because levels and releases are subject to flood-control and power-generation agreements. The normal operational goal is for annual refill by July 31. Gradual releases are normally maintained through the rest of the summer, increasing after late October in preparation for maximum flood-control drawdown between December 1 and March 1. Refill then begins with snowmelt runoff. The Case I example would be contained during the winter drawdown period and much of the remaining period. Runouts of Case II and III flows are not of concern at any time.

The risk of dam failure resulting from a wave generated by a volcanically induced inflow is greatly reduced by the improbability of a large debris avalanche extending to the reservoir. A lahar inflow would be far more gradual than either a landslide inflow, as at Vaiont, Italy (Kiersch, 1964), or a hypothetical debris avalanche like the one that could possibly enter Swift Reservoir near Mount St. Helens (Major and Scott, 1988). Given the large attenuation that would occur in the lahar flood wave through deposition on

the Cowlitz River flood plain upstream, it is unlikely that a lahar-generated wave by the Case I example could cause failure. The prehistoric Case I inundation area is, in fact, similar to the flood-plain area upstream of Riffe Lake.

Riffe Lake could be drawn down in response to an emergency if precursor volcanic activity has occurred and the risk of a lahar is high. Once a lahar has been initiated, though, time would be too short for any significant draw-down. The maximum drawdown rate, without presently causing inundation downstream at Castle Rock, is in the approximate range of 1,100 to 1,400 m³/s, or about 0.3 percent of usable storage in 1 hour with zero inflow (data from Department of Public Utilities, City of Tacoma). Probable travel times of both the maximum lahar and the Case I lahar are less than approximately 4 hours (table 8).

NISQUALLY RIVER

Alder Dam (fig. 1) is a small version of Mossyrock Dam, likewise of concrete-arch design and with similar operational modes. Usable capacity, corrected for the most recent sediment survey, is about 198 million m³. This value is a negligible portion of the Maximum lahar but is approximately 86 percent of the Case I example (table 7). However, sedimentation rate and trap efficiency are high, and several additional percent of capacity have probably been lost. As at Riffe Lake, this capacity is never entirely available.

The dam could clearly be destroyed by the maximum lahar. It is also the most vulnerable to a Case I flow of the three reservoirs potentially affected by volcanic debris flow. It is the reservoir most vulnerable to failure caused by a wave of translation, because the relatively confined valley upstream is capable of conveying a large lahar without great volume loss. Consequently, a high priority needs to be given to drawing down this reservoir in the event of probable volcanic activity.

Inflowing lahars will generate long-period waves that will translate through the reservoir to affect the dam. In a model of the behavior of Swift Reservoir in response to rapid inflow (Pacific Power and Light, 1980), peak wave action in the reservoir occurred before significant water level rise. That reservoir is closer to Mount St. Helens (13 km by the most direct route) than Alder Reservoir is to Mount Rainier (45 km). Thus, the time to peak of a lahar wave is probably greater at Alder Reservoir, resulting in a more gradual rise. However, given the variety of attenuation rates and wave shapes possible for different flows at Mount Rainier, this is not certain. What is certain, however, is that the riskiest potential lahar reaching Alder Reservoir from Mount Rainier is far larger than that reaching Swift Reservoir from Mount St. Helens and that volumetric impacts probably will dominate as hazards at Alder Reservoir. Crandell (1988, fig. 18) shows Alder Reservoir to be within range of a debris avalanche that has not transformed to a lahar.

Loss of capacity in Alder Reservoir, because of the high "background" sedimentation rate, will probably make the structure uneconomic in a fraction of the recurrence interval of the Case I flow. When the reservoir is filled with sediment, decisions either to modify the structure and increase capacity or to abandon it need to consider the possibility of a Case I lahar. The same aspects of emergency response that apply to Riffe Lake also apply to Alder Reservoir. Total streamflow at the highway bridge near Yelm cannot exceed 227 m³/s without causing flooding of habitation there (data from Department of Public Utilities, City of Tacoma). If a release of 150 m³/s from the reservoir is possible (depending on downstream tributary inflows), drawdown with zero inflow is at a rate of 0.3 percent of total capacity per hour. The travel time of a Case I flow from the volcano is less than about two hours (table 8).

CONCLUSIONS

Two types of debris flow have occurred periodically throughout postglacial time at Mount Rainier: (1) cohesive debris flows, containing at least 3 to 5 percent clay, which have flowed untransformed more than 100 km from the volcano; and (2) noncohesive debris flows, containing less than 3 to 5 percent clay, which commonly transform downstream to more dilute flows, passing through the range of hyperconcentrated flow. The noncohesive debris flows form most commonly by bulking of a flood surge with volcanoclastic and morainal sediment, and during formation they also pass through the range of hyperconcentration.

Three subgroups of a mixed population of lahars and glacially related debris flows were studied over time intervals related to their frequency, and from this spectrum of case histories an example of each was selected for consideration in flow-hazard analysis. Case I, a large cohesive lahar formed by mobilization of a deep-seated landslide, is capable of inundating parts of the Puget Sound lowland or the Cowlitz River valley. It is suitable for consideration in hazards planning in lowland areas. Case II is a noncohesive lahar of intermediate size and sufficient frequency that it may be applicable to the design of some structures such as dams and power plants around the volcano. Case III originates as a debris avalanche of a typical size observed at Mount Rainier, and which probably will mobilize to form a lahar. It poses risk primarily to local areas within Mount Rainier National Park.

The maximum lahar is typified by the largest flow in the postglacial history of Mount Rainier. It is a statistical outlier of the group of large cohesive lahars. The smallest and most frequent flows are dominated by glacial-outburst floods that bulk to debris flows and provide behavioral models of the larger noncohesive debris flows. They commonly attenuate rapidly at the base of the volcano through the rapid debulking of sediment, yielding hyperconcentrated streamflow and

secondary debris flow by any of three types of transformations. Their inundation potential can be assessed and hazard zones can be established based on the level of erosion of tephra set W, on dendrochronology, and on numerous historic flows.

Each of the five major river systems draining the volcano has a record of lahars. Although the records indicate that flows differ in size and frequency among river systems, the risk of future lahars may not correlate highly with the record in each individual system. Rather, extrapolation of the entire volcano's past history to the future is more appropriate, with the risk dispersed among the individual drainages. Sites of future instability of the type producing major areas of collapse and the large cohesive lahars cannot be forecast. This is likewise true of the sites where intensified geothermal activity will produce noncohesive lahars by melting of ice and snow, and the places where renewed explosive volcanism will greatly increase the risks of all types of flows. However, the types of flows that will recur, as well as their approximate sizes and probabilities, can be forecast for the volcano as a whole. This is the most essential element of flow-hazard analysis.

REFERENCES CITED

- Atwater, B.F., 1988, Buried Holocene wetlands along the Johns River, southwest Washington [abs.]: Proceedings of the Symposium on Holocene Subduction in the Pacific Northwest, May 1988, Quaternary Research Center, University of Washington, p. 4.
- Bacon, C.R., 1983, Eruptive history of Mount Mazama and Crater Lake caldera, Cascade Range, U.S.A.: *Journal of Volcanology and Geothermal Research*, v. 18, p. 57-116.
- Bagnold, R.A., 1962, Auto-suspension of transported sediment—Turbidity currents: *Proceedings of the Royal Society of London*, v. A225, p. 315-319.
- Bethel, J.P., 1981, Volcanic mudflow deposits in the Cowlitz River valley, Washington [abs.]: *Geological Society of America Abstracts with Programs, Cordilleran Section*, March 25-27, 1981, Hermosillo, Sonora, Mexico, v. 13, no. 2, p. 45.
- Bretz, J.H., 1913, Glaciation of the Puget Sound region: *Washington Geological Survey Bulletin* 8, 244 p.
- Brice, J.C., 1981, Stability of relocated stream channels: Federal Highway Administration Report, no. FHWA/RD-80/158, 177 p.
- Brice, J.C., and Blodgett, J.C., 1978, Countermeasures for hydraulic problems at bridges—Volume 1, Analysis and assessment: Federal Highway Administration Report, no. FHWA-RD-78-162, 169 p.
- Burbank, D.W., 1981, A chronology of late Holocene glacier fluctuations on Mount Rainier, Washington: *Arctic and Alpine Research*, v. 13, p. 369-386.
- Costa, J.E., 1984, Physical geomorphology of debris flows, *in* Costa, J.E., and Fleisher, P.J., eds., *Developments and applications of geomorphology*: Berlin, Springer-Verlag, p. 269-317.
- , 1985, Floods from dam failures: U.S. Geological Survey Open-File Report 85-560, 54 p.
- Crandell, D.R., 1963a, Paradise debris flow at Mount Rainier, Washington, *in* *Short papers in geology and hydrology*: U.S. Geological Survey Professional Paper 475-B, p. 135-139.
- , 1963b, Surficial geology and geomorphology of the Lake Tapps Quadrangle, Washington: U.S. Geological Survey Professional Paper 388-A, 84 p.
- , 1969, Surficial geology of Mount Rainier National Park, Washington: U.S. Geological Survey Bulletin 1288, 41 p.
- , 1971, Postglacial lahars from Mount Rainier Volcano, Washington: U.S. Geological Survey Professional Paper 677, 73 p.
- , 1988, Gigantic debris avalanche of Pleistocene age from ancestral Mount Shasta volcano, California, and debris-avalanche hazard zonation: U.S. Geological Survey Bulletin 1861, 32 p.
- Crandell, D.R., and Fahnestock, R.K., 1965, Rockfalls and avalanches from Little Tahoma Peak on Mount Rainier, Washington: U.S. Geological Survey Bulletin 1221-A, 30 p.
- Crandell, D.R., and Miller, R.D., 1974, Quaternary stratigraphy and extent of glaciation in the Mount Rainier region, Washington: U.S. Geological Survey Professional Paper 847, 59 p.
- Crandell, D.R., Miller, C.D., Glicken, H.X., Christiansen, R.L., and Newhall, C.G., 1984, Catastrophic debris avalanche from ancestral Mount Shasta volcano, California: *Geology*, v. 12, p. 143-146.
- Crandell, D.R., and Mullineaux, D.R., 1978, Potential hazards from future eruptions of Mount St. Helens volcano, Washington: U.S. Geological Survey Bulletin 1383-C, 26 p.
- Crosson, R.S., and Frank, David, 1975, The Mount Rainier earthquake of July 18, 1973, and its tectonic significance: *Seismological Society of America Bulletin*, v. 65, p. 393-401.
- Crosson, R.S., and Lin, J.W., 1975, A note on the Mt. Rainier earthquake of April 20, 1974: *Seismological Society of America Bulletin*, v. 65, p. 549-556.
- Cullen, J.M., 1977, Impact of a major eruption of Mount Rainier on public service delivery systems in the Puyallup Valley, Washington: Seattle, Wash., University of Washington, M.S. thesis, 202 p.
- Cullen Tanaka, Janet, 1983, Volcanic hazards assessment for Mt. Rainier, Washington: Olympia, Wash., Washington State Department of Emergency Services, 28 p.
- Cummins, John, 1981, Chronology of mudflows on the South Fork and North Fork Toutle River following the May 18 eruption, *in* Lipman, P.W., and Mullineaux, D.R., eds., *The 1980 eruptions of Mount St. Helens*, Washington: U.S. Geological Survey Professional Paper 1250, p. 479-486.
- Dethier, D.P., and Bethel, John, 1981, Surficial deposits along the Cowlitz River near Toledo, Lewis County, Washington: U.S. Geological Survey Open-File Report 81-1043, 11 p.
- Dibble, R.R., Nairn, I.A., and Neall, V.E., 1985, Volcanic hazards of North Island, New Zealand—Overview: *Journal of Geodynamics*, v. 3, p. 369-396.
- Driedger, C.L., and Kennard, P.M., 1986, Ice volumes on Cascade volcanoes—Mount Rainier, Mount Hood, Three Sisters and Mount Shasta: U.S. Geological Survey Professional Paper 1365, 28 p.
- Erdmann, C.E., and Johnson, A., 1953, Preliminary report, flood problem on Nisqually River at Longmire, Washington:

- National Park Service unpublished report [available at National Park Service library, Longmire, Wash.], p. 2–11.
- Evans, S.G., 1989, Earthquake-induced landslides in the Canadian Cordillera [abs.]: *Geological Society of America Abstracts with Programs*, v. 21, no. 5, p. 77.
- Fairchild, L.H., 1985, Lahars at Mount St. Helens, Washington: Seattle, Wash., University of Washington Ph.D. thesis, 374 p.
- Fisher, R.V., 1983, Flow transformations in sediment gravity flows: *Geology*, v. 11, p. 273–274.
- Fisher, R.V., and Schmincke, H.U., 1984, *Pyroclastic rocks*: Berlin, Springer-Verlag, 472 p.
- Fiske, R.S., Hopson, C.A., and Waters, A.C., 1963, *Geology of Mount Rainier National Park*, Washington: U.S. Geological Survey Professional Paper 444, 93 p.
- Fiske, R.S., and Jackson, E.D., 1972, Orientation and growth of Hawaiian volcanic rifts—The effect of regional structure and gravitational stresses: *Proceedings of the Royal Society of London, ser. A*, v. 329, p. 299–326.
- Folk, R.L., 1980, *Petrology of sedimentary rocks*: Austin, Tex., Hemphill Publishing Company, 182 p.
- Francis, Peter, and Self, Stephen, 1987, Collapsing volcanoes: *Scientific American*, v. 256, p. 90–97.
- Frank, D.G., 1985, Hydrothermal processes at Mount Rainier: Seattle, Wash., University of Washington, Ph.D. thesis, 195 p.
- Frank, D.G., and Friedman, J.D., 1974, Newly detected infrared anomalies at Mount Rainier, Washington [abs.], in *Symposium on applications of satellite and airplane remote sensing of natural resources in the Pacific Northwest*, Tumwater, Washington, May 2, 1974: Washington Department of Natural Resources, p. 22.
- Franklin, J.F., Cromack, Kermit, Jr., Denison, William, McKee, Arthur, Maser, Chris, Sedell, James, Swanson, Fred, and Juday, Glen, 1981, Ecological characteristics of old-growth Douglas-fir forests: U.S. Forest Service, Pacific Northwest Forest and Range Experiment Station, General Technical Report PNW-118, 48 p.
- Frizzell, V.A., Jr., Tabor, R.W., Booth, D.B., Ort, K.M., and Waitt, R.B., Jr., 1984, Preliminary geologic map of the Snoqualmie Pass 1:100,000 Quadrangle, Washington: U.S. Geological Survey Open-File Map 84-693.
- Glicken, Harry, 1986, Rockslide-debris avalanche of May 18, 1980, Mount St. Helens volcano: Santa Barbara, Calif., University of California, Ph.D. thesis, 303 p.
- Glicken, Harry, and Schultz, P.H., 1980, Martian channel erosion—The lahar analogy: *Planetary Science*, v. 11, no. 5.
- Gower, H.D., 1978, Tectonic map of the Puget Sound region, Washington, showing locations of faults, principal folds, and large-scale Quaternary deformation: U.S. Geological Survey Open-File Report 78-426, 21 p.
- Grater, R.K., 1948a, A report on the Kautz Creek flood studies: National Park Service unpublished report [available at National Park Service library, Longmire, Wash.], 9 p.
- 1948b, The flood that swallowed a glacier: *Natural History*, v. 57, p. 276–278.
- Guy, H.P., 1970, Fluvial sediment concepts, chapter C1 of Book 3, Applications of hydraulics: U.S. Geological Survey Techniques of Water-Resources Investigations, TWI 3-C1, 55 p.
- Hampton, M.A., 1975, Competence of fine-grained debris flows: *Journal of Sedimentary Petrology*, v. 45, p. 834–844.
- Heaton, T.H., and Hartzell, S.H., 1987, Earthquake hazards on the Cascadia subduction zone: *Science*, v. 236, p. 162–168.
- Hooke, R. LeB., 1967, Processes on arid-region alluvial fans: *Journal of Geology*, v. 75, p. 438–460.
- Iverson, R.M., 1989, Pore-water effects in mass-movement mechanics: International Geological Congress, 28th, Washington, 1989, Abstracts, v. 2, p. 104–105.
- Iverson, R.M., and Denlinger, R.P., 1987, The physics of debris flows—A conceptual assessment, in Beschta, R.L., Blinn, T., Grant G.E., Ice, G.G., and Swanson, F.J., eds., *Erosion and sedimentation in the Pacific Rim*: International Association of Hydrological Sciences Publication 165, p. 155–165.
- Jahns, R.H., 1949, Desert floods: Engineering and Science Monthly, California Institute of Technology Contribution No. 499, p. 10–14.
- Johnson, A.M., 1965, A model for debris flow: University Park, Pa., Pennsylvania State University, Ph.D. thesis, 305 p.
- 1970, Physical processes in geology: San Francisco, Freeman, Cooper, and Co., 577 p.
- 1984, Debris flow (*with contributions by* Rodine, J.R.), in Brunsden, Denys, and Prior, D.B., eds., *Slope instability*: New York, John Wiley and Sons, Ltd., p. 257–361.
- Kellerhals, Rolf, and Bray, D.I., 1971, Sampling procedures for coarse fluvial sediments: *Proceedings of the American Society of Civil Engineers, Journal of Hydraulics Division*, v. 97, no. HY8, p. 1165–1180.
- Kiersch, G.A., 1964, The Vaiont River disaster: *Civil Engineering*, v. 34, p. 32–39.
- Kiver, E.P. and Steele, W.K., 1972, Summit fir caves, Mount Rainier, Washington: *Science*, v. 173, p. 320–322.
- Kurdir, R.D., 1973, Classification of mudflows: *Soviet Hydrology*, no. 4, p. 310–316.
- Laenen, Antonius, Scott, K.M., Costa, J.E., and Orzol, L.L., 1987, Hydrologic hazards along Squaw Creek from a hypothetical failure of the glacial moraine impounding Carver Lake near Sisters, Oregon: U.S. Geological Survey Open-File Report 87-41, 48 p.
- 1992, Modeling flood flows from a hypothetical failure of the glacial moraine impounding Carver Lake near Sisters, Oregon, in Subitzky, Seymour, ed., *Selected papers in the hydrologic sciences 1988–92*: U.S. Geological Survey Water-Supply Paper 2340, p. 151–164.
- Latter, J.H., Houghton, B.F., and Hackett, W.R., 1981, Volcanic risk assessment at Ruapehu volcano, chap. 4 of Houghton, B.F., and Smith, I.E.M., eds., *New Zealand Volcanological Workshop, Turangi, New Zealand, November 27–29, 1981*, Handbook and proceedings: unpaginated.
- Linsley, R.K., Jr., Kohler, M.A., and Paulhus, J.L.H., 1958, *Hydrology for engineers*: New York, McGraw-Hill Book Company, Inc., 340 p.
- Lokey, W.M., Mack, Ross, Miller, M.M., Prather, B.W., and Kiver, E.P., 1972, Project Crater—Mt. Rainier glacio-volcanological research, 1970–72, in *Arctic and Mountain Environments Symposium*, Michigan State University, April 22–28, 1972, Program with Abstracts: East Lansing, Mich., Glaciological and Arctic Science Institute, Michigan State University [unpaginated].
- Lowe, D.R., 1976, Grain flow and grain flow deposits: *Journal of Sedimentary Petrology*, v. 46, p. 188–199.

- 1979, Sediment gravity flows—Their classification and some problems of application to natural flows and deposits: *Society of Economic Paleontologists and Mineralogists, Special Publication 27*, p. 75–82.
- 1982, Sediment gravity flows—II. Depositional models with special reference to the deposits of high-density turbidity currents: *Journal of Sedimentary Petrology*, v. 52, p. 279–297.
- Lowe, D.R., and LoPiccolo, R.D., 1974, The characteristics and origins of dish and pillar structures: *Journal of Sedimentary Petrology*, v. 44, p. 484–501.
- Luzier, J.E., 1969, Geology and ground-water resources of southwestern King County, Washington: Washington Department of Water Resources, Water-Supply Bulletin 28, 260 p.
- Major, J.J., 1984, Geologic and rheologic characteristics of the May 18, 1980, southwest flank lahars at Mount St. Helens, Washington: University Park, Pa., Pennsylvania State University, M.S. thesis, 225 p.
- Major, J.J., and Scott, K.M., 1988, Volcaniclastic sedimentation in the Lewis River valley, Mount St. Helens, Washington—Processes, extent, and hazards: *U.S. Geological Survey Bulletin 1383-D*, 38 p.
- Middleton, G.V., and Hampton, M.A., 1976, Subaqueous sediment transport and deposition by sediment gravity flows, in Stanley, D.J., and Swift, D.J.P., eds., *Marine sediment transport and environmental management*: New York, Wiley, p. 197–218.
- Mullineaux, D.R., 1974, Pumice and other pyroclastic deposits in Mount Rainier National Park, Washington: *U.S. Geological Survey Bulletin 1326*, 83 p.
- 1986, Summary of pre-1980 tephra-fall deposits erupted from Mount St. Helens, Washington State, U.S.A: *Bulletin of Volcanology*, v. 48, p. 17–26.
- National Research Council, 1988, *Estimating probabilities of extreme floods—Methods and recommended research*: Washington, National Academy Press, 141 p.
- Nelson, L.M., 1987, Flood characteristics for the Nisqually River and susceptibility of Sunshine Point and Longmire facilities to flooding in Mount Rainier National Park, Washington: *U.S. Geological Survey Water-Resources Investigations Report 86-4179*, 18 p.
- Nemec, W., and Steel, R.J., 1984, Alluvial and coastal conglomerates—Their significant features and some comments on gravelly mass-flow deposits, in Koster, E.H. and Steel, R.J., eds., *Sedimentology of gravels and conglomerates*: Canadian Society of Petroleum Geologists Memoir 10, p. 1–31.
- Norris, R.D., in press, Seismicity of rockfalls and avalanches at three Cascade Range volcanoes—Implications for seismic detection of hazardous mass movements: *Seismological Society of America Bulletin*.
- North American Commission on Stratigraphic Nomenclature, 1983, *North American Stratigraphic Code*: *American Association of Petroleum Geologists Bulletin*, v. 67, p. 841–875.
- Osterkamp, W.R., Hupp, C.R., and Blodgett, J.C., 1985, Magnitude and frequency of debris flows, and areas of hazard on Mount Shasta, northern California: *U.S. Geological Survey Open-File Report 85-425*, 35 p.
- Pacific Power and Light, 1980, Study of effects of potential volcanic activity on Lewis River Projects: Portland, Oreg., Board of Consultants Report, paginated sections. Available from Pacific Power and Light Co., 920 Southwest 6th Ave., Portland, OR 97204.
- Packwood History Committee, 1954, *Packwood on the march*: Unpublished compilation of early historical accounts, unpaginated. Available at Packwood Branch, Lewis County Public Library, Packwood, WA 98361.
- Pierson, T.C., 1980, Erosion and deposition by debris flows at Mount Thomas, North Canterbury, New Zealand: *Earth Surface Processes*, v. 5, p. 227–247.
- 1985, Initiation and flow behavior of the 1980 Pine Creek and Muddy River lahars, Mount St. Helens, Washington: *Geological Society of America Bulletin*, v. 96, p. 1056–1069.
- Pierson, T.C., and Costa, J.E., 1987, A rheologic classification of subaerial sediment-water flows, in Costa, J.E., and Wieczorek, G.F., eds., *Debris flows/avalanches—Process, recognition, and mitigation*: *Reviews in Engineering Geology*, v. 7, p. 1–12.
- Pierson, T.C., Janda, R.J., Thouret, J.-C., and Borrero, C.A., 1990, Perturbation and melting of snow and ice by the 13 November 1985 eruption of Nevado del Ruiz, Colombia, and consequent mobilization, flow and deposition of lahars: *Journal of Volcanology and Geothermal Research*, v. 41, p. 17–66.
- Porter, S.C., and Denton, G.H., 1967, Chronology of Neoglaciation in the North American Cordillera: *American Journal of Science*, v. 265, p. 177–210.
- Postma, George, 1986, Classification for sediment-gravity deposits based on flow conditions during sedimentation: *Geology*, v. 14, p. 291–294.
- Prych, E.A., 1987, Flood-carrying capacities and changes in channels of the lower Puyallup, White, and Carbon Rivers in western Washington: *U.S. Geological Survey Open-File Report 87-4129*, 69 p.
- Qian Yiyang, Yang Wenhai, Zhao Wenlin, Cheng Xiuwen, Zhang Longrong, and Xu Wengui, 1980, Basic characteristics of flow with hyperconcentration of sediment, in Li Boning, chairperson, *Proceedings of the International Symposium on River Sedimentation*, March 24–29, 1980, Beijing, China: Beijing, Gaunghua Press, p. 175–184.
- Reich, B.M., 1973, How frequently will floods occur?: *Water Resources Bulletin*, v. 9, p. 187–188.
- Richardson, Donald, 1968, Glacier outburst floods in the Pacific Northwest, in *Geological Survey Research 1968*: *U.S. Geological Survey Professional Paper 600-D*, p. D79–D86.
- Rodolfo, K.S., 1989, Origin and early evolution of lahar channel at Mabinit, Mayon Volcano, Philippines: *Geological Society of America Bulletin*, v. 101, p. 414–426.
- Scheidegger, A.E., 1973, On the prediction of the reach and velocity of catastrophic landslides: *Rock Mechanics*, Springer-Verlag, v. 5, p. 231–236.
- Schumm, S.A., 1960, The shape of alluvial channels in relation to sediment type: *U.S. Geological Survey Professional Paper 352-B*, 30 p.
- 1961, Effect of sediment characteristics on erosion and deposition in ephemeral-stream channels: *U.S. Geological Survey Professional Paper 352-C*, 70 p.
- Schuster, R.L., and Chleborad, A.F., 1989, Historic earthquake-induced landslides in western Washington: *Geological Society of America Abstracts with Programs*, v. 21, no. 5, p. 141.
- Scott, K.M., 1981, Erosion and sedimentation in the Kenai River, Alaska: *U.S. Geological Survey Professional Paper 1235*, 35 p.

- 1988a, Origin, behavior, and sedimentology of catastrophic lahars at Mount St. Helens, Washington, *in* Clifton, H.E., ed., *Sedimentologic consequences of convulsive geologic events*: Geological Society of America Special Paper 229, p. 23–36.
- 1988b, Origins, behavior, and sedimentology of lahars and lahar-runout flows in the Toutle-Cowlitz River system: U.S. Geological Survey Professional Paper 1447–A, 76 p.
- 1989, Magnitude and frequency of lahars and lahar-runout flows in the Toutle-Cowlitz River system: U.S. Geological Survey Professional Paper 1447–B, 33 p.
- 1992, Risk analysis of sediment gravity flows at Cascade Range volcanoes—Approaches and analogies with alluvial fans, *in* Jones, M.E., and Laenen, Antonius, eds., *Interdisciplinary approaches in hydrology and hydrogeology*: Minneapolis, Minn., American Institute of Hydrology, p. 222–230.
- Scott, K.M., and Janda, R.J., 1987, Multiple origins of catastrophic lahars at Cascade Range volcanoes—Probabilities of precursor events, and hazards in downstream areas: Hawaii Symposium on How Volcanoes Work, Hawaiian Volcano Observatory, Hilo, Hawaii, January 19–25, 1987, Abstract Volume, p. 229.
- Scott, K.M., Laenen, Antonius, and Kresch, D.L., 1987, Hydrologic hazards downstream from volcanoes—Techniques of risk analysis, *in* Accurti, Dante, chairperson, *Realistic approaches to better floodplain management*: Association of State Floodplain Managers, 11th Annual Conference, Seattle, Wash., June 8–13, 1987, Proceedings; Natural Hazards Research and Applications Information Center Special Publication 18, p. 286–291.
- Siebert, Lee, 1984, Large volcanic debris avalanches—Characteristics of source areas, deposits, and associated eruptions: *Journal of Volcanology and Geothermal Research*, v. 22, p. 163–197.
- Siebert, Lee, Glicken, Harry, and Ui, Tadahide, 1987, Volcanic hazards from Bezymianny- and Bandai-type eruptions: *Bulletin of Volcanology*, v. 49, p. 435–459.
- Sigafoos, R.S., and Hendricks, E.L., 1961, Botanical evidence of the modern history of Nisqually Glacier, Washington: U.S. Geological Survey Professional Paper 387–A, 20 p.
- 1972, Recent activity of glaciers of Mount Rainier, Washington: U.S. Geological Survey Professional Paper 387–B, 24 p.
- Smith, G.A., and Fritz, W.J., 1989, Penrose Conference report—Volcanic influences on sedimentation: *Geology*, p. 375–376.
- Southard, J.B., and Mackintosh, M.E., 1981, Experimental test of autosuspension: *Earth Surface Processes and Landforms*, v. 6, p. 103–111.
- Stuiver, Minze, and Becker, Bernd, 1986, High-precision decadal calibration of the radiocarbon time scale, AD 1950–2500 BC: *Radiocarbon*, v. 28, p. 863–910.
- Summers, C.G., 1978, *Go to the Cowlitz*, Peter Crawford: Longview, Wash., Speedy-Litho Press, 324 p.
- Unger, J.D., and Decker, R.W., 1970, The microearthquake activity of Mt. Rainier, Washington: *Seismological Society of America Bulletin*, v. 60, p. 2033–2035.
- Unger, J.D., and Mills, K.F., 1972, Microearthquakes at Mt. Rainier—1969: *Seismological Society of America Bulletin*, v. 62, p. 1079–1081.
- U.S. Army Corps of Engineers, 1985, Toutle River sediment-retention structure—Mudflow design criteria: Portland, Oreg., Portland District Letter Report, 7 p.
- Varnes, D.J., 1978, Slope movement types and processes, *in* Schuster, R.L., and Krizek, R.J., eds., *Landslides—Analysis and control*: National Research Council, Transportation Research Board, Special Report 176, p. 11–35.
- Voight, Barry, Glicken, Harry, Janda, R.J., and Douglas, P.M., 1981, Catastrophic rockslide avalanche of May 18, *in* Lipman, P.W., and Mullineaux, D.R., eds., *The 1980 eruptions of Mount St. Helens, Washington*: U.S. Geological Survey Professional Paper 1250, p. 347–377.
- Walder, J.S., and Driedger, C.L., 1993, Glacier-generated debris flows at Mount Rainier: U.S. Geological Survey Open-File Report 93-124 (Volcano Hazards Fact Sheet), 2 p.
- 1994, Geomorphic change caused by outburst floods and debris flows at Mount Rainier, Washington, with emphasis on Tahoma Creek valley: U.S. Geological Survey Water Resources Investigations Report 93-4093, 93 p.
- Webb, R.H., Pringle, P.T., and Rink, G.R., 1989, Debris flows from tributaries of the Colorado River, Grand Canyon National Park, Arizona: U.S. Geological Survey Professional Paper 1492, 39 p.
- Wentworth, C.M., 1967, Dish structure, a primary sedimentary structure in coarse turbidites [abs.]: *American Association of Petroleum Geologists Bulletin*, v. 51, p. 485.
- Wolman, M.G., 1954, A method of sampling coarse river-bed material: *American Geophysical Union Transactions*, v. 35, p. 951–956.
- Yamaguchi, D.K., 1983, New tree-ring dates for recent eruptions of Mount St. Helens: *Quaternary Research*, v. 20, p. 246–250.
- 1985, Tree-ring evidence for a two-year interval between recent prehistoric explosive eruptions of Mount St. Helens: *Geology*, v. 13, p. 554–557.
- Yano, Katsumasa, and Daido, Atsuyuki, 1965, Fundamental study on mud-flow: *Bulletin of the Disaster Prevention Institute (Japan)*, v. 14, p. 69–83.
- Yesenov, U.Ye., and Degovets, A.S., 1979, Catastrophic mudflow on the Bol'shaya Almatinka River in 1977: *Soviet Hydrology, Selected Papers*, v. 18, p. 158–160.